

BIOSURFACTANT (MONORHAMNOLIPID) COMPLEXATION OF METALS AND
APPLICATIONS FOR AQUEOUS METALLIFEROUS WASTE REMEDIATION

by

David E. Hogan

Copyright © David E. Hogan 2016

A Dissertation Submitted to the Faculty of the

DEPARTMENT OF SOIL, WATER AND ENVIRONMENTAL SCIENCE

In Partial Fulfillment of the Requirements

For the Degree of

DOCTOR OF PHILOSOPHY

In the Graduate College

THE UNIVERSITY OF ARIZONA

2016

**THE UNIVERSITY OF ARIZONA
GRADUATE COLLEGE**

As members of the Dissertation Committee, we certify that we have read the dissertation prepared by David E. Hogan, titled Biosurfactant (Monorhamnolipid) Complexation of Metals and Applications for Aqueous Metalliferous Waste Remediation and recommend that it be accepted as fulfilling the dissertation requirement for the Degree of Doctor of Philosophy.

_____ Date: 09/12/2016

Raina M. Maier

_____ Date: 09/12/2016

Jeanne E. Pemberton

_____ Date: 09/12/2016

Joan E. Curry

_____ Date: 09/12/2016

J. Brent Hiskey

Final approval and acceptance of this dissertation is contingent upon the candidate's submission of the final copies of the dissertation to the Graduate College.

I hereby certify that I have read this dissertation prepared under my direction and recommend that it be accepted as fulfilling the dissertation requirement.

_____ Date: 09/12/2016

Dissertation Director: Raina M. Maier

STATEMENT BY AUTHOR

This dissertation has been submitted in partial fulfillment of the requirements for an advanced degree at the University of Arizona and is deposited in the University Library to be made available to borrowers under rules of the Library.

Brief quotations from this dissertation are allowable without special permission, provided that an accurate acknowledgement of the source is made. Requests for permission for extended quotation from or reproduction of this manuscript in whole or in part may be granted by the head of the major department or the Dean of the Graduate College when in his or her judgment the proposed use of the material is in the interests of scholarship. In all other instances, however, permission must be obtained from the author.

SIGNED: David E. Hogan

ACKNOWLEDGEMENTS

I would like to thank all of my peers alongside whom I have had the pleasure of working and learning, especially those members of the Environmental Microbiology Laboratory. Countless people have helped me develop as a student, researcher, teacher, and person, without whom, this dissertation would not have been possible. These people have enriched my life and provided me with irreplicable experiences, knowledge, skills, and perspectives I trust to guide my future endeavors.

I would especially like to thank Ryan Eismin, a good friend and patient counsel whose advice, guidance, and expertise helped me navigate many scholarly hurdles and furthered my skills and knowledge in the field of chemistry.

I would like to thank Drs. Jeanne Pemberton, Joan Curry, and Brent Hiskey for serving on my committee. I am honored to have had the opportunity to learn from them, and I am grateful for the knowledge and expertise they have shared with me.

I owe a great deal of gratitude to Mary Kay Amistadi in the Arizona Laboratory for Emerging Contaminants. She helped me meet more deadlines than I would like to admit when I found myself in tight spots needing samples analyzed.

I would like to thank Dr. Julie Neilson for fielding years of questions and tolerating countless interruptions. She was always a dependable source of information, experience, and wisdom.

With the utmost gratitude, I thank my primary advisor Dr. Raina Maier for offering me an opportunity to explore my interest in using microorganisms to address environmental issues. To be cliché, she always reminded me to look for the forest despite the trees and not lose sight of the big picture. She pushed my boundaries and helped me to find and improve my weaknesses (literary writing be damned). I appreciate her unwavering support, empathy, encouragement, and uncanny ability to find and divert me from my mental hang-ups. She gave me the opportunity not only to learn, but showed me the joy of teaching as well. I have been fortunate to be a recipient of her knowledge, experiences, and wisdom, and she is the epitome of an outstanding advisor.

Lastly, I would like to thank my parents. The completion of this dissertation is a testament to the foundation they laid not so many years ago as they raised me. They have been a constant source of encouragement and provided me with so many opportunities to explore the world and learn. While I may not have always been the best listener, their advice and guidance has always led me in the right direction, and I am grateful to have such a good compass on my journey through life.

DEDICATION

Life's journey carves a wandering path through an uncharted wilderness. As we wander, we inevitably encounter the paths of others. Sometimes the paths merely intersect, and other times they meander together before parting ways. Those people who have a lasting impact on our lives shift our paths in new directions.

I dedicate this dissertation to those who shifted my path by encouraging me to question more, look deeper, try harder, and strive for excellence, especially my educators.

I also dedicate this dissertation to my loving wife and best friend Kourtney. May our paths forever wander together.

TABLE OF CONTENTS

LIST OF FIGURES	13
LIST OF TABLES	18
ABSTRACT	20
CHAPTER 1 INTRODUCTION	23
1.1. Abstract	23
1.2. Introduction	23
1.3. Metals and Metal Contamination	24
1.4. Sources of Metals	27
1.4.1. Atmospheric Environments	27
1.4.2. Aquatic Environments	28
1.4.3. Soil Environments	28
1.4.4. Summary	29
1.5. Biosurfactant Complexation of Metals	29
1.5.1. Rhamnolipids	30
1.5.1.1. Metal Interactions with Rhamnolipid	31
1.5.1.2. Effects of Metals on Rhamnolipid Production	36
1.5.2. Lipopeptides	37
1.5.2.1. Metal Complexation by Lipopeptides	37
1.5.2.2. Effects of Metals on Lipopeptides	39

1.5.3.	Other Biosurfactants	40
1.5.3.1.	Siderolipids.....	41
1.5.3.2.	Glycoglycerolipids	41
1.5.3.3.	Saponins	42
1.5.3.4.	Sophorolipids	42
1.5.3.5.	Spiculisporic acids.....	43
1.6.	Remediation Applications	44
1.6.1.	Solid Media.....	46
1.6.1.1.	Soil Washing	46
1.6.1.1.1.	Soil Washing: Efficacy of Biosurfactant on Artificial Contamination.....	48
1.6.1.1.2.	Soil Washing: Efficacy of Biosurfactants on Aged Contamination.....	49
1.6.1.1.2.1.	Sediments	50
1.6.1.1.2.2.	Mine Tailings	51
1.6.1.1.2.3.	Industrial Waste	52
1.6.1.1.3.	Summary	52
1.6.1.2.	Phytoremediation	53
1.6.1.3.	Remediation of Co-Contaminated Systems	56
1.6.2.	Liquid Media	58

1.6.3.	Recovery of Metal from Biosurfactant-Metal Complexes	60
1.7.	Conclusion.....	61
1.8.	Note about Chapter 1.....	62
CHAPTER 2 RHAMNOLIPID BIOSURFACTANTS PREFERENTIALLY COMPLEX		
RARE EARTH ELEMENTS.....		
65		
2.1.	Abstract	65
2.2.	Introduction	66
2.3.	Materials and Methods	68
2.3.1.	Monorhamnolipid Production.....	68
2.3.2.	Monorhamnolipid Purification	69
2.3.3.	Metals	70
2.3.4.	Determination of Stability Constants	70
2.3.5.	Stability Constant Calculation.....	71
2.3.6.	Metal Competition Study.....	72
2.4.	Results and Discussion.....	73
2.4.1.	Single Metal Studies.....	73
2.4.2.	Mixed Metal Studies.....	80
2.4.3.	Determinants of Complexation Strength	84
2.4.4.	Potential Monorhamnolipid Metal-Remediation Applications	91
2.5.	Conclusion.....	92

CHAPTER 3 ENVIRONMENTAL COMPATIBILITY AND METAL CONDITIONAL
STABILITY CONSTANTS OF NOVEL MONORHAMNOLIPID BIOSURFACTANT

DIASTEREOMERS	93
3.1. Abstract	93
3.2. Introduction	94
3.3. Materials and Methods	97
3.3.1. Monorhamnolipids.....	97
3.3.1.1. Biosynthesized Rhamnolipid	97
3.3.1.1.1. Bio-mRL Production.....	97
3.3.1.1.2. Bio-mRL purification.....	98
3.3.1.2. Synthetic Monorhamnolipids	99
3.3.2. Biodegradability Testing	99
3.3.3. Microtox Acute Toxicity Assay	100
3.3.4. Zebrafish Toxicity Assay.....	101
3.3.5. Metal Conditional Stability Constant Assay	102
3.4. Results	103
3.4.1. Biodegradation Assay.....	103
3.4.2. Microtox Acute Toxicity Assay	106
3.4.3. Zebrafish Toxicity Assay.....	107
3.4.4. Metal Conditional Stability Constant Assay	109

3.5. Discussion	112
3.5.1. Biodegradability of Synthetic Monorhamnolipids	112
3.5.2. Toxicity of Synthetic Monorhamnolipids.....	113
3.5.2.1. Microtox	114
3.5.2.2. Zebrafish.....	116
3.5.3. Synthetic Monorhamnolipid and Metal Complexation	117
3.6. Conclusion.....	118
 CHAPTER 4 REMEDIATING METAL CONTAMINATED WASTEWATERS USING ION FLOTATION WITH MONORHAMNOLIPID COLLECTOR.....	 119
4.1. Abstract	119
4.2. Introduction	120
4.3. Materials and Methods	123
4.3.1. Monorhamnolipid Production and Purification.....	123
4.3.2. Monorhamnolipid Purification	124
4.3.3. Metals	125
4.3.4. Flotation Column Design.....	125
4.3.5. Ion Flotation Experiments	127
4.3.5.1. Effect of Collector to Colligend Ratio	130
4.3.5.2. Metal Mass Balance	130
4.3.5.3. La ³⁺ Flotation by Foam Fraction.....	131

4.3.5.4. Metal Competition.....	131
4.3.6. Calculations	134
4.4. Results and Discussion.....	135
4.4.1. Column Design.....	135
4.4.2. Effect Collector to Colligend Ratio.....	139
4.4.3. Mass Balance.....	145
4.4.4. Foam Fraction.....	149
4.4.5. Mixed Metal Ion Flotation.....	151
4.5. Conclusion.....	156
APPENDIX A ELABORATION ON SCHUBERT’S METHOD AND ITS RELEVANCE HEREIN	158
A.1. Introduction	158
A.2. Schubert’s Method	159
A.2.1. Foundation.....	159
A.2.2. Determination of Stability Constant.....	160
A.2.3. Fundamental Assumptions	161
A.3. Examination of Schubert’s Method as Used Herein	165
A.3.1. Chapters 2 and 3: Conformity to Schubert’s Assumption.....	165
A.3.2. Revised Experimental Materials and Methods.....	167
A.3.2.1. Monorhamnolipid Production	167

A.3.2.2.	Monorhamnolipid Purification.....	168
A.3.2.3.	Metals.....	169
A.3.2.4.	Ion Exchange Reactions.....	169
A.3.3.	Revised Experiment's Conformity to Schubert's Assumptions.....	170
A.3.4.	Results and Discussion.....	173
A.4.	Conclusion.....	181
REFERENCES	183

LIST OF FIGURES

Figure 1.1 Metals (White), Metalloids (Grey), and Non-metals (Black) of the Periodic Table.	25
Figure 1.2 Mono- and dirhamnolipids (C10,C10) produced by <i>Pseudomonas aeruginosa</i>	31
Figure 1.3 (A) An energy-minimized molecular mechanics model of monorhamnolipid (C10,C10) showing the oxygen-rich cavity which may serve as an cation binding pocket (B) A model showing how a Pb^{2+} ion might interact with the binding pocket of monorhamnolipid (C10,C10). ²²	33
Figure 1.4 Surfactin produced by <i>Bacillus subtilis</i>	37
Figure 1.5 Siderolipid (U9,U9) produced by <i>Pedobacter</i> sp. MTN11. ¹³	41
Figure 1.6 The dimannosyl-glycerolipid produced by a marine <i>Micrococcus luteus</i> . ⁵⁵ ..	42
Figure 1.7 A sophorolipid of <i>R. bogoriensis</i> (R = H or COCH ₃). ⁵⁹	43
Figure 1.8 The modification scheme of spiculisporic acid to DCMA Na-salts. ⁶⁵	44
Figure 2.1 (A) Effect of monorhamnolipid concentration on the complexation of Pb^{2+} and Sr^{2+} . (B) Determination of the conditional stability constant and stoichiometry of monorhamnolipid:metal complexes by ion-exchange equilibrium method for Pb^{2+} and Sr^{2+} . Each metal was tested independently. Each point represents the mean and standard deviation of 6 replicates. Insert: Structure of monorhamnolipids utilized in this study. The varying chain lengths of the monorhamnolipid congeners are represented by ‘m’ and ‘n’ which vary from 4 to 12.....	74

Figure 2.2 Determination of the conditional stability constant and stoichiometry of monorhamnolipid:UO₂²⁺ complexes by ion-exchange equilibrium method. The circled symbol indicates the monorhamnolipid concentration where the monorhamnolipid:metal ratio is 2:1. Region 1 and 2 indicate the two distinct binding regions of monorhamnolipid with uranyl. Each point represents the mean and standard deviation of 6 replicates..... 79

Figure 2.3 Effect of monorhamnolipid concentration on complexation of Pb²⁺, Cd²⁺, and Ca²⁺ in an equimolar metal mixture (each metal was added at a concentration of 0.167 mM). Each point represents the mean and standard deviation of 6 replicates. 81

Figure 2.4 Effect of monorhamnolipid concentration on complexation of Pb²⁺, Cd²⁺, and Ca²⁺ in a 100:10:1 (Ca²⁺: Cd²⁺: Pb²⁺) metal mixture. Each bar represents the mean and standard deviation of 6 replicates..... 82

Figure 2.5 Log β values for the first row transition elements from Mn(II) to Zn(II) demonstrating the Irving-Williams effect. Error bars represent 95% confidence intervals..... 87

Figure 3.1 Structures of biosynthesized (left) and synthetic (right) monorhamnolipids utilized in this study. The varying chain lengths of bio-mRL are represented by ‘m’ and ‘n’ values which vary from 4 to 12. 96

Figure 3.2 CO₂ production due to mineralization of **(A)** diastereomer *R,R*; *R,S*; *S,S*; and *S,R* and **(B)** diastereomer *R,R*, diastereomer mixture, and bio-mRL. C_{mRL} represents the moles of carbon added as monorhamnolipid. Closed symbols indicate the estimated transition from exponential phase to stationary phase where

mineralization was calculated. Each point represents the mean and standard deviation of 3 replicates.	104
Figure 3.3 Mortality incidences (out of 32) at 120 hpf for monorhamnolipid treatments from 0 to 640 μM . Stars indicate a significant difference in mortality compared to a toxicant free control.	108
Figure 3.4 Detail of light micrograph showing 120 hpf zebrafish in a 96-well plate. Left wells: control (no monorhamnolipid added); Right wells: bio-mRL (640 μM).	108
Figure 4.1 Structure of monorhamnolipids utilized in this study. The varying chain lengths of the monorhamnolipid congeners are represented by ‘m’ and ‘n’ which vary from 4 to 12.....	122
Figure 4.2 Schematic of the initial flotation column design, including the air pump, flow meter, air sparger, sampling port, and foam collection vessel.....	126
Figure 4.3 Final column apparatus used for flotation experiments in this study.	127
Figure 4.4 Effect of collector to colligend ratio (ϕ) on ion flotation was examined for (A) Cs^+ , (B) Cd^{2+} , and (C) La^{3+} individually at ϕ ratios of 2(\bullet), 5(\blacktriangle), and 10(\blacksquare). The open symbol indicates the raffinate sample collected after column foam was allowed to collapse. In part C, \bullet represents the apparent metal concentration in the column and the half-filled circles represent the actual column metal concentration.....	141
Figure 4.5 Typical appearance of a coarse foam (left) at $\phi = 2$ and a fine foam (right) at $\phi = 10$	143
Figure 4.6 Scum concentrating on the solution surface and adsorbing to the column while floating La^{3+} at $\phi = 2$	144

- Figure 4.7** Effect of collector to colligend ratio (ϕ) on ion flotation was examined for (●) Cs⁺, (▲) Cd²⁺, and (■) La³⁺ individually at ϕ ratio 10. The open symbol indicates the raffinate sample collected after column foam was allowed to collapse..... 148
- Figure 4.8** Metal recovery during ion flotation of La³⁺ at $\phi = 10$ measured by foam collected during different time frames of foam production. Bars represent averages and standard deviations of triplicate columns..... 150
- Figure 4.9** Efficacy of ion flotation of mixed metal solutions with (●) Cs⁺, (▲) Cd²⁺, and (■) La³⁺ each 3.3 μ M (total $\phi = 10$). The open symbol indicates the raffinate sample collected after column foam was allowed to collapse. Symbols represent mean and standard deviation values from triplicate columns. 154
- Figure 4.10** Efficacy of ion flotation of mixed metal solutions with (●) Cs⁺, (▲) Cd²⁺, and (■) La³⁺ at 9, 0.9, and 0.009 μ M (total $\phi = 10$), respectively. The open symbol indicates the raffinate sample collected after column foam was allowed to collapse. Symbols represent mean and standard deviation values from triplicate columns. The same data is presents on a (A) semi-log graph and (B) linear graph. 155
- Figure A.1 (A)** Effect of monorhamnolipid concentration on the complexation of Pb²⁺ and La³⁺ under conditions which meet the Schubert method assumptions. Each point represents the mean and standard deviation of 3 replicates. **(B)** Effect of monorhamnolipid concentration on the complexation of Pb²⁺ and La³⁺ under the original conditions of Chapter 2. Each point represents the mean and standard deviation of 6 replicates. 175

Figure A.2 Determination of the conditional stability constant and stoichiometry of monorhamnolipid:metal complexes by ion-exchange equilibrium method for La^{3+} under conditions which meet the Schubert method assumptions. Each point represents the mean and standard deviation of 3 replicates..... 176

LIST OF TABLES

Table 2.1 Conditional stability constants, molar ratios, and statistical analysis for metal complexes with monorhamnolipids	75
Table 2.2 Estimated and observed complexation of metals across complexation experiments	83
Table 2.3 Values used to determine correlations between monorhamnolipid:metal conditional stability constants and physical parameters	88
Table 2.4 Pearson's correlation coefficients for monorhamnolipid:metal conditional stability constants and the physical parameters of metals	90
Table 3.1 Characteristics of the monorhamnolipid treatments	105
Table 3.2 Bacterial acute toxicity EC_{50} values at 5, 15, and 30 minutes for Microtox assay (μM)	106
Table 3.3 Conditional stability constants, stoichiometric ratios, and statistical analysis for Pb^{2+} complexes with monorhamnolipid treatments	110
Table 3.4 Conditional stability constants, stoichiometric ratios, and statistical analysis for Cd^{2+} complexes with monorhamnolipid treatments	111
Table 3.5 Bacterial acute toxicity EC_{50} values at 5, 15, and 30 minutes for Microtox assay (mg l^{-1}).....	115
Table 4.1 Ion flotation parameters for all experiments in this study.....	132
Table 4.2 Results of ion flotation for Cs^+ , Cd^{2+} , and La^{3+} at varying collector to colligend ratios.....	142
Table 4.3 Metal mass balance for ion flotation of Cs^+ , Cd^{2+} , and La^{3+} at a collector to colligend ratio of 10	146

Table 4.4 Results of ion flotation for Cs^+ , Cd^{2+} , and La^{3+} at a collector to colligend ratio of 10	147
Table 4.5 Results of ion flotation for mixed metal solutions of Cs^+ , Cd^{2+} , and La^{3+} at equimolar and order-of-magnitude difference concentrations.....	153
Table A.1 Summary of experimental conditions for the original (chapter 2 & 3) and modified (appendix A) methodologies	177

ABSTRACT

Biosurfactants are compounds that exhibit surface activity (e.g., reduce surface and interfacial tension) and are derived from natural, biological sources. They are considered green substances due to their natural derivation, biodegradability, and relatively low toxicity. Biosurfactants from multiple classes have been shown to interact with metals, and a review of these interactions is provided. Rhamnolipids produced by *Pseudomonas aeruginosa* are attracting attention for metal remediation applications. The purpose of this dissertation is to evaluate rhamnolipids' ability to complex rare earth elements, determine the environmental compatibility of novel rhamnolipid diastereomers, and assess the efficacy of rhamnolipid as a collector in ion flotation.

Previous research shows rhamnolipids selectively bind elements of environmental concern over common soil and water cations, but there had been no examination of transition metals from the f-block of the periodic table. The f-block elements include the rare earth elements, which are a vital component of nearly every modern technology and subject to supply risk. The interaction between monorhamnolipids and the rare earth elements was investigated by determining conditional stability constants using a resin-based ion exchange method. For the 27 metals examined, the conditional stability constants could be divided into three groups, albeit somewhat subjectively: weakly, moderately, and strongly bound. UO_2^{2+} , Eu^{3+} , Nd^{3+} , Tb^{3+} , Dy^{3+} , La^{3+} , Cu^{2+} , Al^{3+} , Pb^{2+} , Y^{3+} , Pr^{3+} , and Lu^{3+} are strongly bound with conditional stability constants ranging from 9.82 to 8.20; Cd^{2+} , In^{3+} , Zn^{2+} , Fe^{3+} , Hg^{2+} , and Ca^{2+} are moderately bound with stability constants ranging from 7.17 to 4.10; and Sr^{2+} , Co^{2+} , Ni^{2+} , UO_2^{2+} , Cs^+ , Ba^{2+} , Mn^{2+} , Mg^{2+} , Rb^+ , and K^+ are weakly bound with stability constants ranging from 3.95 to 0.96. The

uranyl ion is reported twice due to the ion demonstrating two distinct binding regions. The conditional stability constants were demonstrated to be an effective predictor of metal removal order. The metal parameters of enthalpy of hydration and ionic charge to radius ratio were shown to be determinants of complexation strength.

Naturally produced rhamnolipids are a mixture of congeners. Synthetic rhamnolipid synthesis has recently enabled production of four monorhamnolipid diastereomers of a single congener. The biodegradability, acute toxicity (Microtox assay), embryo toxicity (Zebrafish assay), and metal binding capacity of the diastereomers was investigated and compared to natural monorhamnolipid. Biodegradability testing showed all the diastereomers were inherently biodegradable. By the Microtox assay, all of the monorhamnolipids were categorized as slightly toxic by Environmental Protection Agency ecotoxicity categories. Out of 22 parameters tested, the zebrafish toxicity assay showed only diastereomer toxicity for the mortality parameter, except for diastereomer *R,R* which showed no toxic effects. All the monorhamnolipids interacted with both Cd^{2+} and Pb^{2+} .

Ion flotation is one possible technology for metal recovery and remediation of metal contaminated waters. Ion flotation utilizes charged surfactants to collect and concentrate non-surface active ions at the surface of an aerated solution. Rhamnolipid's suitability as a collector in ion flotation was investigated. A flotation column was designed to test monorhamnolipid efficacy as a collector. Monorhamnolipids form foams and effectively remove Cs^+ , Cd^{2+} , and La^{3+} from solution. The efficacy of the flotation process relies on the collector:colligend ratio and valency of the colligend. Flotation of metal solutions showed a removal order of $\text{Cd}^{2+} > \text{La}^{3+} \gg \text{Cs}^+$ when the metals were

present individually and mixed at equimolar concentrations. When mixed at order of magnitude different concentrations, the flotation order was $\text{Cd}^{2+} \gg \text{Cs}^+ \gg \text{La}^{3+}$.

These studies show rhamnolipid has potential to be used for environmentally-compatible metal recovery and metalliferous water remediation, especially for the rare earth elements.

CHAPTER 1

INTRODUCTION

1.1. Abstract

Metal contamination of the environment is a serious and continuing issue. Metals are introduced to the environment via natural and anthropogenic routes. Natural sources of metals include volcanoes, forest fires, sea spray, and biological mobilization, but in the last century, human activity has become the major global input of metals through fossil fuel combustion, mining, metal production, agriculture, and industrial wastes.

Biosurfactants, i.e., microbially produced surfactants, have been shown to strongly complex metals. Accordingly, numerous strategies have been proposed for use of biosurfactants in metal remediation technologies. The purpose of this chapter is to describe known interactions between metals and different classes of biosurfactants; examine the molecular nature of these interactions where possible; and highlight potential biosurfactant based approaches to metal remediation technologies including: soil washing, phytoremediation, co-contaminant removal, micellar-enhanced ultrafiltration, and ion flotation.

1.2. Introduction

Humanity's ability to access and manipulate metals was the keystone to our advancement from the Stone Age to today's technologically advanced society. While this keystone drove technological innovation and societal development, it simultaneously resulted in unprecedented alterations of natural biogeochemical cycles and, arguably for the first time, affected the environment on a global scale. Indeed, paleopollution

archaeology is a field of study devoted to evaluating this human impact by analyzing metal deposits in polar ice caps, bogs, and aquatic sediments to document and understand mining and smelting practices of ancient civilizations, such as the Roman Empire, as long as 2000 years ago.¹ This analysis has shown that our utilization of metal resources is having local and global effects on human and environmental health. Practical, effective, and economical remediation technologies are needed to address large scale metal contamination; microbially produced surfactants (biosurfactants) meet these requirements, and may be the basis for developing green remediation technologies. The goal of this chapter is to provide a brief introduction of metals and environmental metal contamination,* followed by an in depth examination of metal interactions with biosurfactants. The chapter will conclude with a discussion of potential remediation techniques and technologies based on metal-biosurfactant interactions.

1.3. Metals and Metal Contamination

In general, metals are lustrous solids (except Hg), usually ductile and malleable, capable of conducting both electricity and heat and forming alloys.² On the periodic table (Figure 1.1), they can be found to the left of the diagonal line drawn from B to At (excluding Ge, Sb, and H). Elements which display some physical characteristics of metals are defined as metalloids and include B, Si, Ge, As, Sb, and Te.² The two common terms used to describe metals, especially those of concern environmentally, are ‘trace elements’—elements in the Earth’s crust at or below 100 mg kg⁻¹, e.g., Zn, Ni, Cu,Co³—

* For a more extensive review see Nriagu¹⁰ and Callender⁴.

and ‘heavy metals’—elements with densities greater than 5 g cm^{-3} , e.g., Cu, Co, Fe, Mn;⁴ these terms are used synonymously for the purpose of this chapter.

H																	He
Li	Be											B	C	N	O	F	Ne
Na	Mg											Al	Si	P	Se	Cl	Ar
K	Ca	Sc	Ti	V	Cr	Mn	Fe	Co	Ni	Cu	Zn	Ga	Ge	As	Se	Br	Kr
Rb	Sr	Y	Zr	Nb	Mo	Tc	Ru	Rh	Pd	Ag	Cd	In	Sn	Sb	Te	I	Xe
Cs	Ba	La*	Hf	Ta	W	Re	Os	Ir	Pt	Au	Hg	Tl	Pb	Bi	Po	At	Rn
Fr	Ra	Ac**	Rf	Db	Sg	Bh	Hs	Mt	Uun	Uuu							

*	Ce	Pr	Nd	Pm	Sm	Eu	Gd	Tb	Dy	Ho	Er	Tm	Yb	Lu
**	Th	Pa	U	Np	Pu	Am	Cm	Bk	Cf	Es	Fm	Md	No	Lr

Figure 1.1 Metals (White), Metalloids (Grey), and Non-metals (Black) of the Periodic Table.

Trace metals generally do not occur as discrete minerals, but are rather “minor substituents in silicates and aluminosilicates (olivines, pyroxenes, amphiboles, micas, and feldspars); hydrous metal (iron, aluminum, and manganese) oxides; iron sulfides; calcium and magnesium carbonates; calcium, iron, and aluminum phosphates.”³ Anthropogenic activities, as discussed in the next section, have resulted in sites where soils are contaminated with metal concentrations well above background levels. The metals, as a result of processing, are no longer incorporated into mineral components, e.g., silicates. As a result, they have increased bioavailability and the potential to exert toxicity. Such

metal contaminants can become widely dispersed. For example, aerosols generated from metal-processing or from metal-containing waste sites can contain elevated metal concentrations resulting in higher metal distribution via aerosol emission/deposition.⁵ These aerosols can be dispersed over large areas and since deposition is often a gradual process, elevated levels develop over time as metals accumulate.

Metal contamination cannot be mineralized to innocuous end products such as carbon dioxide and water like organic contaminants. Once in a system, metals can only be modified through changes in redox state, and thus speciation. For example, toxic species of selenium (Se^{6+} , Se^{4+} , and Se^0) can be methylated by bacteria to the volatile and less toxic species dimethylselenide $[(\text{CH}_3)_2\text{Se}]$ or dimethyldiselenide $[(\text{CH}_3)_2\text{Se}_2]$.⁶ Thus, in order to treat a metal contamination event, the metal must either be physically removed or chemically modified to reduce toxicity and mobility. Due to the large area of most contamination events, the former solution is often infeasible or economically prohibitive; the latter solution is inevitably temporary as changes in environmental conditions due to natural processes or lack of management may result in the contamination returning to its initial or potentially worse condition. In the above example, microbial methylation of selenium accomplishes both chemical treatment via the generation of less toxic methylated species and physical removal via the generation of a volatile compound which is released to the atmosphere.

1.4. Sources of Metals[†]

Trace element contamination occurs both naturally and as a result of anthropogenic activities. The source and degree of contamination varies for atmospheric, aquatic, and soil environments.

1.4.1. Atmospheric Environments

Natural sources of atmospheric trace elements include volcanic activity, forest fires, wind-borne soil particles, seasalt spray, and biogenic, *i.e.*, biologically mediated volatilization and biological particulates. The level of trace elements emitted from each of these sources varies. Volcanic emanations account for 40-50% of naturally emitted As, Cr, Cu, Ni, Pb, and Sb annually. Atmospheric particulates derived from soils can account for over 50% of Cr, Mn, and V. Seasalt spray and forest fires are relatively minor contributors to natural trace-element emissions with less than 10% of annual emissions for most elements. Biogenic contributions of metals in the atmosphere can account for over 50% of Se, Hg, and Mo annually, and 30-50% of As, Cd, Cu, Mn, Pb, and Zn.⁷

Anthropogenic atmospheric metal sources include fuel combustion (coal and oil), metal production (mining and smelting), secondary metal production (non-ferrous and ferrous), refuse incineration, cement production, and wood combustion. Like naturally occurring sources, the amount and types of metals emitted from each source varies and depends on the source material for each process. For example, coal combustion represents a major contributor of Hg, Mo, Sn, Se, As, Cr, Mn, Sb, and Tl while

[†] Those interested in quantitative information regarding metal contamination should review Niagru⁸ and Pacyna.¹² From our literature review, it does not appear that there is a more recent global inventory of metal emissions than that supplied by these authors.

combustion of oil is a major contributor of V and Ni. Consumption of leaded gasoline, primarily in developing countries, represents the largest contributor to Pb emissions. Non-ferrous metal production produces significant amounts of Pb, As, Cd, Cu, In, and Zn emissions, while ferrous metal production is the primary source of Cr and Mn.^{8,9} In 1990 anthropogenic emissions into the atmosphere exceeded natural emissions by a factor of 28 for Pb, 6 for Cd, and 3 for V and Zn.

1.4.2. Aquatic Environments

Natural contributions of trace elements to aquatic environments are primarily from settling of atmospheric particulates and fluvial movement of weathered material into bodies of water. The trace elements introduced vary by source. The primary anthropogenic sources of water contamination are domestic wastewater effluents (As, Cr, Cu, Mn, and Ni); sewage discharges (As, Mn, and Pb); coal consumption (As, Hg, and Se); ferrous and non-ferrous metal production, *i.e.*, mining and smelting, (Cd, Ni, Pb, Se, Cr, Mo, Sb, and Zn); and urban run-off.^{8, 10} Atmospheric fallout from sources listed in the previous section is also a contributing factor. Anthropogenic metal inputs into aquatic environments are roughly twice those to the atmosphere (with the exception of Pb and Cd).⁴

1.4.3. Soil Environments

The primary natural source of trace metals in soil environments is derived from pedogenesis and metal content depends on the parent material. Like water, soils may also accumulate metals from atmospheric deposition. Deposited aerosols may contain background or elevated levels of metals; elevated levels can be generated from industrial or contaminated site point sources or from non-point sources which might simply be a

highly populated region. Such atmospheric contributions are important especially in soils found in rural and remote areas.¹⁰

Anthropogenic inputs of trace elements to soils come from many different sources including fertilizers, pesticides, biosolids, metal mining and processing, and industrial wastes.^{8, 10, 11} In 1990, antimony, Cu, Pb, and Zn anthropogenic soil emissions exceeded natural weathering flux three-fold, and for Hg, ten-fold.¹⁰ Anthropogenic metal inputs to soil are several times greater than inputs into both air and water.⁴

1.4.4. Summary

It is difficult to separate the atmosphere, hydrosphere, and pedosphere when examining the movement and cycling of trace elements considering their innate connectedness and interdependence. Overall, data reveal that anthropogenic trace element emissions are greater than natural emissions and humanity has now become the driving influence over the biogeochemical cycling of these elements globally.^{4, 7, 8, 10} In fact it has been shown that Pb, V, As, Sn, Zn, Cd, Hg, Sb, Cu, Ag, and Se emissions have caused perturbation of natural geochemical cycles at the global level (i.e., intercontinentally).¹²

1.5. Biosurfactant Complexation of Metals

Biosurfactants are surface active compounds derived from natural, biological sources; they are amphiphilic molecules consisting of two parts: a hydrophilic head group and a hydrophobic tail group. The hydrophilic group can be composed of a mono-, oligo- or polysaccharide, peptide, citric acid with two cadaverines, or a protein. The hydrophobic group is composed of saturated, unsaturated and/or hydroxylated fatty acids or fatty alcohols.^{13, 14} Due to their amphiphilic nature, these molecules accumulate at interfaces. At the interface of immiscible fluids, surfactants increase the solubility and

mobility of the hydrophobic or insoluble organic phase within the aqueous phase.¹⁵

Surfactants are characterized by their physical and chemical properties: ability to reduce surface tension, critical micelle concentration, hydrophile-lipophile balance, aggregate formation, charge, chemical structure, and source.¹⁶

The study of metal interactions with biosurfactants is a relatively new field of study. To the best of our knowledge, the first reports of biosurfactants interacting with metals involved the lipopeptide surfactin and some of the group I and II metals from a medical perspective.^{17, 18} Tan et al.¹⁹ was the first report of the interactions between a glycolipid, rhamnolipid, and a heavy metal, Cd, from an environmental perspective. A Web of Science search in 2012 showed 160 publications examining metal-biosurfactant interactions, an indication of the great interest in this area. The following sections review what is currently known about biosurfactant-metal interactions. It is not possible at this time to directly compare metal-surfactant complexation constants in all cases since different methodologies were used; however, we do so where possible.

1.5.1. Rhamnolipids

Rhamnolipids are glycolipidic biosurfactants first discovered as extracellular products of *Pseudomonas aeruginosa*, but they have recently been found to be produced by other species within and outside of *P. aeruginosa*'s phylum (Figure 1.2).²⁰

Rhamnolipids are characterized by a hydrophilic mono- or di-rhamnose moiety (head group) and a hydrophobic lipid moiety consisting of one or two (in rare cases three) hydrocarbon chains (tail group); nearly 60 congeners of the rhamnolipid molecule have been reported, and congener distribution varies depending on bacterial strain and/or

carbon source. The hydrophilic moiety contains a carboxylic acid group which makes rhamnolipid an anionic surfactant.²⁰

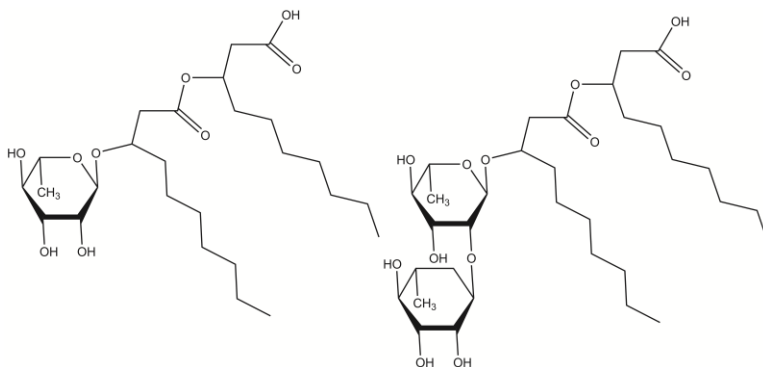


Figure 1.2 Mono- and dirhamnolipids (C10,C10) produced by *Pseudomonas aeruginosa*.

1.5.1.1. Metal Interactions with Rhamnolipid

Tan et al.¹⁹ reported a strong interaction between Cd^{2+} and monorhamnolipid. The monorhamnolipid was capable of complexing Cd^{2+} both rapidly (equilibrium within 15 min) and stably (for at least 27 h). The complexation reaction was independent of pH in a narrow range (6-7), buffer concentration, and temperature. The ability of rhamnolipid to complex Cd^{2+} was higher than reported values for bacterial cell and exopolymer complexation (previously described materials utilized for metal recovery). The stability constant of the monorhamnolipid- Cd^{2+} complex ($\log K = 6.9$) was also stronger than reported stability constants for Cd^{2+} with other organic ligands that have carboxylate functional groups, including acetic acid, oxalic acid, citric acid, and fulvic acid (ranging from $\log K = 1.2$ to 4.5), all commonly found in soil.²¹ This study provided evidence that a biosurfactant could offer a versatile and powerful tool for dealing with heavy metal contamination.

Following this discovery, it was shown that monorhamnolipid forms strong complexes with many elements in addition to Cd with the following conditional stability constant sequence (from strongest, $\log K = 10.30$, to weakest, 0.96): $\text{Al}^{3+} > \text{Cu}^{2+} > \text{Pb}^{2+} > \text{Cd}^{2+} > \text{Zn}^{2+} > \text{Fe}^{3+} > \text{Hg}^{2+} > \text{Ca}^{2+} > \text{Co}^{2+} > \text{Ni}^{2+} > \text{Mn}^{2+} > \text{Mg}^{2+} > \text{K}^+$.²¹ This sequence shows that naturally-occurring, abundant metal cations (Ca^{2+} , Mg^{2+}) have lower stability constants than trace elements of environmental concern (Pb^{2+} , Cd^{2+} , Hg^{2+}). These results, combined with the fact that monorhamnolipid complexed metals more strongly than other organic ligands that might compete in the soil environment, suggested that monorhamnolipid was a good candidate for metal removal applications.

Insight into the nature of the interactions of monorhamnolipid with metals has recently been elucidated at the molecular level using a combination of ^1H NMR, FTIR, and H/D exchange mass spectrometry.²² 600 MHz ^1H NMR studies of monorhamnolipid solutions containing Pb^{2+} provide the surprising result that the carboxylate moiety is only weakly involved in the metal complexation. This assertion is supported by the insignificant chemical shift difference observed for the methylene protons immediately adjacent to the carboxylic acid in the absence and presence of metal cations in solution. For strong carboxylate metal ion complexation, chemical shift changes of >2 ppm are typically observed.²³ In contrast, chemical shift changes for these methylene protons for the monorhamnolipids with Pb^{2+} are only 0.012-0.013 ppm, far smaller than the 2 ppm shift expected for carboxylate binding.

Given the large formation constants measured for these metal complexes as noted above, one must conclude that strong complexes are formed by binding of the metal cation to other parts of the monorhamnolipid molecule. Indeed, the small chemical shift

changes observed are similar to those for metal-crown ether and carbohydrate-metal complexes.²⁴⁻²⁸ This similarity implies that strong binding might occur by the involvement of multiple atoms in the monorhamnolipid, possibly through formation of a binding pocket involving the carboxylate and the rhamnose sugar. Indeed, an energy-minimized molecular mechanics model of the C10:C10 monorhamnolipid shown in Figure 1.3A documents hydrogen-bonding interactions between two of the rhamnose sugar hydroxyls and the carboxylic acid. This leads to formation of an oxygen-rich cavity that might serve as a metal cation binding pocket in which shared coordination of metal cations can occur in much the same way as in a crown ether.

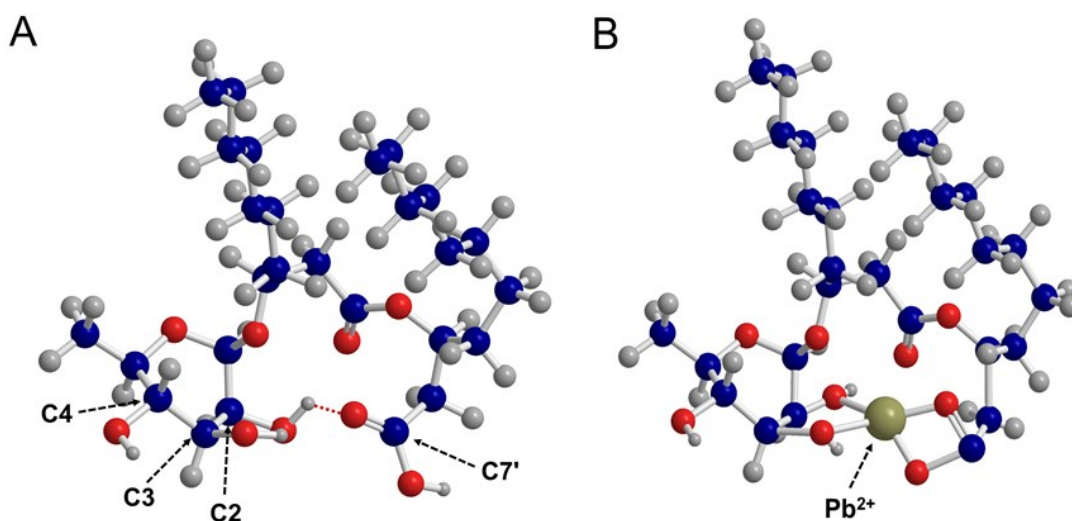


Figure 1.3 (A) An energy-minimized molecular mechanics model of monorhamnolipid (C10,C10) showing the oxygen-rich cavity which may serve as an cation binding pocket (B) A model showing how a Pb^{2+} ion might interact with the binding pocket of monorhamnolipid (C10,C10).²²

FTIR spectroscopy provides further evidence for metal complexation in a binding pocket involving both the carboxylate and the sugar hydroxyls. Fruitful spectral results

can be found in two frequency regions of the spectrum. In one frequency region, the frequency difference between the $\nu_{as}(\text{COO}^-)$ and $\nu_s(\text{COO}^-)$ bands ($\Delta\nu$) of carboxylate species is sensitive to chemical environment and is useful for insight into metal cation binding. The value of $\Delta\nu$ is different for free carboxylates compared to those complexed to metal cations, thus providing an indicator of coordination that is sensitive to coordination type.²⁹⁻³² Due to symmetry differences between the free ionic species and monodentate metal carboxylate complexes, large increases in $\Delta\nu$ are observed. However, bidentate chelation, even weak bidentate coordination in which the interaction strength between the two carboxylate oxygen atoms and the metal cation is unequal, does not alter overall symmetry, and therefore, does not significantly alter the spectral behavior from that of the ionic form, or gives rise to small decreases in $\Delta\nu$. For the free monorhamnolipid, $\Delta\nu$ is on the order of 160 cm^{-1} . For the Pb^{2+} complex, this $\Delta\nu$ decreases slightly to 154 cm^{-1} , consistent with bidentate or weak (i.e. asymmetric) bidentate binding.

Involvement of the sugar hydroxyls in the metal cation binding is also indicated in the FTIR spectra in the second useful spectral region. Sugar vibrational modes are known to undergo frequency shifts upon metal coordination.³³⁻³⁵ For monorhamnolipid- Pb^{2+} complexes, the most significant spectral changes occur for the $[\delta(\text{COH}) + \nu(\text{C-O})]$ band, observed at 1233 cm^{-1} for the monorhamnolipid- Pb^{2+} complex but at 1191 cm^{-1} for the free monorhamnolipid, and the $[\delta_{ip}(\text{OH}) + \nu(\text{C-O})]$ band, observed at 1210 cm^{-1} for the monorhamnolipid- Pb^{2+} complex but at 1170 cm^{-1} for free monorhamnolipid. This shift to higher frequency is indicative of an increase in bond strength with a concomitant decrease in bond length upon Pb^{2+} coordination. Collectively, the data in these two

spectral regions support involvement of both the carboxylate and the sugar in metal cation binding.

Further evidence for the existence of a binding pocket was sought through gas-phase hydrogen-deuterium exchange (HDX) ESI-MS experiments. This approach is predicated on changes in the rate of H/D exchange based on the acidity/basicity of labile hydrogen atoms in addition to the details of the three-dimensional structure of the molecule that dictates accessibility of these labile hydrogen atoms.³⁶⁻³⁸ It has been shown that, although HDX occurs in the gas phase, the exchange rates are directly related to the solution conformation and structure of a molecule. Thus, HDX was performed for the free monorhamnolipid and the monorhamnolipid-Pb²⁺ complex. Fully-protonated free monorhamnolipid contains four exchangeable hydrogen atoms on the hydroxyls on carbons 2, 3, and 4 of the sugar and the oxygen of the carboxylic acid involving carbon 7' in addition to the ionizing proton which gives the ion its positive charge (Figure 1.3A). Exchange of four of these hydrogen atoms can be experimentally monitored (exchange of the carboxylic acid hydrogen is too rapid to be measurable). For the free monorhamnolipid, H/D exchange is complete for all four hydrogen atoms within 1 second. In contrast, for the complexed monorhamnolipid, which contains only three exchangeable hydrogen atoms, one of these hydrogen atoms, of the hydroxyl group on the rhamnose sugar C4 atom, exchanges at the same rate in the complex as in the free monorhamnolipid, suggesting that this hydroxyl is not involved in the metal binding. However, the hydrogen atoms of the hydroxyls on the rhamnose C3 and C2 atoms exchange more slowly by factors of 10 and 100, respectively. These results clearly indicate that these hydroxyl groups are highly inaccessible in the complex relative to the

free monorhamnolipid, supporting the involvement of the sugar in a metal cation binding pocket. A model for what this metal binding in a pocket might look like is shown in Figure 1.3B.

1.5.1.2. Effects of Metals on Rhamnolipid Production

The strong monorhamnolipid-metal stability constants suggested that there may be a physiological reason for the interaction of this biosurfactant with metals. In fact, it has been shown that when *P. aeruginosa* IGB83 (which produces a mixture of mono- and dirhamnolipid) was exposed to sub-toxic levels of Cd^{2+} , expression of one of the rhamnolipid genes, *rhlB*, was enhanced in mid-stationary phase and sustained through late stationary phase.³⁹ The RhlB enzyme is responsible for catalyzing the addition of a second rhamnose sugar onto monorhamnolipid to form dirhamnolipid. As a result of this increased expression, there was an increase in the ratio of dirhamnolipid to monorhamnolipid produced. This is significant because the complexation constant for dirhamnolipid is several orders of magnitude higher than monorhamnolipid. Thus, it appears that the presence of Cd^{2+} during growth may increase production of dirhamnolipid as a detoxification mechanism. This is supported by an earlier study showing that the addition of monorhamnolipid to soils co-contaminated with phenanthrene and Cd^{2+} (levels high enough to exert toxicity) resulted in enhanced degradation of phenanthrene.⁴⁰

Research has also linked rhamnolipid production to iron and magnesium status in the environment. Multiple studies have reported that iron limitation increases rhamnolipid production while sufficient growth levels of iron suppress rhamnolipid

production.⁴¹⁻⁴⁴ In contrast, magnesium limitation reduces rhamnolipid production while sufficient levels of magnesium enhance production.^{42, 45}

1.5.2. Lipopeptides

Lipopeptides are a class of biosurfactants with the general structure of a cyclic seven- to ten- amino acid peptide connected to a fatty acid chain. The best studied member of this class is the anionic surfactant surfactin, produced by *Bacillus subtilis*. Surfactin has a seven amino acid peptide head group and a fatty acid chain of 13 to 16 carbons (Figure 1.4). Lesser studied members of this class include iturin (7 amino acid peptide with a C14 to C17 fatty acid), fengycins (10 amino acid peptide with a C14 to C18 fatty acid), and viscosin (9 amino acid peptide and a C10 fatty acid tail group).^{14, 46}

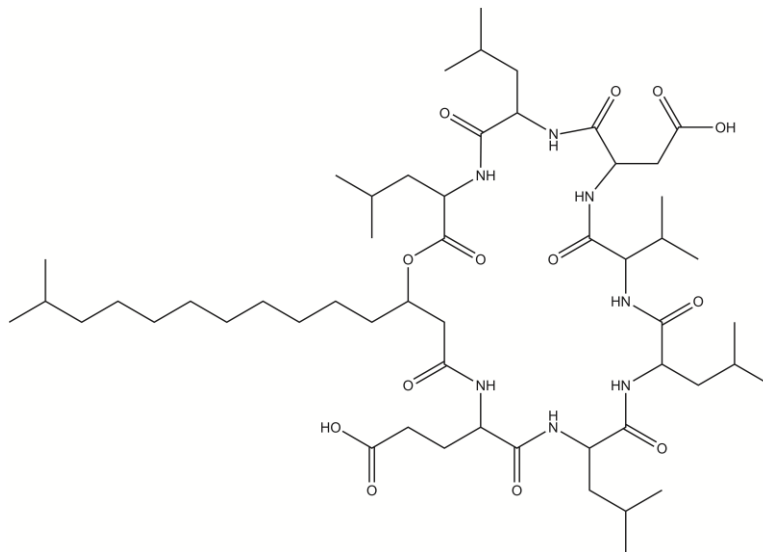


Figure 1.4 Surfactin produced by *Bacillus subtilis*.

1.5.2.1. Metal Complexation by Lipopeptides

Early studies of surfactin interaction with cations focused on understanding their ability to disrupt erythrocyte membranes.¹⁷ These studies showed that surfactin can complex Ca^{2+} and Mg^{2+} with constants of $1.5 \times 10^5 \text{ M}^{-1}$ and $1.9 \times 10^4 \text{ M}^{-1}$, respectively.¹⁸

More recently, surfactin has been shown to interact strongly with Fe^{3+} , weakly with Cu^{2+} , and not at all with Nd^{3+} —biphasic liquid-liquid extraction percentages were >95%, $\approx 12\%$, and <5% respectively.⁴⁷ This binding is associated with the negative charge generated by two carboxylic groups from the aspartate and glutamate residues of the peptide structure.¹⁷ Spatial arrangement studies of surfactin suggest that the peptide portion of the molecule forms a “claw-like” structure with the aspartate and glutamate residues on opposite tips of the claw, creating a position for metals to bind.⁴⁸ As a result of the two charged groups, there are different association behaviors of surfactin with mono- and divalent cations. Divalent cations exhibit a single associated binding constant value which is higher than for monovalent cations. Monovalent cations have a choice of two binding sites on surfactin each of which has different affinity for the cation. For example, for Rb^+ there is a site with high affinity (association constant of 71 M^{-1}) and a site with low affinity (association constant of 11 M^{-1}). Accordingly, surfactin shows a 1:1 molar ratio with Ca^{2+} and a 2:1 molar ratio with Rb^+ .⁴⁹

Other lipopeptides have also been shown to bind metals. Lichenysin is a lipopeptide produced by *Bacillus licheniformis* which structurally resembles surfactin. It has seven amino acids attached to a C13-C15 fatty acid tail. It differs from surfactin through the substitution of a glutamyl residue for glutamic acid in the number one peptide position. This reduces the molecular charge from -2 in surfactin to -1 in lichenysin. Lichenysin has been reported to bind Ca^{2+} and Mg^{2+} 4-fold and 10-fold, respectively, more strongly than surfactin.⁵⁰ The affinity for Ca^{2+} over Mg^{2+} is only 2-fold higher for lichenysin in comparison to 10-fold for surfactin. This may result from the replacement of the more specific “claw” binding structure of surfactin with a less

discriminate binding structure in lichenysin. Lichenysin also forms a 2:1 molar ratio with Ca^{+2} instead of the 1:1 reported for surfactin.⁵⁰

Viscosin is a lipopeptide produced by a variety of *Pseudomonas* sp. and is characterized by a fatty acid tail connected to two amino acids and a seven member cyclic peptide. Viscosin has a conditional stability constant of 5.87 with Cd^{2+} .⁴⁶

1.5.2.2. Effects of Metals on Lipopeptides

It has been reported that solution cations (Mg^{2+} , Mn^{2+} , Ca^{2+} , Ba^{2+} , Li^+ , Na^+ , K^+ , and Rb^+) can reduce the critical micelle concentration of surfactin from 4- to 12-fold depending on the cation and concentration.¹⁷ The shape of the aggregates is affected by both pH and cation concentration and type (mono- vs. divalent).^{17, 49} Higher pH and lower cation concentration both result in smaller and rounder aggregates while lower pH and higher cation concentration result in aggregates that are rod-like to lamellar. These findings can be explained by the neutralization of charge in the surfactin head group by added cations. When the charge in the peptide ring is neutralized by a cation, the effective size of the head-group ring is reduced, allowing molecules to interact more closely. This results in a reduction of curvature in the aggregate which favors larger rod-like and lamellar structures. A divalent cation can completely neutralize the charge of the surfactin head group while a monovalent cation only partially neutralizes the charge and so the effect is not as great (the same concept applies to any charged surfactant molecule).

Surfactin effectively attaches to and integrates with lipid membranes. Its ability to do so is highly enhanced when combined with metals. Surfactin has been shown to produce ion-conducting pores in artificial lipid membranes when complexed with a metal

cation. Further, surfactin has been shown to carry metal ions across a hydrocarbon barrier phase from one aqueous phase to another.^{18, 51} This ability can be attributed to its interaction with the metal cations; surfactin will not exhibit ionopore formation if not allowed to interact with cations first.¹⁸ Recent data suggests that the complexation of surfactin with cations, especially divalent cations, reduces the hydrophilicity of the head group by neutralizing the charged residues in the peptide ring, allowing the surfactin-metal complex to integrate into hydrophobic structures.⁴⁹ This ionophore activity has garnered a great deal of interest in the medical field due to its ability to cause hemolysis of erythrocytes, but has yet to be extensively explored for potential remediation applications.

Similar to rhamnolipids, metals have been found to influence surfactin production. Manganese added as $MnSO_4$ has been shown to increase the production of surfactin roughly 10-fold. In the same study, additions of Fe resulted in a reduction of surfactin produced on a per biomass basis.⁵² A more recent study of surfactin production by a thermophilic *B. subtilis* showed varying responses to a range of individual metal concentrations with the best productivity resulting from a mixture of added metals.⁵³ It is not yet clear whether the metal effects reported are a result of the metals alone or whether the presence/absence of other medium components also influenced surfactin production.

1.5.3. Other Biosurfactants

There are a variety of other biosurfactants produced but few are well characterized in terms of their interactions with metals. The following section provides some examples of studies that have used these biosurfactants to complex metals in

various applications even though, in some cases, the strength of the interaction is not characterized.

1.5.3.1. Siderolipids

Siderolipids (formerly flavolipids) are a recently described class of biosurfactants produced by *Pedobacter* sp. MTN11 (formerly *Flavobacterium* sp. MTN11) (Figure 1.5).^{13, 54} The polar moiety of this anionic biosurfactant is composed of a citric acid and two cadaverine molecules, and the non-polar moiety is composed of two branched chain acyl groups with 6-10 carbons each. It is reported to complex Cd with a conditional stability constant of $\log K = 3.6$,¹³ which is weaker than the stability constant reported for rhamnolipid (6.9). The siderolipid-Cd complexation constant is comparable to those reported for natural organic acids: acetic acid, 1.2 to 3.2; oxalic acid, 4.1; and citric acid, 4.5. The structure of the siderolipid headgroup is similar to the siderophore aerobactin which suggests that siderolipids may be iron chelators.¹³

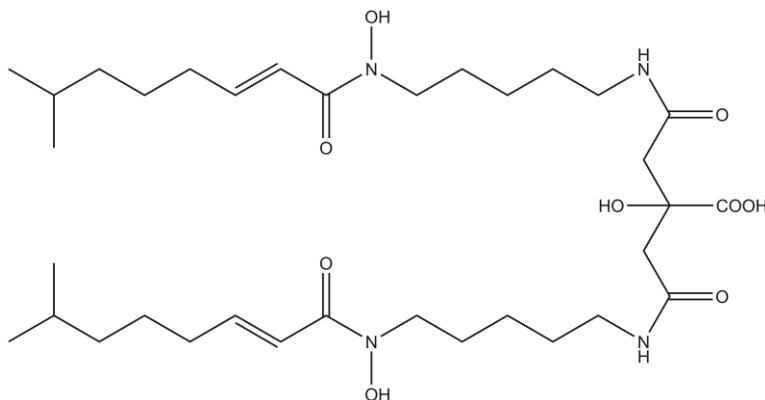


Figure 1.5 Siderolipid (U9,U9) produced by *Pedobacter* sp. MTN11.¹³

1.5.3.2. Glycoglycerolipids

Glycoglycerolipids are produced by *Microbacterium* spp., *Micrococcus luteus*, and *Bacillus pumilus*. Figure 1.6 depicts a dimannosyl-glycerolipid produced by a strain

of *M. luteus* isolated from the North Sea. These biosurfactants are an abundant constituent of plant and bacterial membranes. They are composed of carbohydrate unit(s), a glycerol moiety, and a variety of short or long chained saturated or unsaturated fatty acids.⁵⁵ A recent study showed that the partially purified glyco-glycerolipids from four strains of *Microbacterium* sp. could be used to extract Zn^{2+} and Cd^{2+} from an industrial residue. The study reports varying efficiencies based on strain and carbon source.⁵⁶

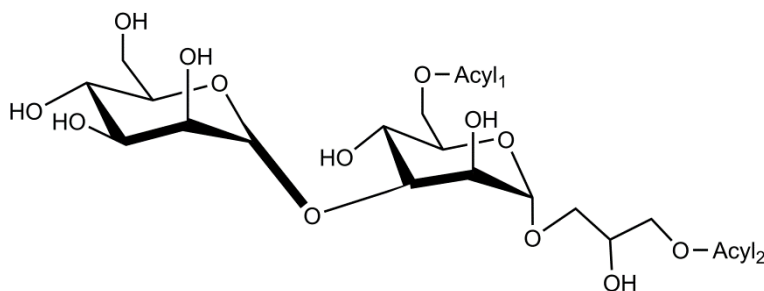


Figure 1.6 The dimannosyl-glycerolipid produced by a marine *Micrococcus luteus*.⁵⁵

1.5.3.3. Saponins

Saponins are plant- and microorganism-derived biosurfactants. They are non-ionic, acidic, high molecular weight glycosides characterized by a hydrophilic sugar moiety and hydrophobic triptene or steroid aglycone group.^{57, 58} Recent studies report their use as a soil washing agent of metal contaminated materials.

1.5.3.4. Sophorolipids

Sophorolipids are produced by various species of yeast including *Candida bombicola*, *Candida apicola*, *Wicherhamiella domercqiae*, *Pichia anomala*, and *Rhodotorula bogoriensis*. The sophorolipid of *R. bogoriensis* is illustrated in Figure 1.7. These molecules are characterized by a hydrophilic moiety composed of a disaccharide sophorose, a diglucose with a β -1,2 bond. The hydrophobic moiety is a terminal or

subterminal hydroxylated fatty acid, β -glycosidically linked to the sophorose. Like rhamnolipids, sophorolipids are produced as a variety of congeners.⁵⁹ A recent report shows that sophorolipids could be used to help synthesize silver nanoparticles.⁶⁰

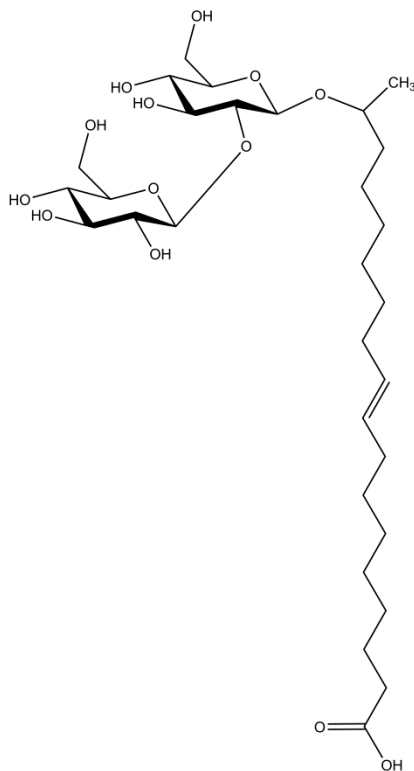


Figure 1.7 A sophorolipid of *R. bogoriensis* (R = H or COCH₃).⁵⁹

1.5.3.5. Spiculisporic acids

Spiculisporic acids (S-acid) are microbially produced surfactants with two carboxylic moieties and a lactone ring composing the hydrophilic head group; the hydrophobic portion is a decyl chain. The molecular structure can be modified through neutralization and saponification with NaOH to a tricarboxylic acid 2-(2-carboxyethyl)-3-decyl maleic anhydride (DCMA). This acid can further form mono-, di-, and tri-Na DCMA salts (DCMA-xNa where x is 1, 2, or 3 respectively) (Figure 1.8). The surfactant characteristics vary from form to form with the fully neutralized and saponified forms

exhibiting the highest hydrophilicity and lowest surface activity.⁶¹ DCMA-xNa salts have been shown to disperse titanium dioxide and ferric oxide and sequester Ca^{2+} . The ability to sequester Ca^{2+} is strongest for the DCMA-3Na with decreasing sequestration from DCMA-3Na to DCMA-1Na.⁶² Later work showed that DCMA-3Na is capable of complexing various cations including Ca^{2+} , Cd^{2+} , Co^{2+} , Cu^{2+} , Mg^{2+} , Ni^{2+} , and Zn^{2+} .^{63, 64} A binding affinity sequence of $\text{Cd}^{+2} > \text{Cu}^{+2} \approx \text{Zn}^{+2} > \text{Ni}^{+2}$ has been reported.⁶⁴

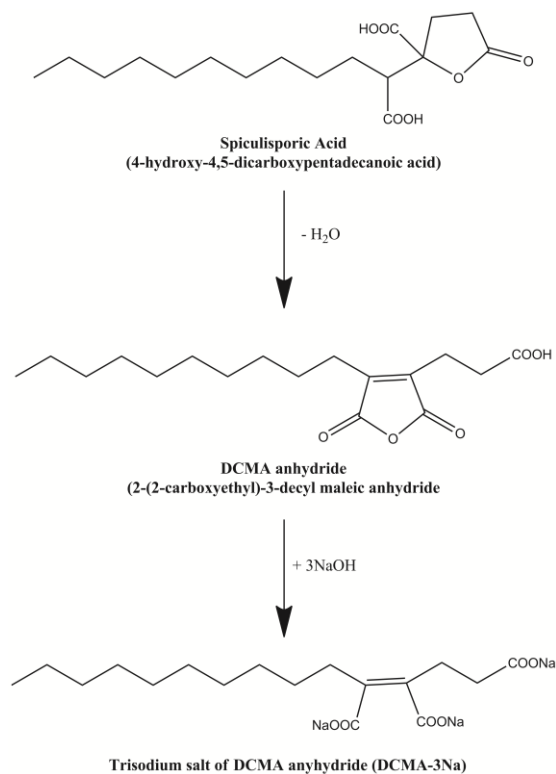


Figure 1.8 The modification scheme of spiculisporic acid to DCMA Na-salts.⁶⁵

1.6. Remediation Applications

Biosurfactants are considered “green” materials with several advantages for use in bioremediation applications. They are naturally produced, i.e., not fossil fuel derived, with potential to be produced *in situ*. Apart from the bioemulsifiers, they are of small molecular size with molecular weights generally less than 1500.⁶⁶ Biosurfactants

accumulate at interfaces which is beneficial for desorbing metal and organic contaminants, and they increase the apparent solubility of organic compounds which is beneficial for physical and biodegradative removal. Biosurfactants are biodegradable and generally perceived as less toxic than synthetic analogues.^{16, 40} A small number of studies have examined the biodegradation of rhamnolipid in soil. One showed that it took 8 weeks for rhamnolipid to biodegrade in a Brazito sandy loam.⁴⁰ A more recent study compared the biodegradation of EDTA (ethylenediamine tetraacetic acid: a common and strong metal chelant), citric acid, and rhamnolipid in three soils.⁶⁷ Results showed that in the soils tested the biodegradability of these materials increased in the order EDTA < rhamnolipid < citric acid. Rhamnolipid degradation was not complete in any of the soils in 20 days, the length of the experiment. Both studies show that rhamnolipids are biodegradable but the process is not rapid. This suggests that there would be an effective “window” of remediation time before their removal through biodegradation.

For the reasons provided above, biosurfactants have potential as remediation materials. In fact, much of the technology required to apply biosurfactants for remediation applications has already been developed for use with synthetic surfactants, meaning remediation procedures must only be adapted for use with biosurfactants. Their use has been constrained by lack of availability which is primarily due to high costs of production. There is a need for research and avenues for commercialization to realize the potential for biosurfactants in remediation. The following sections will discuss research that has demonstrated the application of biosurfactants to various remediation technologies.

1.6.1. Solid Media

1.6.1.1. Soil Washing

Heavy metal remediation of soils, sediment, mine tailings, and industrial wastes has primarily focused on two strategies. The first is isolation and stabilization. Common approaches include: excavation and landfilling; capping with impermeable materials; covering with soil; mixing or injecting inorganic or organic amendments (e.g., liming agents, organic media; aluminosilicates, phosphates, metal oxides, etc.); and/or developing plant covers (phytostabilization). The goal of this strategy is to prevent the spread of contamination. The major disadvantage is that the metal contamination is not removed. Thus, extended management, monitoring, and maintenance is required, and there is generally a long-term risk of spreading contamination in the event of design failure.⁶⁸

The second strategy is physical and chemical treatment applied to remove metal contamination. This technique generally involves washing soils with strong acids or metal chelating compounds in order to mobilize metals, followed by a step that captures and re-concentrates the metals from solution. The use of strong acids has drawbacks because it leads to the disruption of the physical, chemical, and biological structure of soils, thus reducing possibilities for subsequent use as a soil medium.⁶⁹⁻⁷¹ Metal chelators can be effective and are less destructive. Many synthetic chelators, including some surfactants, have been studied; the most common of which is EDTA.⁶⁹⁻⁷¹ The need for an additive to facilitate metal removal has led to the notion of examining whether there are green additives, with reduced toxicity, that can be used in place of traditional chelators/surfactants.

There are several approaches to the mobilization step of soil washing. *In situ* soil washing is a viable technique for applications where the contaminated zone is underlain by a non-permeable layer. This allows the washing solution to be leached through the contaminated zone and then pumped out and treated above ground to remove metals.⁶⁸ *Ex situ* treatment basically involves removal and treatment of the contaminated soil. This can be done in a batch system, such as a soil slurry reactor, or can be done using heap or column leaching where the treatment solution is either gravimetrically percolated or pumped through the contaminated soil and then collected and treated. Finally, soils can be treated electrokinetically (generally *ex situ*) to remove metals by applying a direct current electrical field through a saturated contamination soil. This causes the pore fluid to migrate by electro-osmosis and cationic metal ions to concentrate at the cathode.⁶⁸ For each of these approaches, *in situ* or *ex situ* soil washing or electrokinetic extraction, biosurfactants can be added to increase their efficacy in what is known as surfactant-enhanced soil washing.⁷⁰

The mechanism of biosurfactant-enhanced metal removal from solid surfaces is an interesting area of research. The sorption of metals onto mineral surfaces is controlled by many factors including ion exchange and association with Fe and Mn oxides, carbonates, and organic matter (precipitation/dissolution reactions). Two hypotheses have been offered to explain the mechanism behind surfactant-enhanced soil washing. First, direct complexation between the biosurfactant and solution phase metal effectively removes metal from solution and increases dissolution and desorption according to Le Chateliers principle.⁶⁶ The second is that biosurfactants can accumulate at the solid/liquid interface and interact with sorbed metals. Mulligan et al.⁷² designed a series of

experiments to test these hypotheses using surfactin and a hydrocarbon-contaminated soil that was spiked with metals including Cu, Cd, Pb, and Zn. They conclude that interaction of surfactant with the soil allows direct interaction between the surfactant and the sorbed metal. The surfactant also reduces the interfacial tension at the liquid-solid interface thereby making it easier to release the sorbed metal.^{72, 73}

1.6.1.1.1. Soil Washing: Efficacy of Biosurfactant on Artificial Contamination

Biosurfactants have been shown to be effective additives in soil washing technologies. Rhamnolipid, perhaps the best studied biosurfactant for surfactant-enhanced soil washing, was found to desorb metals from a sandy loam both when the metals were tested individually and in a mixture. An 80 mM monorhamnolipid (4%) solution removed 40% of Zn⁺² and Pb⁺² and nearly 60% of Cd⁺².⁷⁴ A second study showed 99% removal of Pb, Ni, Cu, and Cd after flushing with a 1% glycolipid solution for 30 d.⁷⁵ Yet a third study showed that 0.1% rhamnolipid removed 92% of Cd and 88% of Pb during a 36-hour column leaching study, with no impact on culturable counts of bacteria or fungi.⁷⁶ Using a different approach, Wang and Mulligan⁷⁷ examined whether a rhamnolipid foam could be used as a soil washing agent. Interestingly, a 0.5% rhamnolipid foam was 11% more effective at removing Cd and 17% more effective at removing Ni from a sandy soil than a 0.5% rhamnolipid solution. The authors hypothesized this was due to an increase in the homogeneity of the washing solution flow and surface contact when it was applied as a foam.

Saponin has also been studied as a soil washing agent. Saponin removed nearly 100% of Cd, Zn, and Cu from three soils with the removal efficiency of the soils being sandy loam > loam > silty clay. These batch studies showed that removal efficiency

improved with multiple washings and that triplicate washes yielded optimal efficiency.⁵⁸ Saponin was also shown to have high removal efficiencies for Cd (90-100%) and Zn (85-98%) from an Andosol, Cambisol, and Regosol when applied at a 3% concentration.⁷⁸ Both Cu and Pb were also removed but with lower efficiencies (30-60%).

Finally, surfactin has been demonstrated as a soil washing agent.⁷² Results of this study showed that metal removal by 0.25% surfactin solution was 25% for Cu and 6% for Zn. When the surfactin concentration in the washing solution was increased to 1%, the amount of metal removed decreased. Removal efficiency then increased again as surfactin was increased from 1 to 4%. As shown previously for rhamnolipids, multiple washes with surfactin improved metal recovery. For example, a 0.25% surfactin solution was used in 5 successive washes, removing 70% of Cu, 25% of Zn, and 15% of Cd.

1.6.1.1.2. Soil Washing: Efficacy of Biosurfactants on Aged Contamination

While the above results sound promising, each of the above studies described used an artificially contaminated soil. Soil washing is not nearly as efficient in aged contaminated soils. When two historically contaminated soils were studied, one from a mining site and one from an abandoned army depot, rhamnolipid only removed a small fraction of the metals. Focusing on Pb which was present in both soils, after 10 washings under batch conditions, rhamnolipid removed 14.2 and 15.3% of total Pb from the soils, a relatively small amount; rhamnolipid Pb removal was at least an order of magnitude greater than KNO_3 and $\text{Ca}(\text{NO}_3)_2$ electrolyte solutions, however. The low removal rates of rhamnolipid were attributed to the association of the Pb with stable carbonate and oxide fractions in these soils. Rhamnolipid was effective in removing the soluble and exchangeable fraction of Pb from the soils but was much less effective at removing Pb

bound to carbonates and amorphous iron oxides. This significantly reduced removal efficiency suggests that the longer a contaminant is in the soil, the more recalcitrant and associated with recalcitrant fractions of the soil that contaminant becomes.⁶⁹

A historically contaminated acidic soil from the Palmerton Zinc Pile Superfund site was more successfully treated to remove Zn, Cu, Pb, and Cd (39, 56, 68, and 43%, respectively) with rhamnolipid. The soil was reported to be less toxic to two species of earthworm after the washing.⁷⁹ Taken together, these studies suggest that the contamination age of a soil along with its physical and chemical characteristics must be carefully considered to identify suitable extractants and extraction conditions. Further examination of historically contaminated soils is warranted, not only for biosurfactant application, but for the technology as a whole.

1.6.1.1.2.1.Sediments

Sediments have different characteristic properties than soil, e.g., higher clay and organic matter content, and they too have been studied for surfactant-enhanced soil washing process efficacy. Mulligan et al.⁷³ compared the ability of surfactin, rhamnolipid, and sophorolipid for removal of metals from a zinc and copper contaminated sediment. Results showed that rhamnolipid was most effective; a single washing of a 0.5% rhamnolipid solution removed 65% Cu and 18% Zn. A 4% sophorolipid solution removed 25% of Cu and 60% of Zn while a 0.25% surfactin solution removed only 15% of Cu and 6% of Zn.⁷³ In a second study which examined metal removal in continuous flow columns, 5% rhamnolipid was able to remove 37% of Cu, 7.5% of Zn, and 33% of Ni. Interestingly, the addition of 1% NaOH to 0.5% rhamnolipid increased the removal efficiency of Cu to levels near the 5% (10-fold higher)

rhamnolipid treatment.⁸⁰ This increase in Cu recovery was due to the solubilization of organic matter by NaOH since Cu tends to partition into the organic fraction of soils and sediments. These results again suggest that the physicochemical characteristics of the system (sediment, soil, or water) must be carefully considered to allow extraction conditions to be optimized.

1.6.1.1.2.2.Mine Tailings

Mine tailings are the leftover waste material generated from mining processes. The materials, especially in older legacy mine tailings sites, can be highly contaminated with metals such as Pb and As. Surfactant-enhanced soil washing has recently been examined for use in remediation of mine tailings. Aniszewski et al.⁵⁶ examined the removal of Zn and Cd from a waste generated from mining zinc. They isolated four *Microbacterium* spp. with bioemulsifying activity and tested both cell free supernatants and partially purified preparations for metal recovery. Cadmium removal ranged from 17 to 41% and Zn removal ranged from 14 to 68% depending on the *Microbacterium* strain and the growth substrate used to produce the bioemulsifier.

Wang and Mulligan⁸¹ used rhamnolipid to remove As from tailings, finding that the mobility of As increased with increasing rhamnolipid concentration and increasing pH. Since As is generally present as an anion, the authors discussed the potential mechanism of removal. The addition of rhamnolipid was found to lower the zeta potential of the tailings, suggesting that rhamnolipid was adsorbed to the tailings particle surfaces. It was hypothesized that this enhanced the mobilization of As anions due to increased charge density (negative) and repulsive electrostatic interactions.⁸¹ In a second study, 70 pore volumes of a 0.1% rhamnolipid solution was applied to a column containing

oxidized mine tailings with elevated levels of As, Cu, Pb, and Zn.⁸² Overall the removal of these metals was low: 7% (As), 7% (Cu), 18% (Pb), and 5% (Zn). The mobilization of all these metals was found to be positively correlated with the removal of Fe.

1.6.1.1.2.3. Industrial Waste

Industrial wastes originating from sectors in aerospace to printed circuit boards to wastewater treatment can contain metal contaminants that range from low to very high in concentration. Several groups have examined the use of biosurfactants to recover metals from these waste streams. Gao et al.⁸³ compared the removal of Pb, Ni, and Cr from an industrial water treatment plant sludge by saponin and sophorolipid. Both surfactants could aid in metal recovery with the amount of metal recovered related to increasing biosurfactant concentration and decreasing pH. Saponin, which removed 73.2, 64.2, and 56.1% of Pb, Ni, and Cr, respectively, performed better than sophorolipid.⁸³ In a second study, saponin was found to remove 20 to 45% of Cr, 50 to 60% of Cu, and up to 100% of Pb from a municipal solid waste incinerator fly ash.⁵⁷

1.6.1.1.3. Summary

The variability in metal removal efficiency of the above studies is a testament to the challenges of using biosurfactants as soil washing agents. Comparing the studies is difficult because each utilized different soils and experimental treatments. Much of the variability is due to the nature of soils as dynamic and heterogeneous systems. Every soil characteristic that makes a soil unique, e.g., soil pH, type, mineralogy, cation exchange capacity, organic matter content, porosity, contamination extent, contaminant age, etc., is a contributing factor that must be considered when developing a soil washing technique. For example, the mineralogy of the soil influences biosurfactant behavior: Ochoa-Loza et

al.⁸⁴ showed that monorhamnolipid sorption at low concentration follows the order hematite > kaolinite > MnO₂ ≈ illite ≈ Ca-montmorillonite > gibbsite (Al(OH)₃) > humic acid coated silica, while monorhamnolipid at high concentration sorbs in the order illite >> humic acid-coated silica > Ca-montmorillonite > hematite > MnO₂ > gibbsite ≈ kaolinite. Adsorption is undesirable because it reduces the amount of solution phase surfactant available and further, can contribute to soil pore plugging.

As a second example, metal removal is optimal at a different pH for different surfactants. Saponin was most effective removing metals from kaolin at a pH of 6.5.⁸⁵ Rhamnolipid was most effective at a pH of 6.8 when tested individually on K-feldspar, sepiolite, quartz, and kaolin,⁸⁶⁻⁸⁸ but was more effective at a higher pH (10-11) when tested in soils,⁷⁷ sediments,⁷³ and mine tailings.⁸¹ Surfactin was more effective at a pH of 10 than a pH of 8.⁷³

As yet a third example, sorption behavior can also change as a function of surfactant type or congener mixture. For example, monorhamnolipid sorbed more strongly than a mix of the mono- and dirhamnolipid.⁸⁴ Sorption has also been shown to be impacted by surfactant concentration, metal contamination (surfactants tend to sorb less when metal contamination is present), and ionic strength.^{86, 88, 89} Clearly, surfactant-enhanced soil washing has the potential to be an effective remediation technique, but careful planning and design is required for every application if the process is to be successful.

1.6.1.2. Phytoremediation

Phytoremediation technologies use plants to clean contaminated sites. Phytoextraction is a type of phytoremediation in which plants are used to concentrate and

remove contaminants from soil.⁶⁸ Effective phytoextraction requires soil metals to be mobilized, absorbed by plant roots, translocated to shoot tissues, and stored, whereafter the biomass can be harvested and disposed of properly. A desirable plant for phytoremediation needs to be tolerant of elevated metal content, effective at accumulating metals in biomass, and productive with high biomass yields. Most of the plants already recognized as good candidates for phytoextraction are crop plants including sunflower (*Heliantus annuus*), corn (*Zea mays*), pea (*Pisum sativum*), and mustard (*Brassica juncea*).⁹⁰ Chelates can be utilized to augment phytoextraction of contaminated soils. Chelate-assisted phytoextraction is based on the same principles as soil washing except that plants are used to remove the metals from the soil rather than a soil-water separation step. Thus, biosurfactants have the potential for use in chelate-assisted phytoextraction as long as they are compatible with plant growth, i.e., not toxic. Indeed, many synthetic chelants, especially EDTA, have been shown to effectively increase concentrations of metals in plant tissues.⁶⁸

Rhamnolipid has been examined in multiple studies to test its potential for chelate-assisted phytoextraction. Jordan et al.⁹⁰ tested rhamnolipid with *Z. mays* and *Atriplex numilaria* (saltbrush) and the heavy metals Pb, Cu, and Zn. Rhamnolipid showed no effect on metal accumulation, yet was found in the plant tissues. It was hypothesized that the rhamnolipid micelles (where the metal is bound) are too big and thus excluded from the root, while rhamnolipid monomers are capable of entering the plant tissues. A second study examined the effect of rhamnolipid in a hydroponic system. This study found rhamnolipid did not enhance Cu uptake into *B. juncea* or *Lolium perenne* (ryegrass),⁹¹ even though rhamnolipid complexes with Cu strongly ($\log K = 9.27$).²¹

Exclusion of the soil-Cu sorption factor by this experiment supports the hypothesis that metal-micelle complexes are too big for root absorption. In a third study, rhamnolipid not only failed to enhance uptake of Zn and Cd, but it also showed toxic effects on *Z. mays* and *H. annuus* at concentrations as low as 0.2 mmol/kg of soil/week.⁹² Toxicity is also reported for *B. juncea* and *L. perenne* treated with 200 mg/L of rhamnolipid.⁹¹

Failure of rhamnolipid to act as an effective chelate-assisted phytoextraction amendment may be because experimental parameters were outside of the optimal conditions reported for surfactant-enhanced soil washing studies. For example, the pH range for the chelate-assisted phytoextraction studies was 6-7 while optimal conditions for rhamnolipid were shown to be near the pH of 10 for soils.^{77, 81, 91, 92} Further, the rhamnolipid concentration used in chelate-assisted phytoextraction studies was lower (4-5 mM) than those utilized for surfactant-enhanced soil washing studies (10-80 mM).^{74, 75, 77, 90-92}

Two studies did show a benefit associated with use of rhamnolipid in chelate-assisted phytoextraction. In the first, a moderate enhancement of Cu and Cd uptake by hydroponically grown *L. perenne* was achieved using 0.15 mM rhamnolipid.⁹³ Interestingly, uptake enhancement was significantly increased when rhamnolipid was combined with additional amendments including EDDS (an aminopolycarboxylic acid) or EDDS and citric acid. These combined treatments showed increased shoot Cu, Cd, and Pb concentrations (22- and 38-fold for Cu, 8- and 9-fold for Cd, and 2- and 3-fold for Pb, respectively). These treatments were also toxic to plant growth. The toxicity was attributed to both rhamnolipid, which showed some toxicity when used alone in metal-free controls, and the increased metal concentrations in the plant tissue. The rhamnolipid-

EDDS-citric acid treatment was highly toxic to the plants so was applied only a few days prior to harvesting of the plants. Rhamnolipid-histidine and rhamnolipid-citric acid showed enhanced uptake of Cd, Cu, and Pb, but at lower levels and with less toxicity.⁹³

In the second study, which examined the hydroponic growth of *Brassica napus* (canola) in Zn-limiting conditions, rhamnolipid was found to increase Zn absorption through non-metabolically mediated pathways. Rhamnolipid-Zn complexes were found in the roots when examined by synchrotron XRF and XAS, and root K⁺ efflux was increased, suggesting phytotoxic effects of the treatment.⁹⁴ These studies suggest that physiological state of the plant may be a controlling factor in metal/metal-chelate uptake and accumulation. Indeed, studies have shown that root damage may be helpful for uptake of metal and/or metal-chelate complexes.⁶⁸ More research is required to better understand the mechanisms behind chelate-assisted phytoextraction and its optimization. Studies of additional biosurfactants and synergistic amendments are warranted as well.

1.6.1.3. Remediation of Co-Contaminated Systems

Forty percent of the sites on the Environmental Protection Agency National Priority List are co-contaminated with heavy metals and organic compounds. Heavy metal toxicity in such sites can inhibit the biodegradation of organic contaminants by both aerobic and anaerobic consortia.^{95,96} Toxicity of metals to microorganisms occurs by a variety of mechanisms: competitive replacement of physiologically essential cations rendering enzymes nonfunctional, metal oxyanions may be substituted for similar essential oxyanions (*e.g.*, arsenate for phosphate), and oxidative stress.⁹⁶ Effective techniques for reducing metal toxicity rely either on the use of metal-tolerant bacteria or

on the addition of materials to reduce metal bioavailability, e.g., clays, calcium carbonate, phosphates, or chelating substances.⁹⁶

Biosurfactants can play a dual role in remediation of co-contaminated sites. They can complex metals thereby reducing their bioavailability and toxicity, but they can also increase the aqueous solubility of organic compounds resulting in enhanced biodegradation rates.⁹⁷ This was demonstrated in a study examining the effect of rhamnolipid on the degradation of naphthalene by a *Burkholderia* sp. in the presence of Cd. Results showed that a 1:1 molar ratio of rhamnolipid:Cd reduced cadmium toxicity, while increasing the molar ratio to 10:1 eliminated cadmium toxicity completely.⁹⁵ In a second study rhamnolipid was shown to enhance the degradation of phenanthrene by a soil consortium inhibited by the addition of Cd. In this study, phenanthrene mineralization reached the same levels as metal-free controls when several pulses of rhamnolipid were added. The pulsed addition technique was used to replenish rhamnolipid depleted through biodegradation.⁴⁰

Biosurfactants have also been studied for simultaneous removal of organic and metal contamination from soil. In one study, saponin removed 76% of phenanthrene and 88% of Cd simultaneously.⁹⁸ Interestingly, removal levels for both phenanthrene and Cd were the same whether they were present individually or in combination. This suggests that the two contaminants do not compete with each other. This may be because Cd interacts with the head group of the surfactant and phenanthrene interacts with the micelle interior.⁹⁸ A second study examined removal of Cd and phenanthrene co-contaminants by four biosurfactants including: surfactin; an iturin and fengycin mixture (lipopeptides produced by *Bacillus* sp.); arthrofactin (a lipopeptide produced by

Arthrobacter oxydans); and flavolipid (now siderolipids).⁹⁹ Removal ranged from 79 to 87% and from 66.9 to 71.9% for phenanthrene and Cd respectively, depending on the biosurfactant used. The use of an iodide ligand increased Cd removal to 74 to 99%. The iodide ligand is thought to form a neutral complex with Cd which can then interact with the interior hydrophobic domain of the micelle thereby increasing the amount of Cd associated with each micelle.⁹⁹

1.6.2. Liquid Media

There are a variety of approaches for the removal of metals from aqueous solutions. One is the use of sorbents which can range from ion exchange resins to clays to microbial biomass. A recent report used rhamnolipid to assist in the process of sorption of Cu to clay. In this study, the efficiency of Cu sorption by a Na-montmorillonite clay was increased considerably when modified by rhamnolipid.¹⁰⁰ A small amount of added rhamnolipid (2×10^{-6} M) acted to disperse the clay particles, thus increasing the total available surface area for Cu sorption. The sorbed metals were subsequently removed from the clay using a higher concentration rhamnolipid wash treatment.¹⁰⁰

Metals can also be removed directly from aqueous solution using biosurfactants. Once the aqueous solutions are treated with biosurfactants, the metal-surfactant complex must be removed from the solution. This can be accomplished in two ways: micellar-enhanced ultrafiltration and ion flotation. Micellar-enhanced ultrafiltration is a membrane-based separation process that uses anisotropic membranes with small size pores that do not allow surfactant micelles to pass through. Thus, the micelle-bound metal in solution is retained on the filter and removed from the bulk aqueous solution that passes through the filter.¹⁰¹ Pores sizes can range from 1000 to 50,000 molecular-weight-

cut-off (MWCO). Biosurfactants, because they are biodegradable, are particularly suited for this application; surfactant monomers can leak through the membrane leaving low levels of surfactant in the aqueous solution which can thereafter be biodegraded. The efficacy of this technique with biosurfactants has been examined. Micellar-enhanced ultrafiltration was tested with a spiculisporic acid derivative 2-(2-carboxyethyl)-3-decyl maleic anhydride (DCMA-3Na).⁶⁴ Results showed that DCMA-3Na removed 99, 99, and 93% of Cd, Cu, and Zn respectively when at equimolar concentrations using a 3000 MWCO membrane. DCMA-3Na exhibited a metal binding affinity of $\text{Cd}^{2+} > \text{Cu}^{2+} \sim \text{Zn}^{2+} > \text{Ni}^{2+}$ with Ni removal reaching only 65%.

A second study examined the use of rhamnolipid in micellar-enhanced ultrafiltration.¹⁰² Optimized conditions were determined for use of rhamnolipid to remove metals from six wastewater samples from the metal-refining industry. The wastewater samples contained Zn (60 to 130 mg/L); Cd (10 to 30 mg/L); and Pb, Cu, and Ni which were all below 10 mg/L. The optimal conditions identified were: membrane pressure, 69 ± 2 kPa; rhamnolipid:metal molar ratio, 2:1; temperature, 21 ± 1 °C; and pH, 6.9 ± 0.1 . Operating under these conditions, the level of all metals in the six wastewater samples was reduced to below 1.2 mg/L meeting Canadian Federal discharge limits.¹⁰²

A second approach to removing biosurfactant-metal complexes from solution is ion flotation, also known as dissolved air flotation or foam fractionation. This technique employs air sparging into a surfactant solution. The surfactant will absorb to the air bubbles generating a foam that can be harvested and removed from the solution. In the presence of metal ions, the surfactants can complex the ions and carry them into the foam.¹⁰³ Using this technique, H. Chen¹⁰³ showed surfactin was able to remove 45% of

the Hg from a 2 mg/L Hg solution. To achieve this removal, the optimal conditions were determined to be surfactin applied at 10 times the critical micelle concentration (10 x CMC) at a pH of 8 or 9. Overnight mixing prior to removal also helped increase Hg removal. In a second study, a 3:1 molar ratio of saponin to metal was used to remove lead, copper, and cadmium from wastewater with efficiencies of 90, 81 and 71%, respectively.¹⁰⁴ A third study used surfactants produced by *Candida* (likely sphorolipids) to achieve a removal of $\geq 98\%$ of Fe (62 mg/L) and Mn (4 mg/L) from neutralized acid mine drainage using a 0.02% (200 mg/L) surfactant solution.¹⁰⁵

Adsorbing colloid flotation is a method that combines the use of a colloidal sorbent material (*e.g.*, clays and goethite) with the flotation technique.¹⁰⁶ This method essentially follows sorbent treatment of wastewater with surfactant flotation. Since the sorbent is present as a colloid, the surfactant foam will collect the metal ions adsorbed to the colloid particles by floating the sorbent. Similarly, compounds like Fe^{+3} can be used to co-precipitate metals for subsequent flotation. Using this technique, surfactin and lichenysin were used to collect either goethite (pH 4-7) or ferric hydroxide (pH 4) colloids that had sorbed Cr, resulting in removal of Cr with almost 100% efficiency. Surfactin could also remove $\sim 95\%$ Zn when collecting ferric hydroxides (pH 6). Lichenysin, however, was ineffective for Zn removal.¹⁰⁶

1.6.3. Recovery of Metal from Biosurfactant-Metal Complexes

It is worth noting that once a biosurfactant-metal complex has been formed and used to remove the metal from a contaminated soil, sediment or solution, the complex can be separated again through a simple pH adjustment. This allows recovery and recycling of both the metal and the biosurfactant. For anionic surfactants such as rhamnolipid or

surfactin, the solution can be acidified (~ pH 2) to precipitate the surfactant and release the metal ion. The biosurfactant can then be removed by centrifugation and recycled for reuse.^{73, 74} For a non-ionic surfactant, such as saponin, a pH adjustment to 11 will precipitate the complexed metals; the metals can then be removed by centrifugation and the biosurfactant collected for reuse.⁸³

1.7. Conclusion

As shown in this chapter, the body of literature on biosurfactant-metal interactions is large and continuing to grow. The potential for green, economical remediation technologies based on these interactions is enormous, but there remain several challenges that must be resolved before biosurfactants are viable alternatives for use in remediation technologies.

The first challenge is material cost. There is still no biosurfactant that can be competitively produced, in terms of cost, when compared to synthetic surfactants. The second challenge is in understanding the chemical properties of individual biosurfactant congeners so that they can be optimized for application in remediation technologies. For example, up to 60 rhamnolipid congeners are produced naturally by bacteria, but these congeners can have very different chemical properties (e.g., CMC, interaction with metals). The ability to genetically manipulate bacteria to produce single congeners or alternatively, to chemically synthesize single congeners, has the potential to increase the efficacy of biosurfactants dramatically. The third challenge is to move research from the bench-scale and into field testing. Optimally this can be done by creating academic-industry partnerships which can be implemented in two stages: first to demonstrate effectiveness, and second to scale-up production of biosurfactants for commercial use.

To close, it is clear humanity's impact on the biogeochemical cycling of metals is significant and resulting in increasing risks to public health due to metal exposures. As we continue to increase global consumption of new technologies, including cell phones and computers, the need for a variety of metals increases along with the resulting impacts of mining and metal consumption. As our demand for metals increases, we must find a way to reduce emissions and the impacts related to their use. The foundation for preserving the health and stability of our environment while encouraging innovation and economic growth lies in the development of green technologies and green chemicals; in the realm of metals, biosurfactants are one of the most promising possibilities available today.

1.8. Note about Chapter 1

This chapter was originally written for and published in the 2014 special topic book *Biosurfactants: Research Trends and Applications*.¹⁰⁷ Since its publication, numerous reviews—primarily chapters in special topic books—have been published discussing biosurfactants and metals,¹⁰⁸⁻¹¹² but there have been few notable additions of primary research to the literature.

Abyaneh and Fazaelipour¹¹³ tested rhamnolipid as collector in precipitate flotation and found that rhamnolipid could successfully float Cr(IV) from water after it had been precipitated as Cr(III) using a ferrous salt. Up to 95% recovery of Cr(IV) was achieved from an initial concentration of 40 ppm. Bodagh et al.¹¹⁴ report the use of rhamnolipid collector in ion flotation of Cd²⁺. Cd²⁺ was floated, individually and separately mixed with Zn and Cu, with Cd²⁺ removal efficiencies of 57, 36, and 48%, respectively.

Rhamnolipid selectivity coefficients of cadmium > zinc, cadmium > copper, and zinc > copper were reported.

An anionic glycolipid biosurfactant from *Candida sphaerica* was used to wash metals from a soil contaminated by metals in an automotive battery industrial area. Removal percentages of 95, 90, and 79% Fe, Zn, and Pb were achieved using a cell free broth, but amendments of 0.1%, 0.25, and 2.5% of purified biosurfactant had moderately lower removals. Sequential extractions of heavy metals from the contaminated soil revealed Fe was removed from the oxide and exchangeable fractions of the soil, Pb was removed from the exchangeable and carbonate fractions, and Zn was removed from the carbonate and organic fractions.¹¹⁵ These results demonstrate that metal removal from different soil fractions is metal-specific during biosurfactant mediated soil washing.

Haryanto and Change¹¹⁶ examined metal recovery from artificially contaminated sands using surfactin and rhamnolipid. Initial experiments flushing surfactant solution through the sand yielded poor metal removal efficiencies for copper and cadmium with 3-10% and 13-36% removed, respectively. Removal efficiencies were improved by flushing the sand with surfactant foams because channeling effects were reduced. Removal efficiencies for copper and cadmium increased to 10-30% and 20-46%, respectively. Rhamnolipid had greater removal efficiencies compared to surfactin for both metals, and the authors attribute the difference to rhamnolipid's higher dynamic foam capacity.

Singh and Cameotra¹¹⁷ also reported success using biosurfactants as soil washing agents. Surfactin and fengycin obtained from *Bacillus subtilis* were used to wash soils collected from an industrial dumping site. Removals of 44.2% for Cd, 35.4% for Co,

40.3% for Pb, 32.2% for Ni, 26.2% for Cu, and 32.1% for Zn were achieved. The soil washing was effective enough to enable the germination of mustard seeds in soils where germination was previously inhibited.

Numerous reports of novel biosurfactants or biosurfactant producing organisms interacting with metals were found, but if the type of biosurfactant was not reported, they were excluded from discussion in this chapter.

CHAPTER 2

RHAMNOLIPID BIOSURFACTANTS PREFERENTIALLY COMPLEX RARE EARTH ELEMENTS

2.1. Abstract

Rare earth elements (REEs) are a vital component of many modern technologies, and some of these elements are considered critical materials subject to supply risk. We are investigating monorhamnolipid biosurfactants for interactions with REEs. Conditional stability constants were determined using a resin-based ion exchange method. 27 metals were examined, and the conditional stability constants could be divided into three groups, albeit somewhat subjectively: weakly, moderately, and strongly bound. UO_2^{2+} , Eu^{3+} , Nd^{3+} , Tb^{3+} , Dy^{3+} , La^{3+} , Cu^{2+} , Al^{3+} , Pb^{2+} , Y^{3+} , Pr^{3+} , and Lu^{3+} are strongly bound with conditional stability constants ranging from 9.82 to 8.20; Cd^{2+} , In^{3+} , Zn^{2+} , Fe^{3+} , Hg^{2+} , and Ca^{2+} are moderately bound with stability constants ranging from 7.17 to 4.10; and Sr^{2+} , Co^{2+} , Ni^{2+} , UO_2^{2+} , Cs^+ , Ba^{2+} , Mn^{2+} , Mg^{2+} , Rb^+ , and K^+ are weakly bound with stability constants ranging from 3.95 to 0.96. The uranyl ion is reported twice due to the ion demonstrating two distinct binding regions. A study of mixed metals confirmed monorhamnolipids preferentially remove metals with large $\log \beta$ values over those with smaller values. $\log \beta$ values have significant, strong correlation to enthalpy of hydration and significant, less strong correlation to the ionic charge to radius ratio. The preferential complexation of monorhamnolipids with REEs may constitute a green pathway for recovery of REEs from alternative, non-traditional sources.

2.2. Introduction

An Intel computer chip requires nearly 60 periodic elements to produce,¹¹⁸ and a widely recognized future challenge will be maintaining a steady supply of these elements.¹¹⁹ This is especially true for rare earth elements (REEs) which are essential components of every modern technology including green energy, personal electronics, data transmission, medical technologies, reaction catalysts, aircraft, and optics.¹²⁰ The U.S. Department of Energy lists the rare earth metals dysprosium, neodymium, terbium, europium, and yttrium as critical materials subject to supply risk;¹²¹ the European Union has identified a longer list of materials which includes indium and additional REEs.¹²² Demand for REEs was estimated at 136,100 tons in 2010 and is estimated to increase to 160,000-210,000 tons by 2016.¹²³ Due to the limited number of economically viable ore bodies for mining these materials, it is critical that alternative technologies be developed to utilize all possible REE resources.

One untapped source for REEs is waste streams generated by different industries. Despite considerable REE concentrations in aqueous waste streams from hard rock mining¹²⁴⁻¹²⁹ and coal mining,¹³⁰⁻¹³² REEs are not currently targeted for recovery from these sources. Possible other sources also include industrial waste streams,¹³³ municipal wastewaters,^{134, 135} and landfill leachates.¹³⁶

One approach to recover metals from waste streams is the use of metal complexing agents. These compounds should be selective for target metals even when they are at low concentration, because most waste streams will contain competing metals (K^+ , Ca^{2+} , etc.) at orders-of-magnitude higher concentrations. A second consideration is that the use of complexing agents to capture metals from waste streams will ultimately

lead to the release of some of this material to the environment even under controlled conditions. Thus, agents that are non-toxic, naturally-derived, and renewable would be ideal for minimizing the potential for environmental contamination during the metal recovery process. Biosurfactants are green molecules with properties that may suit this challenge well.

Biosurfactants are compounds that exhibit surface activity (e.g., reduce surface and interfacial tension) and are derived from natural, biological sources. They are considered green substances due to their natural derivation, biodegradability, and relatively low toxicity.²⁰ Rhamnolipids produced by *Pseudomonas aeruginosa* are a class of biosurfactants known to complex metals, and they are attracting a great deal of attention for metal remediation applications. Rhamnolipids are most often produced as a complex congener mixture where the molecule may have a monorhamnose or dirhamnose hydrophilic moiety linked by an O-glycosidic linkage to a hydrophobic moiety of one, two, or three (rarely) hydrocarbon chains which are primarily saturated, although mono- and polyunsaturated congeners exist.²⁰

Monorhamnolipids (rhamnosyl- β -hydroxyalkanoyl- β -hydroxyalkanoates), (Figure 2.1A insert) are the best studied rhamnolipids for metal complexation behavior. Cadmium was the first metal reported to be complexed by monorhamnolipids,¹⁹ and subsequent studies expanded the list of transition metals.^{21, 74} Monorhamnolipid-metal complexes are typically reported in terms of their conditional stability constants, a measure of the affinity of a complexing agent for a metal cation under specific solution conditions.¹³⁷ These studies showed that monorhamnolipids have conditional stability

constants for heavy metal cations (Pb^{2+} , Cd^{2+} , Zn^{2+}) that are several orders of magnitude larger than for common soil/water cations.²¹

To date, rhamnolipid interactions with REEs have not yet been examined, but given the strong complexing ability of these biosurfactants with transition metals, we hypothesized that they would also complex REEs. Toward this end, the objectives of this study were to (1) determine the ability of monorhamnolipids to complex REEs and other metals identified as critical with a supply risk and (2) assess the ability of monorhamnolipids to selectively remove metals from mixed metal solutions.

Monorhamnolipids from *Pseudomonas aeruginosa* ATCC 9027 were used for all experiments. An ion exchange technique was used to determine the conditional stability constants for monorhamnolipids with Y^{3+} , La^{3+} , Pr^{3+} , Nd^{3+} , Eu^{3+} , Tb^{3+} , Dy^{3+} , In^{3+} , UO_2^{2+} and Lu^{3+} . In addition, the ability of monorhamnolipids to selectively remove metals in the presence of competing metals at equimolar and order-of-magnitude higher concentrations was tested using ion exchange with the metals Ca^{2+} , Cd^{2+} , Pb^{2+} .

2.3. Materials and Methods

2.3.1. Monorhamnolipid Production

Pseudomonas aeruginosa ATCC 9027 was obtained from the American Type Culture Collection and kept as a glycerol freezer stock at -80°C . This strain is a natural mutant that has been previously shown to exclusively produce monorhamnolipid congeners.^{138, 139} *P. aeruginosa* was cultured for 24 h at 37°C on a PTYG agar (0.5% protease peptone, 0.5% tryptone, 1% yeast extract, 0.06% $\text{MgSO}_4 \cdot 7\text{H}_2\text{O}$, $7 \times 10^{-4}\%$ $\text{CaCl}_2 \cdot 2\text{H}_2\text{O}$, and 1% glucose). The agar culture was transferred to Kay's mineral medium for 24 h growth at 37°C and 200 rpm. Kay's mineral medium contains 100 ml of

solution A (0.3% $\text{NH}_4\text{H}_2\text{PO}_4$, 0.2% K_2HPO_4 , and 0.2% glucose), 1 ml solution B (0.025% $\text{FeSO}_4 \cdot 7\text{H}_2\text{O}$) and 1 ml solution C (10% $\text{MgSO}_4 \cdot 7\text{H}_2\text{O}$). The pre-culture was transferred to a pH 7 minimal salts medium (MSM) with 2% glucose at a ratio of 1 ml pre-culture per 100 ml MSM. MSM is composed of 1 l of solution A (0.25% NaNO_3 , 0.04% $\text{MgSO}_4 \cdot 7\text{H}_2\text{O}$, 0.1% KCl , 0.1% NaCl , 0.005% $\text{CaCl}_2 \cdot 2\text{H}_2\text{O}$, and 0.4% H_3PO_4) mixed with 1 ml of solution B (0.05% $\text{FeSO}_4 \cdot 7\text{H}_2\text{O}$, 0.15% $\text{ZnSO}_4 \cdot 7\text{H}_2\text{O}$, 0.15% $\text{MnSO}_4 \cdot \text{H}_2\text{O}$, 0.03% H_3BO_3 , 0.015% $\text{CoCl}_2 \cdot 6\text{H}_2\text{O}$, 0.015% $\text{CuSO}_4 \cdot 5\text{H}_2\text{O}$, and 0.01% $\text{Na}_2\text{MoO}_4 \cdot 2\text{H}_2\text{O}$). The MSM culture is placed in a 37° C gyratory shaker and shaken for 72 h at 200 rpm.

2.3.2. Monorhamnolipid Purification

Monorhamnolipids produced by *Pseudomonas aeruginosa* ATCC 9027 are a congener mixture of up to 30 molecules in which the rhamnose headgroup is preserved but the alkyl chains can vary in chain length and, to a lesser extent, saturation.¹⁴⁰ The protocol used for this work generates a pure native mixture in which the major congener, rhamnosyl- β -hydroxydecanoyl- β -hydroxydecanoate (Rha-C10-C10), typically dominates at 75-85 wt% of the mixture.^{140, 141} This complex assembly of congeners is referred to herein as either the native monorhamnolipid mixture or simply monorhamnolipids.

The native monorhamnolipid mixture was concentrated by centrifugation (10,000 rpm for 10 min) to remove cells and cellular debris, followed by removal and acidification of the supernatant to pH 2 using HCl. Monorhamnolipids have pK_a values of ~5.5, below which they become poorly soluble¹³⁸ and can be collected by centrifugation. Pelleted monorhamnolipids were dissolved in a 9:1 chloroform:methanol mixture and separated from remnant water using a separatory funnel. The solvent was removed by

rotoevaporation. The concentrated monorhamnolipids were purified using a solvent mixture of 6:6:6:1:1 (v/v) of hexane:dichloromethane:ethyl acetate:chloroform:methanol (containing 0.1% acetic acid) by elution through a 22 x 300 mm gravity-based, glass chromatography column packed with 45 g of 60-Å-pore silica gel. Monorhamnolipids were collected when column eluent tested positive for rhamnose with anthrone reagent dissolved in H₂SO₄. The solvent mixture was removed from the monorhamnolipids by rotoevaporation, and purity is checked by reversed phase high performance liquid chromatography on a C18 column.¹³⁸

2.3.3. Metals

Pb(NO₃)₂, Cd(NO₃)₂•4H₂O, Y(NO₃)₃•4H₂O, Ba(NO₃)₂, Sr(NO₃)₂, Cs(NO₃), In(NO₃)₃•xH₂O, Lu(NO₃)₃•xH₂O, La(NO₃)₃•6H₂O, UO₂(NO₃)₂•6H₂O, Rb(NO₃), Eu(NO₃)₃•5H₂O, Tb(NO₃)₃•5H₂O, Pr(NO₃)₃•6H₂O, Nd(NO₃)₃•6H₂O, Dy(NO₃)₃•xH₂O, and Al(NO₃)₃•9H₂O were purchased from Sigma-Aldrich with a purity of ≥99% and were used as received. Appropriate trace ICP/AA grade standard solutions for each metal were obtained from Fisher Scientific.

2.3.4. Determination of Stability Constants

Stability constants of monorhamnolipids with each metal were determined using an ion-exchange technique which is described in detail in Appendix A. In brief, this technique involves mixing various concentrations of ligand with a resin onto which metal is bound in an aqueous system. It suits only mononuclear complexes¹⁴² in which the ligand-to-metal ratio is ≥1.¹⁴³ This technique was originally described by Schubert¹⁴⁴ and Schubert and Richter¹⁴⁵ and later adapted for metal-biosurfactant interactions.^{21, 74} The ion exchange resin SP Sephadex C25 (GE Healthcare) was prepared by soaking in

ultrapure water ($\geq 18 \text{ M}\Omega\text{-cm}$) overnight. The hydrated resin was washed with equal parts ultrapure water, then pH 6.9 disodium PIPES buffer [Piperazine-N,N'-bis(2-ethanesulfonic acid)], and air-dried; sufficient buffer was used to saturate the resin with Na^+ . Ion exchange reactions were allowed to occur in 15-ml metal-free centrifuge tubes. Each reaction contained 100 mg of prepared resin and a total volume of 10 ml with final concentrations of 0.5 mM metal, 0.01 M PIPES buffer at pH 6.9, and 0, [0.1 or 0.25], 0.5, 1, 2, or 4 mM of the native monorhamnolipid mixture. Uranyl was also examined with the additional monorhamnolipid concentrations of 0.75 and 1.5 mM. In the absence of monorhamnolipids, 99% of the metal is bound for polyvalent ions and about 50% for monovalent ions. A 10 mM monorhamnolipid solution was generated using a molecular weight of 504 g mol^{-1} for the native monorhamnolipid mixture. Monorhamnolipids were measured gravimetrically, dissolved in ultrapure water, and the solution adjusted to pH 6.9. Metal solutions were mixed with ultrapure water 0.5 h before use. Reactions were shaken horizontally on a gyratory shaker (200 rpm) for 2 h, allowed to settle vertically for a minimum of 1 h, and then a sample of supernatant was removed and diluted in 2% HNO_3 . Metal concentrations were measured by inductively coupled plasma atomic emission spectroscopy (ICP-AES). Calibration curves were prepared using standard solutions in trace-metals grade 2% HNO_3 .

2.3.5. Stability Constant Calculation

The monorhamnolipid-metal stability constant was calculated as described previously.^{21, 74, 144} The formation constant, or stability constant, β , is calculated by $\beta = [ML_\chi]/([M][L]^\chi)$ where M is the metal (mol l^{-1}), L is the monorhamnolipid ligand (mol l^{-1}), ML_χ is the metal:ligand complex (mol l^{-1}), and χ is the stoichiometry of the

monorhamnolipid:metal complex (mol mol⁻¹). The conditional stability constant has previously been reported as K, but because multiple binding events have been shown to occur in this system, β is a more appropriate designation for the overall stability constants reported herein; K is related to β by $\beta = K_1 \cdot K_2 \cdots K_n$ where each K value is a stability constant for stepwise addition of 1 to χ ligands.¹⁴⁶ The overall stability constant is determined using the linear relationship in Eq. 2.1.

$$\log(\lambda_o/\lambda - 1) = \log \beta + \chi \log L \quad [2.1]$$

A linear regression of data plotted with $\log L$ vs. $\log(\lambda_o/\lambda - 1)$ yields a y-intercept representing the stability constant, $\log \beta$, and a slope representing the molar ratio of ligand to metal, χ . λ_o and λ are distribution coefficients where $\lambda_o = [MR]/[M]$ and $\lambda = [MR]/[(M + ML_\chi)]$. MR is the metal bound to resin (mol kg⁻¹). These constants are determined experimentally. It should be noted that stability constants determined using this method are only valid for the conditions of the experiment; thus, they are considered conditional stability constants. A derivation of Eq. 2.1 can be found in Appendix A.

2.3.6. Metal Competition Study

The preference of monorhamnolipids for different metals was examined in two mixed metal studies. Ca²⁺, Cd²⁺, and Pb²⁺ were selected as model elements for their small, intermediate, and large stability constants, respectively. The first study examined Ca²⁺, Cd²⁺, and Pb²⁺ at equimolar concentrations, and the second, at a ratio of 100:10:1, respectively. Reactions for the former were set up following the procedure outlined above for the determination of stability constants except that each metal was present at a concentration of 0.167 mM (0.5 mM total). During the second study, the same method was used except that only 0, 1, or 2 mM monorhamnolipid was examined with metal

concentrations of 0.45, 0.045, and 0.0045 mM (0.5 mM total) for Ca^{2+} , Cd^{2+} , and Pb^{2+} , respectively. Metal concentrations were measured by ICP-AES. Calibration curves were prepared using standard solutions in trace-metals grade 2% HNO_3 .

2.4. Results and Discussion

2.4.1. Single Metal Studies

Thirteen previously unstudied metals, including a group of REEs, were reacted with monorhamnolipids to determine the conditional stability constant and stoichiometry of monorhamnolipid:metal complexes using an ion exchange technique. As would be expected, metal complexation increases with increasing monorhamnolipid concentrations. Figure 2.1A compares the increase in aqueous metal concentration of Pb^{2+} and Sr^{2+} with increasing monorhamnolipid concentration. Pb^{2+} is the more effectively complexed, with 97% of the Pb^{2+} in the aqueous phase at 4 mM monorhamnolipid, but only 6.7% of the Sr^{2+} .

Complexation data were then used to calculate the conditional stability constants ($\log \beta$), a measure of complexation efficiency, and the monorhamnolipid:metal complex stoichiometry (molar ratio, χ) using Eq. 2.1. Figure 2.1B shows plots of $\log(\lambda_o/\lambda - 1)$ as a function of $\log L$ for Pb^{2+} and Sr^{2+} ; these plots were subjected to linear fits from which values for $\log \beta$ and χ were determined. Pb^{2+} , the better complexed metal as seen in Figure 2.1A, exhibits larger slope and y-intercept indicating larger $\log \beta$ and χ values than Sr^{2+} . Conversely, as the less effectively complexed metal, Sr^{2+} exhibits a smaller slope and y-intercept.

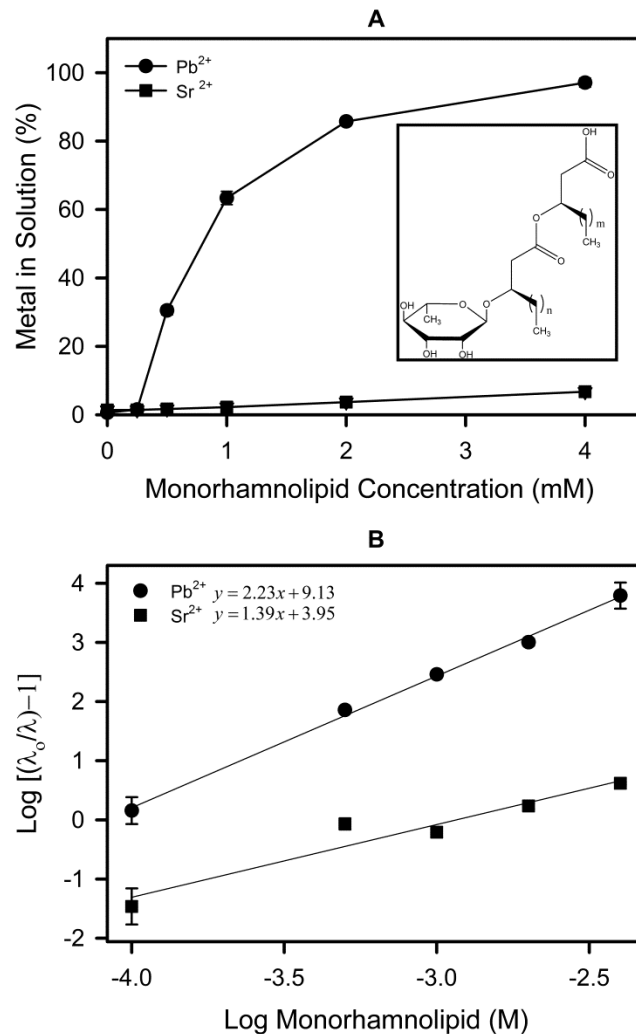


Figure 2.1 (A) Effect of monorhamnolipid concentration on the complexation of Pb²⁺ and Sr²⁺. **(B)** Determination of the conditional stability constant and stoichiometry of monorhamnolipid:metal complexes by ion-exchange equilibrium method for Pb²⁺ and Sr²⁺. Each metal was tested independently. Each point represents the mean and standard deviation of 6 replicates. **Insert:** Structure of monorhamnolipids utilized in this study. The varying chain lengths of the monorhamnolipid congeners are represented by ‘m’ and ‘n’ which vary from 4 to 12

Table 2.1 Conditional stability constants, molar ratios, and statistical analysis for metal complexes with monorhamnolipids

Metal Ion	Log β	Std. Error log β	95% Conf. Limits		χ	Std. error χ	95% Conf. Limits χ		R^2	Coefficient of Variation (%)		
			Lower	Upper			Lower	Upper		Log β	χ	λ_0
$\dagger\text{UO}_2^{2+}$	9.82	1.328	6.99	11.74	2.93	0.467	1.90	3.58	0.975	13.5	16.0	17
Eu^{3+}	9.77	0.202	9.34	10.62	2.17	0.065	2.00	2.45	0.997	2.1	3.0	2790
Nd^{3+}	9.69	0.459	8.28	11.32	2.19	0.147	1.65	2.71	0.987	4.7	6.7	1880
Tb^{3+}	9.65	0.382	8.27	10.88	2.01	0.122	1.49	2.39	0.989	4.0	6.1	8080
Dy^{3+}	9.57	0.592	7.27	10.93	2.14	0.189	1.29	2.51	0.977	6.2	8.8	1330
La^{3+}	9.29	0.432	8.14	10.86	2.07	0.138	1.77	2.61	0.987	4.6	6.7	3330
$*\text{Cu}^{2+}$	9.27	0.659	7.43	11.10	2.31	0.218	1.70	2.91	0.966	7.1	9.4	
Al^{3+}	9.22	0.937	5.08	11.13	2.35	0.299	0.95	2.86	0.954	10.2	12.7	63
Pb^{2+}	9.13	0.223	8.71	10.12	2.23	0.071	2.12	2.56	0.997	2.4	3.2	166
Y^{3+}	9.11	0.201	8.59	9.96	2.04	0.064	1.88	2.32	0.997	2.2	3.2	2350
Pr^{3+}	9.04	0.223	8.53	9.83	1.98	0.071	1.84	2.25	0.996	2.5	3.6	2440
Lu^{3+}	8.20	0.247	7.69	9.16	1.72	0.079	1.51	2.02	0.994	3.0	4.6	1230
Cd^{2+}	7.17	0.735	5.28	9.41	2.04	0.235	1.50	2.86	0.962	10.3	11.5	90
In^{3+}	6.70	1.129	3.65	10.18	1.75	0.361	0.92	3.03	0.886	16.8	20.7	81
$*\text{Zn}^{2+}$	5.62	0.214	5.03	6.22	1.58	0.071	1.39	1.78	0.992	3.8	4.5	
$*\text{Fe}^{3+}$	5.16	0.710	3.19	7.13	1.22	0.235	0.55	1.85	0.867	13.8	19.3	
$*\text{Hg}^{2+}$	4.49	0.135	4.11	4.87	1.21	0.045	1.09	1.34	0.995	3.0	3.7	

Table 2.1 Conditional stability constants, molar ratios, and statistical analysis for metal complexes with monorhamnolipids

Metal Ion	Log β	Std. Error log β	95% Conf. Limits $\log \beta$		χ	Std. error χ	95% Conf. Limits χ		R^2	Coefficient of Variation (%)		
			Lower	Upper			Lower	Upper		Log β	χ	λ_0
*Ca ²⁺	4.10	0.635	2.33	5.86	1.32	0.210	0.74	1.90	0.908	15.5	15.9	
Sr ²⁺	3.95	0.095	3.52	4.13	1.39	0.030	1.24	1.44	0.999	2.4	2.2	71
*Co ²⁺	3.58	0.150	3.17	4.00	1.03	0.049	0.89	1.17	0.991	4.2	4.8	
*Ni ²⁺	3.53	0.176	3.04	4.02	0.93	0.058	0.77	1.09	0.984	5.0	6.2	
†UO ₂ ²⁺	3.43	0.419	2.25	5.09	0.78	0.128	0.44	1.30	0.949	12.2	16.5	17
§Cs ⁺	(3.43)				(1.47)				0.9635			1.6
Ba ²⁺	3.22	0.438	1.97	4.36	1.10	0.140	0.66	1.40	0.954	13.6	12.7	84
*Mn ²⁺	2.85	0.452	1.59	4.10	0.90	0.150	0.49	1.32	0.901	15.9	16.7	
*Mg ²⁺	2.66	0.315	1.80	3.55	0.84	0.104	0.55	1.13	0.942	11.8	12.4	
Rb ⁺	1.57	0.291	1.13	2.30	0.85	0.096	0.72	1.09	0.963	18.6	11.3	1.2
*K ⁺	0.96	0.115	0.64	1.28	0.57	0.038	0.47	0.68	0.983	12.0	6.7	

*Values from Ochoa-Loza et al.²¹

† UO₂²⁺ had two distinct binding regions, and each region is included separately.

§ Values for Cs⁺ are tentative due to inconsistent and irregular results during replicate trials. Cs⁺ is included in this table because it is utilized during the subsequent ion flotation study (see Chapter 4).

The metals Al^{3+} , Pb^{2+} , and Cd^{2+} were tested in this study as a comparison to values reported previously by Ochoa-Loza et al.²¹ Log β values for Al^{3+} , Pb^{2+} , and Cd^{2+} obtained here were 9.22, 9.13, and 7.17; these values are within the 95% confidence intervals reported by Ochoa-Loza et al., demonstrating good agreement between the studies.

Table 2.1 shows the log β and χ values determined for the 17 metals examined combined with data for 10 metals from Ochoa-Loza et al.²¹ Log β values range from 9.82 to 0.96. A stability constant sequence could not be generated because there is significant overlap of the conditional stability constants when the standard error is considered. As a result, the 27 metals were divided into three groups, albeit somewhat subjectively: weakly, moderately, and strongly bound. UO_2^{2+} , Eu^{3+} , Nd^{3+} , Tb^{3+} , Dy^{3+} , La^{3+} , Cu^{2+} , Al^{3+} , Pb^{2+} , Y^{3+} , Pr^{3+} , and Lu^{3+} are strongly bound with conditional stability constants ranging from 9.82 to 8.20; Cd^{2+} , In^{3+} , Zn^{2+} , Fe^{3+} , Hg^{2+} , and Ca^{2+} are moderately bound with stability constants ranging from 7.17 to 4.10; and Sr^{2+} , Co^{2+} , Ni^{2+} , UO_2^{2+} , Cs^+ , Ba^{2+} , Mn^{2+} , Mg^{2+} , Rb^+ , and K^+ are weakly bound with stability constants ranging from 3.95 to 0.96. The uranyl ion is reported twice due to the ion demonstrating two distinct binding regions (see below). These groups reveal that the REEs, metals of environmental concern (e.g., Pb^{2+} , Cd^{2+} , Hg^{2+}), and metals listed as critical (e.g., In^{3+}) have relatively large log β values, while common soil and water cations (e.g., Mg^{2+} , Mn^{2+} , K^+) have small log β values. The groups show that monorhamnolipids exhibit selectivity for REEs which are concentrated in the strongly bound stability constant group.

The coefficients of variation (CV) for these log β values [(standard error / log β)·100%] range from 2.1 to 18.6%. The molar ratio values, χ , range from 2.93 to 0.57.

Non-integer values for χ are counterintuitive, as it is impossible to have 2.93 monorhamnolipid molecules, but there are several possibilities for why non-integer values are calculated. First, the values could be the result of analytical error in a system with only a single complex formed.¹⁴² χ could also represent the average of a complex population distribution if multiple monorhamnolipid:metal complexes are present,¹⁴⁷⁻¹⁴⁹ as has been shown for complexes of $\text{Pb}^{2+}/\text{UO}_2^{2+}$ and monorhamnolipids.²² The presence of monorhamnolipid congeners might also explain non-integer molar ratios, as different congeners may have different metal affinities, leading to different metal removal rates and non-uniform molar ratios. Finally, in aqueous media, metal hydroxo complexes or mixed hydroxo-monorhamnolipid complexes may also form resulting in ligand competition that would complicate determination of χ values using Eq 2.1.

Uranyl (UO_2^{2+}), the only oxyanion in this study, was selected because there is significant interest in recovering uranium from seawater in an environmentally compatible manner.¹⁵⁰ Interestingly, all of the metals tested exhibited plots like those shown in Figure 2.1B, except for UO_2^{2+} . When initially examined, uranyl appeared to exhibit two distinct binding regions (data not shown). To confirm these results, a second series of experiments with additional monorhamnolipid concentrations was conducted (Figure 2.2). Uranyl clearly exhibits two distinct binding regions. Region 1 has a conditional stability constant value of 3.43, while region 2 has a value of 9.82. The χ value determined for region 1 is 0.78, while region 2 is 2.93. These two results are included as separate entries in Table 2.1. The point of this incongruity occurs when the ratio of monorhamnolipids to metal reaches 2:1.

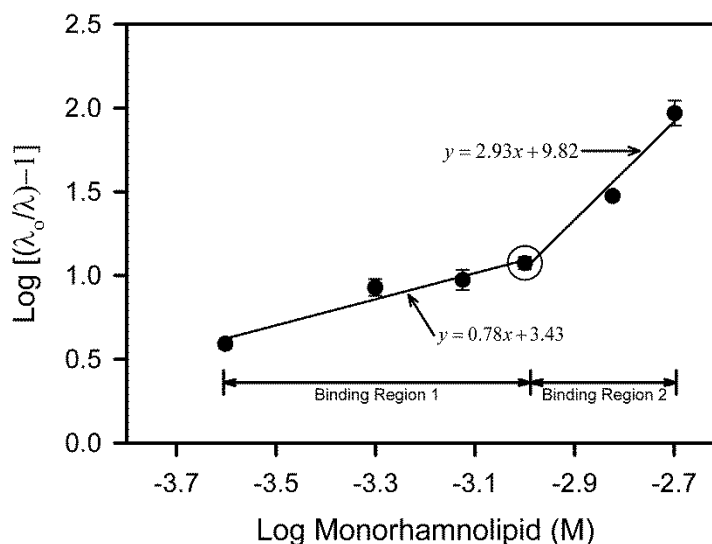


Figure 2.2 Determination of the conditional stability constant and stoichiometry of monorhamnolipid:UO₂²⁺ complexes by ion-exchange equilibrium method. The circled symbol indicates the monorhamnolipid concentration where the monorhamnolipid:metal ratio is 2:1. Region 1 and 2 indicate the two distinct binding regions of monorhamnolipid with uranyl. Each point represents the mean and standard deviation of 6 replicates.

There are several possibilities for this unusual behavior. At pH 7, uranyl can form a complex mixture of positively to negatively charged hydroxo species in aqueous media.¹⁵¹ It is possible that the cation binding resin has a greater affinity for a subset of the aqueous uranyl species (e.g., those with higher charge). A second possibility is the formation of mixed ligand species. Positively charged hydroxo species would remain bound to the resin until monorhamnolipid replaced the hydroxo ligands. During ligand exchange, positively-charged mixed-ligand complexes may form and remain bound to the resin. In both possible explanations, release of uranyl complexes would require higher concentrations of monorhamnolipid for effective competition.

A third possible explanation relates to the stoichiometry of the monorhamnolipid:UO₂²⁺ complex. Previous work²² reveals that at a equimolar concentrations of metal and monorhamnolipid, the 2:1 monorhamnolipid:UO₂²⁺ complex is the most abundant species. Thus, under conditions where the ratio of monorhamnolipid:UO₂²⁺ < 2:1 (Figure 2.2, Region 1), the amount of complex formed with UO₂²⁺ is limited by monorhamnolipid, resulting in a smaller conditional stability constant. However, when this ratio exceeds the 2:1 threshold, monorhamnolipid is no longer limiting and the measured stability constant increases (Figure 2.2, Region 2).

2.4.2. Mixed Metal Studies

Complexation results using single metals suggest that monorhamnolipids have potential for use as metal complexing ligands. However, commercial and industrial applications rarely involve single metal solutions. Since conditional stability constants are reported as log values, a difference of one log β value means a ten-fold difference in preference, favoring the metal with the larger log β. Log β values of individual metals should, therefore, predict removal order when monorhamnolipids are applied in a mixed metal solution. This was tested with two mixed metal studies.

The complexation preference of monorhamnolipids for metals with larger log β values was examined using a mixture of three metals. Pb²⁺, Cd²⁺ and Ca²⁺ were selected for the mixed metal study, because these metals represent large (9.13), intermediate (7.17), and small (4.10) log β values. In the first series of experiments, an equimolar amount of each metal was added (0.167 mM) for a total concentration of 0.5 mM metal. As expected, monorhamnolipids complexed Pb²⁺ much more effectively than Cd²⁺ or Ca²⁺ with 81, 97, and 100% of Pb²⁺ detected in the aqueous phase at concentrations of 1,

2, and 4 mM of monorhamnolipids, respectively (Figure 2.3). In contrast, aqueous phase Cd^{2+} and Ca^{2+} were 62 and 15% of added metal, respectively, at the 4 mM monorhamnolipid concentration.

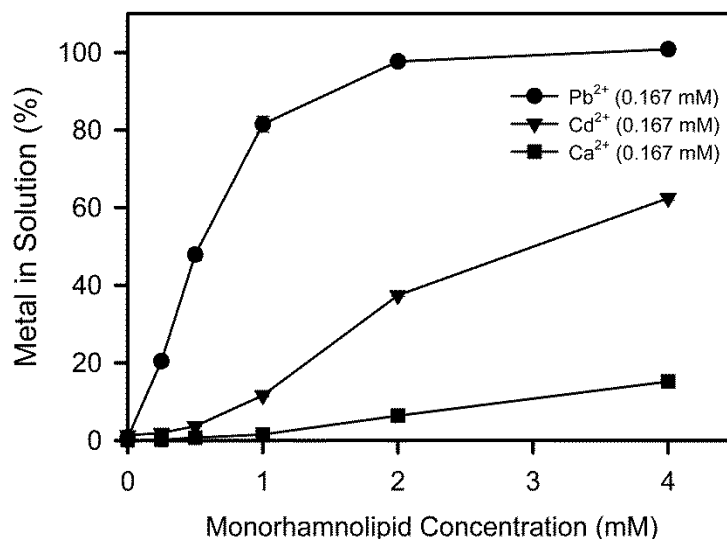


Figure 2.3 Effect of monorhamnolipid concentration on complexation of Pb^{2+} , Cd^{2+} , and Ca^{2+} in an equimolar metal mixture (each metal was added at a concentration of 0.167 mM). Each point represents the mean and standard deviation of 6 replicates.

A second experiment was performed to confirm that complexation of metals added at varying concentrations were dependent on their relative conditional stability constants. This experiment was performed because environmental samples are likely to contain a mixture of target metals and non-target metals in which the latter are present at considerably higher concentrations (e.g., Ca^{2+} , K^{+} etc.). The ability of monorhamnolipids to complex target metals over non-target metals was tested with 10-fold differences in metal concentrations: 0.45 mM Ca^{2+} , 0.045 mM Cd^{2+} , and 0.0045 mM Pb^{2+} (0.5 mM total metal concentration). Results show that 80 and 86% of Pb^{2+} , 14 and 27% of Cd^{2+}

and 3 and 5% of Ca^{2+} were complexed by 1 and 2 mM monorhamnolipid, respectively (Figure 2.4). As expected, in both experiments, removal of metals occurred in the order $\text{Pb}^{2+} \gg \text{Cd}^{2+} > \text{Ca}^{2+}$. These results confirm the usefulness of conditional stability constants as predictors for metal selectivity and removal order by monorhamnolipids.

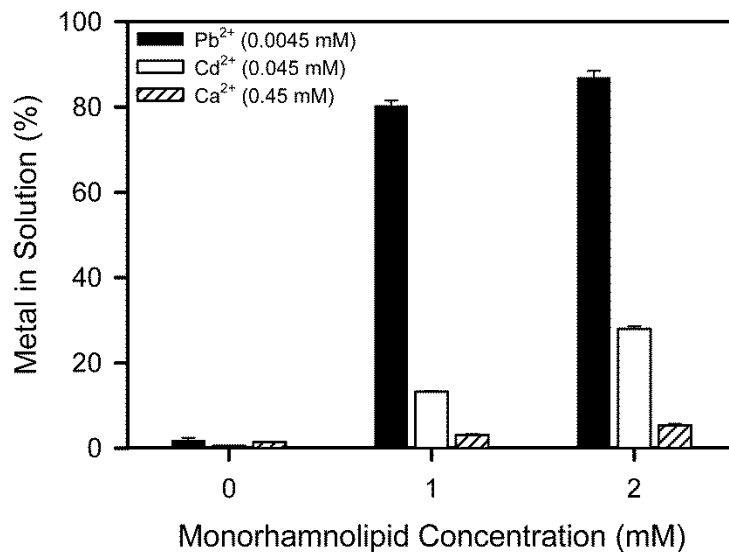


Figure 2.4 Effect of monorhamnolipid concentration on complexation of Pb^{2+} , Cd^{2+} , and Ca^{2+} in a 100:10:1 (Ca^{2+} : Cd^{2+} : Pb^{2+}) metal mixture. Each bar represents the mean and standard deviation of 6 replicates

Table 2.2 Estimated and observed complexation of metals across complexation experiments

		Monorhamnolipid Concentration					
		1 mM		2 mM		4 mM	
		Estimated ^c (μM)	Observed (μM)	Estimated ^c (μM)	Observed (μM)	Estimated ^c (μM)	Observed (μM)
Individual Metal Studies	Pb ²⁺ (500 μM)	386	343	498	466	500	524
	Cd ²⁺ (500 μM)	304	97	463	190	495	288
	Ca ²⁺ (500 μM)	230	11.5 ^a	354	21.5 ^a	438	44.0 ^a
Equimolar Mixed Metal Study	Pb ²⁺ (167 μM)	165	141	167	169	167	175
	Cd ²⁺ (167 μM)	142	19.5	162	62.5	166	104
	Ca ²⁺ (167 μM)	90.0	2.6	126	10.4	149	24.7
Order of Magnitude Mixed Metal Study^b	Pb ²⁺ (4.5 μM)	4.5	3.9	4.5	4.2		
	Cd ²⁺ (45 μM)	40.7	6.4	44.0	13.4		
	Ca ²⁺ (450 μM)	212.4	14.0	322	24.2		

^a Values calculated based on data from Ochoa Loza et al.²¹

^b 1 Pb²⁺ : 10 Cd²⁺ : 100 Ca²⁺

^c Values were calculated using Eq. 2.1. Metal bound to the resin is assumed to be free metal. Table 2.1 β and χ values and the concentrations given in this table were used as initial reaction conditions. Metal removal concentrations were calculated for each metal alone as an estimation of removal in the mixed reactions.

The equilibrium values of metal complexes were estimated using the stability constant equation $\beta = [ML_\chi]/([M][L]^\chi)$, log β and χ values from Table 2.1, and different initial concentrations of metal and monorhamnolipid (Table 2.2). For these calculations, it was assumed that all monorhamnolipids were in their anionic form, metal bound to the resin is free metal, the metals are present alone, and the observed metal concentrations are due to ML_χ where χ is equal to the value given in Table 2.1. A comparison of the estimated values to the observed values shows that estimates for Pb^{2+} are similar to what is observed, while estimates for Cd^{2+} and Ca^{2+} were generally much higher than what was observed. Given that there is more ligand available than the total metal for all treatments in the table, the ligand should not be limiting. The most probable explanation of the differences may be retention of monorhamnolipid:metal complexes on the resin, especially 1:1 complexes which would retain a net positive charge. Because Pb^{2+} estimates are essentially equivalent to the observed values, Pb^{2+} would be forming neutrally charged 2:1 complexes which are not retained on the resin. If true, this explanation highlights a failure to satisfy one of the foundational assumptions in the Schubert method: no anions or complex species are adsorbed to the resin.¹⁴⁴ If complexes are being retained, the numbers reported for the conditional stability constants and stoichiometries may be underreported.

2.4.3. Determinants of Complexation Strength

Conditional stability constants for 27 metals are reported herein; the coverage of metals across the periodic table enables examination of the data for trends associated with metal cation physical parameters to infer the determinants of monorhamnolipid:metal complexation strength. Identifying a specific determinant of monorhamnolipid:metal

interactions is difficult due to numerous factors that play a role in the coordination chemistry. Factors attributable to metal cations include, but are not limited to, cation charge, ionic radius, preferred coordination geometry, electron configuration, crystal field effects, and the Pearson's hardness of the metal. Monorhamnolipid ligand factors include metal binding pocket size, steric interference between monorhamnolipids, molecular conformation, and Pearson's hardness parameter similarity between monorhamnolipids' oxygen (Lewis base) and the reacting metal (Lewis acid)—the strongest and fastest reactions occur between hard-hard and soft-soft acid-base reactions.

Despite the numerous factors influencing complexation strength, we hypothesized a strong correlation between the stability constants and one or more physical parameters of the metals. Metal:monorhamnolipid conditional stability constants have significant ($p = < 0.0001$), strong (Pearson's $r = 0.71$) correlation to enthalpy of hydration and a significant ($p = 0.0045$), less strong (Pearson's $r = 0.55$) correlation to the ionic charge to radius ratio (using values from salts with 6 coordinating anions). No significant correlations were found for atomic radius, covalent radius, ionic radius (using values from salts with 6 or 8 coordinating anions), Pauling's electronegativity, or Pearson's hardness parameter (see Tables 2.3 for physical parameter values and Table 2.4 for correlation values). The enthalpy of hydration and ionic charge to radius ratio (using values from salts with 6 coordinating anions) are not suitable predictors of monorhamnolipid:metal conditional stability constants, however, because they are confounding parameters with a significant ($p = < 0.0001$) and strong (Pearson's $r = 0.92$) correlation. This is to be expected, as enthalpy of hydration is affected by both ion size and charge.²

Localized periodic trends can be found within groups of metals with similar characteristics. For example, the first row transition metals exhibit the Irving-Williams effect, a general trend in stability constants of $Mn^{2+} < Fe^{2+} < Co^{2+} < Ni^{2+} < Cu^{2+} > Zn^{2+}$ essentially irrespective of the nature of the ligand.^{146, 152} Example ligands following this trend include oxalic acid, glycine, salicylaldehyde, ethylenediamine, and ammonia. The data supporting the existence of this trend is observed with monorhamnolipids (Figure 2.5). The effect is caused by imperfect shielding of the nucleus as the number of protons increases, with a progressively higher apparent nuclear charge (despite equal formal charges) due to imperfect electron shielding of the nucleus. The stability constant decrease at Zn^{2+} is the result of complete filling of the d electron set and loss of crystal field stabilization energy.¹⁴⁶

A second example can be found in the REEs, or lanthanoids, in the first row of the f block. Due to the electron configurations within the f-block elements, the lanthanoids tend to have very similar coordination chemistry.¹⁴⁶ These metals bond with ligands primarily through electrostatic (ionic) interactions with the strongest complexes forming with hard base donors¹⁵³ such as the hydroxyl and carboxyl donors of monorhamnolipids. Examination of Table 2.1 shows that these metals behave somewhat predictably: they group together and have high stability constants as predicted for interactions between the lanthanoids and the hard base donor groups of the monorhamnolipids. The monorhamnolipid:REE stability constants do not, however, exhibit the smooth increase in $\log \beta$ characteristic of the lanthanide contraction, unlike previous studies with other ligands such as carbonate, oxalate, 5-sulfosalicylate, α -hydroxyisobutyrate, and fluoride.¹⁵⁴

Examination of the 95% confidence intervals in Table 2.1 suggests the possibility that this trend may be obscured by the precision of the method.

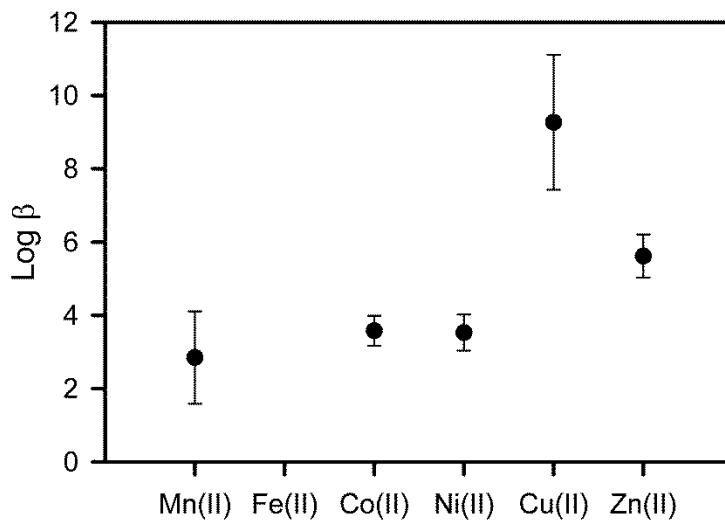


Figure 2.5 Log β values for the first row transition elements from Mn(II) to Zn(II) demonstrating the Irving-Williams effect. Error bars represent 95% confidence intervals.

Table 2.3 Values used to determine correlations between monorhamnolipid:metal conditional stability constants and physical parameters

Metal Ion	Log β	Charge (+)	Atomic Radius ^a (Å)	Covalent Radius ^a (Å)	Ionic Radius ^b		Pauling's Electronegativity ^a	Hydration Enthalpy ^c (-kJ mol ⁻¹)	Pearson's Hardness Parameter ^d (eV)
					6-Coordinated (Å)	8-Coordinated (Å)			
Eu ³⁺	9.77	3	2.56	1.85	0.947	1.066	1.20	3600	
Nd ³⁺	9.69	3	2.64	1.64	0.983	1.109	1.14	3420	
Tb ³⁺	9.65	3	2.51	1.59	0.923	1.04	1.10	3540	
Dy ³⁺	9.57	3	2.49	1.59	0.912	1.027	1.22	3570	
La ³⁺	9.29	3	2.74	1.25	1.032	1.16	1.10	3296	15.4
Al ³⁺	9.22	3	1.82	1.18	0.535		1.61	4665	45.8
Y ³⁺	9.11	3	2.27	1.62	0.9	1.019	1.22	3583	
Pr ³⁺	9.04	3	2.67	1.65	0.99	1.126	1.13	3405	
Lu ³⁺	8.20	3	2.25	1.56	0.861	0.977	1.27	3530	
In ³⁺	6.70	3	2.00	1.44	0.8	0.92	1.78	4112	
Fe ³⁺	5.16	3	1.72	1.17	0.645	0.78	1.83	4430	13.1
Cu ²⁺	9.27	2	1.57	1.17	0.73		1.90	2100	8.3
Pb ²⁺	9.13	2	1.81	1.47	1.19	1.29	2.33	1481	8.5
Cd ²⁺	7.17	2	1.71	1.41	0.95	1.1	1.69	1807	10.3
Zn ²⁺	5.62	2	1.53	1.25	0.74	0.9	1.65	2046	10.8
Hg ²⁺	4.49	2	1.76	1.49	0.72	0.89	2.00	1824	7.7
Ca ²⁺	4.10	2	2.23	1.74	1	1.12	1.00	1577	
Sr ²⁺	3.95	2	2.45	1.91	1.18	1.26	0.95	1443	
Co ²⁺	3.58	2	1.67	1.16	0.745	0.9	1.88	1996	
Ni ²⁺	3.53	2	1.62	1.15	0.69		1.91	2105	8.5
Ba ²⁺	3.22	2	2.78	1.98	1.35	1.42	0.89	1305	12.8
Mn ²⁺	2.85	2	1.79	1.17	0.83	0.96	1.55	1841	

Table 2.3 Values used to determine correlations between monorhamnolipid:metal conditional stability constants and physical parameters

Metal Ion	Log β	Charge (+)	Atomic Radius ^a (Å)	Covalent Radius ^a (Å)	Ionic Radius ^b		Pauling's Electronegativity ^a	Hydration Enthalpy ^c (-kJ mol ⁻¹)	Pearson's Hardness Parameter ^d (eV)
					6-Coordinated (Å)	8-Coordinated (Å)			
Mg ²⁺	2.66	2	1.72	1.36	0.72	0.89	1.31	1921	32.5
Rb ⁺	1.57	1	2.98	2.16	1.52	1.61	0.82	293	11.7
K ⁺	0.96	1	2.77	2.03	1.38	1.51	0.82	322	

^a *Periodic Table of the Elements*. VWR/Sargent-Welch, 1998

^b R. D. Shannon¹⁵⁵

^c D. W. Smith¹⁵⁶.

^d R. G. Parr. & R. G. Pearson¹⁵⁷

Table 2.4 Pearson's correlation coefficients for monorhamnolipid:metal conditional stability constants and the physical parameters of metals

Physical Parameter	Pearson's Correlation Coefficient (r)	Significance Probability (p-value)
Atomic Radius	0.0648	0.7582
Covalent Radius	-0.2080	0.3183
Ionic Radius (Coordination Number 6)	-0.2730	0.1868
Ionic Radius (Coordination Number 8)	-0.2696	0.2251
Pauling's Electronegativity	0.1410	0.5013
Enthalpy of Hydration	0.7145	< 0.0001
Pearson's Hardness Parameter	0.1252	0.6983
Charge/Ionic Radius (Coordination Number 6)	0.5493	0.0045

2.4.4. Potential Monorhamnolipid Metal-Remediation Applications

Metal containing waste streams constitute not only an opportunity for recovery of critical materials, but also a threat to environmental and human health if released to the environment untreated. Unlike organic compounds, metals cannot be biodegraded and are subject to accumulation; the ultimate fate of metals is dependent on the biogeochemical environment into which they are released. Risks associated with metal release and accumulation are widely recognized, and regulations are becoming increasingly stringent regarding permissible metal content of waste effluents. For uranium, interest lies not in recovery from waste streams, but mining seawater's 4 billion tons ($3.3 \mu\text{g l}^{-1}$) of dissolved uranium (primarily as uranyl tricarbonate)^{150, 158} in lieu of opening new terrestrial mines. Metal recovery from aqueous sources should, thus, be of interest as a way of both recovering critical materials and preventing environmental contamination.

Many technologies have been designed to remove metals from aqueous media: chemical precipitation, flotation, ion-exchange, adsorption, membrane filtration, and electrochemical treatment.^{133, 159} Of these technologies, monorhamnolipids may be suitable for use in froth fractionation and membrane filtration, specifically micellar-enhanced ultrafiltration. As demonstrated by this research, monorhamnolipids exhibit high selectivity for REEs, UO_2^{2+} , and metals of environmental concern. Additionally, it has previously been reported that monorhamnolipids are biodegradable, exhibit low toxicity, and can be recovered for reuse by manipulation of pH. When acidified to pH ~ 2 , monorhamnolipids become poorly soluble and release complexed metal ions,⁷⁴ allowing for recovery of both complexing agent and metal. Taken together, these characteristics suggest the potential for recovery of REEs and other metals from aqueous media by

monorhamnolipids. Future research should focus on metal recovery using rhamnolipids in naturally occurring metalliferous waters and waste streams generated by different industries. These aqueous resources are complex, heterogeneous, and vary by source, thus, the operational limits for application of rhamnolipids must be delineated.

2.5. Conclusion

Interactions between metals and monorhamnolipids have now been reported for all regions of the periodic table. Results show that monorhamnolipid selectively complexes economically important metals, such as the critical rare earth elements as well as metals of environmental concern, in comparison to common soil and water cations. Results suggest that the monorhamnolipid:metal conditional stability constants reported here can be used to predict the removal of metals from mixed metal waste streams.

CHAPTER 3

ENVIRONMENTAL COMPATIBILITY AND METAL CONDITIONAL STABILITY CONSTANTS OF NOVEL MONORHAMNOLIPID BIOSURFACTANT DIASTEREOMERS

3.1. Abstract

We have recently reported a novel synthetic pathway for monorhamnolipid. Synthetic monorhamnolipid differs from biologically produced material in that synthetic monorhamnolipid is produced as a single congener depending on the fatty acid used and that it is produced as a mixture of four diastereomers. Here we compare the biodegradability, acute toxicity (Microtox assay), embryo toxicity (Zebrafish assay), and metal binding capacity of synthetic monorhamnolipids with biologically produced monorhamnolipid. All of the monorhamnolipids were found to be inherently biodegradable with mineralization ranging from 42 to 92%. Microtox assay data shows all of the monorhamnolipids are categorized as slightly toxic according to the US Environmental Protection Agency ecotoxicity categories with 5 min EC₅₀ values ranging from 39.1 to 86.5 μM . Of the 22 parameters tested, the zebrafish assay resulted in toxic effects only for mortality at 120 hours post fertilization; all of the monorhamnolipids caused significant mortality at 640 μM except diastereomer *R,R* which showed no toxic effects at the concentrations tested. The conditional stability constants ($\log \beta$) for the monorhamnolipids with Pb^{2+} and Cd^{2+} ranged from 11.29 to 7.33 and 7.49 to 4.85, respectively. These data begin to provide some of the information regarding

monorhamnolipid diastereomers that is pertinent to their use as environmental amendments.

3.2. Introduction

The addition of surfactants to enhance remediation of contaminated sites can lead to dramatic improvements in remediation time and completeness.¹⁶⁰ However, use of surfactant amendments must be carefully considered to ensure the treatment does not cause environmental harm or a secondary contamination event. Surfactants can be toxic to life at all levels;¹⁶¹ in the 1967 Torrey-Canyon oil spill off the English coast, dispersants—a mixture of solvents and surfactants—used to treat the spilled oil were more toxic than the oil alone. In areas “close to dispersant spraying practically all animal life was killed, while many algae... were killed or damaged.”¹⁶² During the 2010 Deepwater Horizon oil spill in the Gulf of Mexico, millions of liters of COREXIT dispersants were released to disperse surface and sub-surface oil. COREXIT dispersants are reported to have negative environmental effects: high toxicity to oil degrading microbial communities,¹⁶³ increased polycyclic aromatic hydrocarbon mobility into anoxic sediments where degradation rates are slower,¹⁶⁴ and formation of mutagenic oil-dispersant mixtures which affect marine organisms.¹⁶⁵ Studies show some dispersant components increase biodegradation while others are inhibitory, and by encouraging selective microbial degradation of specific hydrocarbons, dispersants can result in increased or decreased toxicity of residual oil.¹⁶⁶ In summary, while dispersant use for oil spills is routine, research on the environmental compatibility and efficacy of dispersants yields conflicting results due to variability in environmental conditions, hydrocarbon sources, and dispersant compositions studied.¹⁶⁶

The use of bio-based and biogenic surfactants as amendments in remediation applications is attracting increased interest because they can be less toxic and more biodegradable than synthetic compounds.¹⁶⁰ One example of a biological compound that has been studied extensively with respect to potential environmental applications is rhamnolipid, a family of biosurfactants produced primarily by *Pseudomonas aeruginosa* strains. Rhamnolipids are considered “green” materials; they are a renewable resource and generally accepted as more biodegradable and less toxic than currently used synthetic surfactants.¹⁶⁷ Rhamnolipids have been examined as remediation agents in numerous environmental applications to: increase the solubility and biodegradation of hydrocarbons,^{97, 139, 168} bind metals,^{19, 21, 74} decrease metal toxicity,⁹⁵ modify cellular characteristics and behavior,¹⁶ improve oil recovery,¹⁵ and for biocidal activity.^{169, 170} Despite this list of potential applications, the technical and economic hurdles of biologically producing rhamnolipids has limited the scale-up and use for remediation and other applications.^{171, 172}

Biosynthesized rhamnolipids are composed of one (monorhamnolipid) or two (dirhamnolipid) L-rhamnose sugars connected through a glycosidic bond to two β -hydroxy fatty acids (varying from 8 to 16 carbons) linked by an ester bond.²⁰ The β -hydroxy fatty acids are (*R*)-3-hydroxy fatty acids, resulting in two *R* oriented chirality centers (excluding the chirality centers on the rhamnose moiety).¹⁷³⁻¹⁷⁶ Biosynthetic rhamnolipid is thus composed of a congener mixture of *R,R* rhamnolipids.

Recent advances in glycosylation research have enabled synthetic production of rhamnolipid as an alternative to biological production. The chemical synthesis uses minimal steps, renewable resources, and recyclable materials.¹⁷⁷ There are two major

differences between synthetically and biologically produced rhamnolipids. The first is that the number of congeners can be controlled in synthetic rhamnolipids. Only a single congener is produced if a single β -hydroxy fatty acid is used. If more than one β -hydroxy fatty acid is used then a congener mixture will be produced that reflects the component fatty acids used in the synthesis. The second difference is that chemical synthesis of rhamnolipid results in the production of four diastereomers: *R,R*; *R,S*; *S,S*; and *S,R* (Figure 3.1). The *R,S*; *S,S*; and *S,R* diastereomers represent novel molecules which have not been assessed for toxicity, biodegradability, or useful applications, e.g., metal binding. Yet, it is well-known that modifying chirality centers can alter toxicity,¹⁷⁸ degradability, and transformation products.¹⁷⁹⁻¹⁸¹

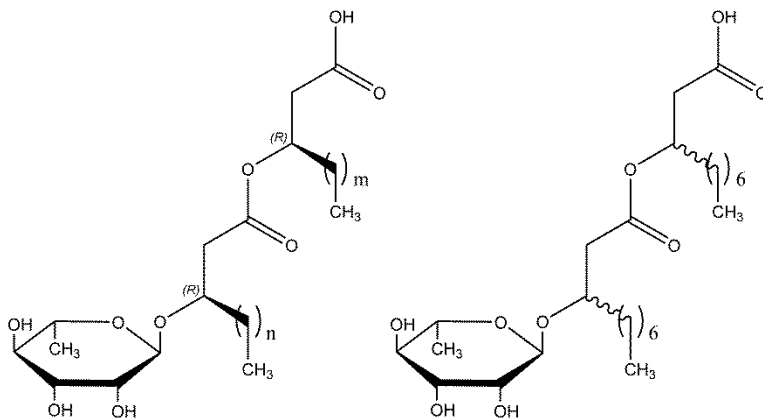


Figure 3.1 Structures of biosynthesized (left) and synthetic (right) monorhamnolipids utilized in this study. The varying chain lengths of bio-mRL are represented by ‘m’ and ‘n’ values which vary from 4 to 12.

The objective of this study is to examine the biodegradability, toxicity, and metal binding characteristics of synthetic monorhamnolipid diastereomers relative to a biosynthetic monorhamnolipid congener mixture. The synthetic monorhamnolipid

studied is Rha-C10-C10 (rhamnosyl- β -hydroxyalkanoyl- β -hydroxyalkanoate). Rha-C10-C10 was selected because it is the most abundant congener (typically 75-85%) produced by *Pseudomonas aeruginosa* ATCC 9027, the model strain used in this study.¹⁴¹

Biodegradability was assessed by CO₂ evolution (mineralization) in biometer flasks. Bacterial acute toxicity was assessed using the Microtox assay and eukaryotic toxicity via zebrafish developmental assays. To determine diastereomer metal complexation performance, conditional stability constants for Pb²⁺ and Cd²⁺ were determined. The synthetic diastereomers were examined individually and as a mixture and were compared to a congener mixture of biosynthetic monorhamnolipid, hereafter referred to as bio-mRL.

3.3. Materials and Methods

3.3.1. Monorhamnolipids

All monorhamnolipid solutions were made in ultrapure water (≥ 18 M Ω -cm) using a molecular weight of 504 g mol⁻¹ and pH adjusted to 7.0 unless otherwise noted.

3.3.1.1. Biosynthesized Rhamnolipid

3.3.1.1.1. Bio-mRL Production

Pseudomonas aeruginosa ATCC 9027 was obtained from the American Type Culture Collection and kept as a glycerol freezer stock at -80° C. This strain has been previously shown to only produce monorhamnolipid congeners.^{138, 139} *Pseudomonas aeruginosa* was initially cultured for 24 h at 37° C on a PTYG agar (0.5% protease peptone, 0.5% tryptone, 1% yeast extract, 0.06% MgSO₄•7H₂O, 7x10⁻⁴% CaCl₂•2H₂O, and 1% glucose). The agar culture was transferred to Kay's mineral medium for 24 h growth at 37° C and 200 rpm. Kay's mineral medium contains 100 ml of solution A

(0.3% $\text{NH}_4\text{H}_2\text{PO}_4$, 0.2% K_2HPO_4 , and 0.2% glucose), 1 ml solution B (0.025% $\text{FeSO}_4 \cdot 7\text{H}_2\text{O}$) and 1 ml solution C (10% $\text{MgSO}_4 \cdot 7\text{H}_2\text{O}$). The pre-culture was transferred to a pH 7 minimal salts medium (MSM) with 2% glucose. MSM is composed of 1 ml of solution A (0.25% NaNO_3 , 0.04% $\text{MgSO}_4 \cdot 7\text{H}_2\text{O}$, 0.1% KCl , 0.1% NaCl , 0.005% $\text{CaCl}_2 \cdot 2\text{H}_2\text{O}$, and 0.4% H_3PO_4) mixed with 1 ml of solution B (0.05% $\text{FeSO}_4 \cdot 7\text{H}_2\text{O}$, 0.15% $\text{ZnSO}_4 \cdot 7\text{H}_2\text{O}$, 0.15% $\text{MnSO}_4 \cdot \text{H}_2\text{O}$, 0.03% H_3BO_3 , 0.015% $\text{CoCl}_2 \cdot 6\text{H}_2\text{O}$, 0.015% $\text{CuSO}_4 \cdot 5\text{H}_2\text{O}$, and 0.01% $\text{Na}_2\text{MoO}_4 \cdot 2\text{H}_2\text{O}$). The MSM culture was placed in a 37° C gyratory shaker, shaken for 72 h at 200 rpm, and bio-mRL was harvested as described below.

3.3.1.1.2. Bio-mRL Purification.

The MSM culture was centrifuged (10,000 rpm for 10 min) to remove cells and cellular debris, followed by removal and acidification of the supernatant to a pH of 2 using HCl to precipitate the bio-mRL.¹³⁸ The precipitate was pelleted by centrifugation and then dissolved in a 9:1 chloroform:methanol mixture and separated from remnant water using a separatory funnel. The solvent was removed by rotoevaporation. The concentrated bio-mRL was purified using a solvent mixture of 6:6:6:1:1 (v/v) of hexane:dichloromethane:ethyl acetate:chloroform:methanol in 0.1% acetic acid by elution through a 22 x 300 mm gravity-based, glass chromatography column packed with 45 g of 60-Å-pore silica gel. Bio-mRL was collected when column eluent fractions tested positive for rhamnose with anthrone reagent dissolved in H_2SO_4 . The solvent mixture was removed from the rhamnolipid by rotoevaporation, and purity was assessed by high pressure liquid chromatography.¹³⁸ Characteristics of the bio-mRL are provided in Table 3.1.

3.3.1.2. Synthetic Monorhamnolipids

The synthetic monorhamnolipid diastereomers were produced as >87% purity oils of individual diastereomers and a mixture of all four diastereomers as described by Coss.¹⁷⁷ The surfactants were used as received. Characteristics of the diastereomers are provided in Table 3.1.

3.3.2. Biodegradability Testing

Mineralization of bio-mRL and synthetic monorhamnolipids was measured by quantitation of CO₂ as described previously with the following specifications.¹⁸² Each experiment was performed in triplicate sealed biometer flasks (Corning Life Sciences) and included a control treatment also in triplicate without added monorhamnolipid. The microbial inoculum was aeration basin mixed liquor suspended solids (MLSS) from the Tres Rios Water Reclamation Facility (Pima County, AZ). The MLSS was kept aerated and used within 4 h of collection. Before addition to flasks, the MLSS was allowed to settle in a graduated cylinder until the apparent volume of solids became constant. The supernatant was decanted and reserved. The total reaction volume in each flask was 25 ml consisting of 2 ml settled MLSS flocculate, 15 ml MLSS supernatant, 6 ml EPA minimal salts medium¹⁸³, and 2 ml monorhamnolipid (5 mg ml⁻¹) solution in ultrapure water (final concentration 400 mg l⁻¹). Control flasks received 2 ml ultrapure water with no monorhamnolipid. Flasks were shaken on a rotary shaker at 25° C for 30 d and assayed for CO₂ evolution every 24 h for the first 6 d and then every 48 h thereafter.

Carbon dioxide produced in the flasks was captured in 10 ml of 0.1 M KOH placed into the biometer flask's sidearm through the formation of K₂CO_{3(aq)}. The amount of CO₂ produced was measured by titration; the sidearm solution was removed and mixed

with phenolphthalein indicator, 1 ml of 1 M BaCl₂, and 5 ml of water used to wash the sidearm. This solution was titrated with 0.05 M HCl. The K₂CO_{3(aq)} reacts with BaCl_{2(aq)} to form BaCO_{3(s)} which prevents the release and recapture of CO₂ by unreacted OH⁻ during titration. All reagents were made with ultrapure water purged of CO₂ for 10 min with nitrogen gas sparging.

Mineralization of the monorhamnolipid treatments was measured as percent mineralization which was calculated using Equation 3.1:

$$\% \text{ mineralization} = \frac{CO_{2 \text{ mRL}}}{C_{\text{mRL}}} \times 100 \quad [3.1]$$

where CO_{2 mRL} is the moles of CO₂ from mineralized monorhamnolipid and C_{mRL} is moles of carbon added as monorhamnolipid (based on MW 504 g mol⁻¹). A monorhamnolipid-free control was used to quantify CO₂ production from mineralization of carbon in the MLSS solids and supernatant. Thus, CO_{2 mRL} was calculated using Equation 3.2:

$$CO_{2 \text{ mRL}} = CO_{2 \text{ treatment}} - CO_{2 \text{ control}} \quad [3.2]$$

Where CO_{2 treatment} is moles of CO₂ produced for each treatment and CO_{2 control} is moles of CO₂ measured in the monorhamnolipid-free control.

3.3.3. Microtox Acute Toxicity Assay

Prokaryotic acute toxicity of the surfactants was assessed using a Microtox[®] Model 500 analyzer (Modern Water Inc., New Castle, DE, USA). The Microtox[®] assay assesses toxicity by determining the effective concentration (EC₅₀) at which a toxicant reduces bioluminescence of the marine bacterium *Vibrio fischeri* by 50% relative to a toxicant-free control. Reagents were sourced from Modern Water Inc. (New Castle, DE). Triplicate experiments with monorhamnolipid solutions were tested as previously

described.¹⁸⁴ In brief, a 2 mM monorhamnolipid stock solution was diluted to adjust the osmotic strength using the Microtox osmotic adjustment solution as instructed by the manufacturer. The adjusted solution was then 1:1 serially diluted using the Microtox diluent to create 9 monorhamnolipid concentrations (3.5-889 μM). Microtox diluent was used as the toxicant free control. Initial bioluminescence was measured then the toxicant solutions were mixed with the bacterium, and bioluminescence was measured at 5, 15, and 30 min to determine the EC_{50} for each time point.

3.3.4. Zebrafish Toxicity Assay

Zebrafish assays were performed in the Sinnhuber Aquatic Research Laboratory, Oregon State University, Corvallis OR. Zebrafish (*Danio rerio*) embryos with intact chorions were exposed to the monorhamnolipid treatments from 6 to 120 h post-fertilization (hpf), following the protocol outlined in Truong et al.¹⁸⁵ Briefly, at 6 hpf, embryos were placed manually in 96-well plates containing embryo medium (90 μL) consisting of (in mg l^{-1}): NaCl (875.0), KCl (37.5), $\text{CaCl}_2 \cdot \text{H}_2\text{O}$ (145.0), KH_2PO_4 (20.5), Na_2HPO_4 (7.1), and $\text{MgSO}_4 \cdot 7\text{H}_2\text{O}$ (4.9). Monorhamnolipid samples were added (10 μL) in the concentration range 0.064-640 μM , and 32 replicates were run for each concentration and controls, all including 0.64% dimethylsulfoxide (DMSO) to ensure dissolution when preparing the stock solutions of the monorhamnolipids. The 96-well plates were covered in foil and incubated at 28° C in the dark. At 24 and 120 hpf, development abnormality and mortality assessments were performed.¹⁸⁵ The endpoints evaluated at 24 hpf included mortality, developmental delay, spontaneous movement, and notochord; and at 120 hpf included: mortality, notochord, yolk sac edema, body axis, eye defect, snout, jaw, optic vesicle, pericardial edema, brain, somite, pectoral fin, caudal fin,

pigment, circulation, truncated body, swim bladder, and touch response. Endpoint scoring and statistical analyses were performed in R software as described previously.¹⁸⁵

3.3.5. Metal Conditional Stability Constant Assay

The conditional stability constant of the surfactants was determined using an ion-exchange method described by Ochoa-Loza²¹ with minor modifications. The ion exchange method utilizes multiple concentrations of monorhamnolipid mixed with metal-complexed SP Sephadex C25 resin (GE Healthcare) to determine the conditional stability between monorhamnolipid and metals. The ion exchange resin was, prepared by soaking in ultrapure water overnight. The hydrated resin was washed with equal parts ultrapure water, then pH 6.9 disodium PIPES buffer [Piperazine-N,N'-bis(2-ethanesulfonic acid)], and air-dried; sufficient buffer was used to saturate the resin with Na⁺. Ion exchange reactions took place in 15-ml metal-free centrifuge tubes. Each reaction contained 100 mg of prepared resin and a total volume of 10 ml with final concentrations of 0.5 mM Pb²⁺ or Cd²⁺, 0.01 M PIPES buffer at pH 6.9, and 0, 0.1, 0.5, 1, 2, and 4 mM of the monorhamnolipid solutions (pH 6.9). In the absence of monorhamnolipids, 99% of the metal is bound by the resin. Metal solutions were mixed with ultrapure water 0.5 h before use. Reactions were shaken horizontally on a gyratory shaker (200 rpm) for 2 h, allowed to settle vertically for a minimum of 1 h, and then a sample of supernatant was removed and diluted in trace-metals grade 2% HNO₃. Metal concentrations were measured by inductively coupled plasma-atomic emission spectroscopy. Calibration curves were prepared using standard solutions in 2% HNO₃. A detailed discussion of this method is located in Appendix A.

3.4. Results

3.4.1. Biodegradation Assay

The bio-mRL and the diastereomers were mineralized—transformed into CO₂, H₂O, and cell mass—to varying extents ranging from 42 to 92% (Figure 3.2, Table 3.1). A limited number of biometer flasks allowed only four treatments and a control to be assayed in each experiment. Therefore two experiments were performed: experiment 1 compared mineralization of the four diastereomers (Figure 3.2A) and experiment 2 compared the bio-mRL, diastereomer *R,R*, and the diastereomer mixture (Figure 3.2B). Mineralization was calculated at the estimated transition from exponential phase to stationary phase (filled symbols in Figure 3.2). It is assumed that CO₂ production measured after this transition point is due to endogenous decay (decay and degradation of new cells produced), and this CO₂ was not included in calculations for estimated monorhamnolipid biodegradation.

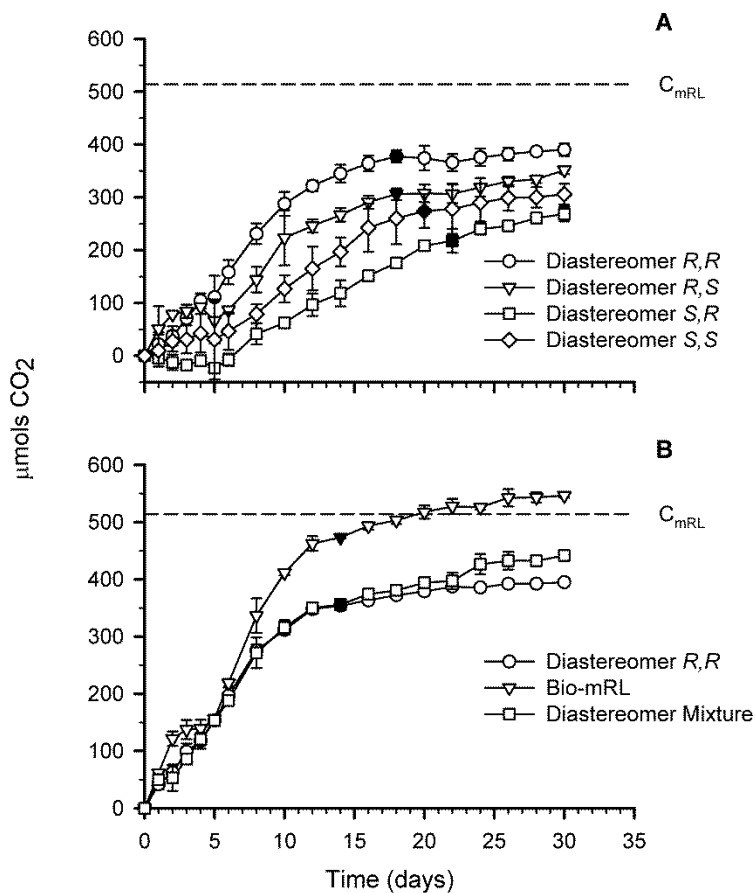


Figure 3.2 CO_2 production due to mineralization of **(A)** diastereomer *R,R*; *R,S*; *S,S*; and *S,R* and **(B)** diastereomer *R,R*, diastereomer mixture, and bio-mRL. C_{mRL} represents the moles of carbon added as monorhamnolipid. Closed symbols indicate the estimated transition from exponential phase to stationary phase where mineralization was calculated. Each point represents the mean and standard deviation of 3 replicates.

Table 3.1 Characteristics of the monorhamnolipid treatments

Monorhamnolipid Treatment	Purity (%)	CMC ^a (μM)	Minimum Surface Tension ^a	Area ^a	Congener Mixture	Mineralization ^b
			(mN m^{-1})	($\text{\AA}^2 \text{ molecule}^{-1}$)		(%)
Bio-mRL		201 \pm 12	29.0 \pm 0.5	85.8 \pm 1.9	Yes	92 ²
Diastereomer Mixture		277 \pm 21	27.9 \pm 0.3	73 \pm 2	No	69 ²
Diastereomer <i>R,S</i> ^c	99	79 \pm 3	27.4 \pm 0.2	82 \pm 1	No	59 ¹
Diastereomer <i>R,R</i> ^c	87	270 \pm 77	28.1 \pm 0.2	119 \pm 10	No	73 ¹ , 69 ²
Diastereomer <i>S,S</i> ^c	92	201 \pm 51	29.5 \pm 0.2	94 \pm 8	No	53 ¹
Diastereomer <i>S,R</i> ^c	92	180 \pm 24	28.5 \pm 0.2	105 \pm 4	No	42 ¹

^a Measured at pH 8

^b Mineralization values were determined using two experiments as indicated by the superscript next to each value. 1 = experiment 1 (Fig. 3.2A), 2 = experiment 2 (Fig. 3.2B). Diastereomer *R,R* was evaluated in both experiments.

^c CMC, minimum surface tension, and molecular area data from Palos Pacheco et al.¹⁸⁶

3.4.2. Microtox Acute Toxicity Assay

Microtox results revealed EC₅₀ values ranging from 39.1 to 86.5 µM at 5 min and 31.3 to 55.9 µM at 30 min (Table 3.2). Over time, within treatments, the bio-mRL, *R,R*, *S,S*, and *S,R*, had significantly increased ($\alpha=0.05$) toxicity between the 5 and 15 min exposures while there was no increase for *R,S* and the diastereomer mixture (data not shown). However, there was no significant change in toxicity between the 15 and 30 min exposure times for any of the treatments (data not shown).

Table 3.2 Bacterial acute toxicity EC₅₀ values at 5, 15, and 30 minutes for Microtox assay (µM)

Monorhamnolipid Treatment	5 minute ^a			15 minute ^a			30 minute ^a		
	(µM)			(µM)			(µM)		
Bio-mRL	79.3	± 10.1	A	50.5	± 7.9	AB	45.0	± 4.8	AB
Diastereomer Mixture	39.1	± 10.3	B	31.3	± 6.9	B	31.3	± 5.9	B
Diastereomer <i>R,S</i>	86.5	± 14.4	A	57.7	± 13.5	A	55.9	± 15.3	A
Diastereomer <i>R,R</i>	77.7	± 4.0	A	53.1	± 3.3	AB	46.7	± 1.2	AB
Diastereomer <i>S,S</i>	63.5	± 8.4	AB	42.1	± 4.4	AB	38.4	± 3.7	AB
Diastereomer <i>S,R</i>	61.1	± 4.6	AB	39.1	± 2.9	AB	36.1	± 2.9	AB

^a Values reported are the means of triplicate trials ± the standard deviations of the mean. Significant treatment differences were determined by one-way ANOVA using the Tukey–Kramer HSD test to compare means ($\alpha = 0.05$). Each column was tested independently. Levels not connected by same letter are significantly different.

Among treatments, a comparison of EC₅₀ values at each time point tested shows that the *R,S*, *R,R*, and bio-mRL treatments were generally least toxic and the diastereomer mix was most toxic (Table 3.2). Statistical analysis of these results shows that the

diastereomer mixture was significantly ($\alpha = 0.05$) more toxic than the *R,S* diastereomer at all time points and more toxic than the bio-mRL and the *R,R*, diastereomer at 5 min (Table 3.2). There was no significant difference between the bio-mRL and individual diastereomers at any time point.

3.4.3. Zebrafish Toxicity Assay

Overall, the only developmental endpoint affected of those measured in the concentration range of 0 to 640 μM monorhamnolipid was mortality. All treatments, except *R,R*, showed significant mortality at 640 μM (Figure 3.3) relative to the no monorhamnolipid treatment. The most toxic diastereomer was *R,S*, with 100% mortality (32 out of 32), followed by *S,S*, with 81% mortality. The diastereomer mixture, *S,R*, and the bio-mRL all exhibited similar 120 hpf mortality ranging from 56 to 66%, while the *R,R* diastereomer showed no mortality among the 32 replicates. Mortality at 120 hpf was also significant, although at a lower percent mortality, for *S,S* at 6.4 μM (19% mortality) and *R,S* at 64 (13%) and 0.064 (13%) μM . Developmental endpoint assessment suggests that mortality occurred at an early stage, before hatching from the chorion (Figure 3.4), suggesting the toxicity may result from the rapid transport of the monorhamnolipid across the chorion at very early developmental stages.

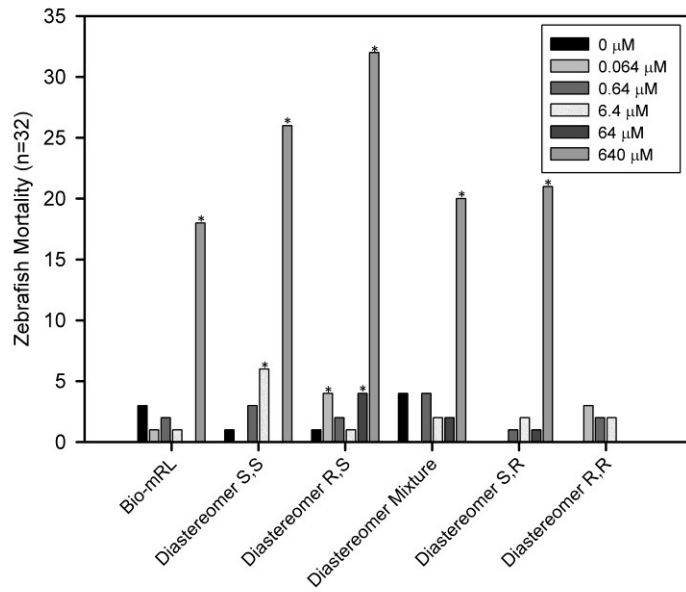


Figure 3.3 Mortality incidences (out of 32) at 120 hpf for monorhamnolipid treatments from 0 to 640 μM . Stars indicate a significant difference in mortality compared to a toxicant free control.

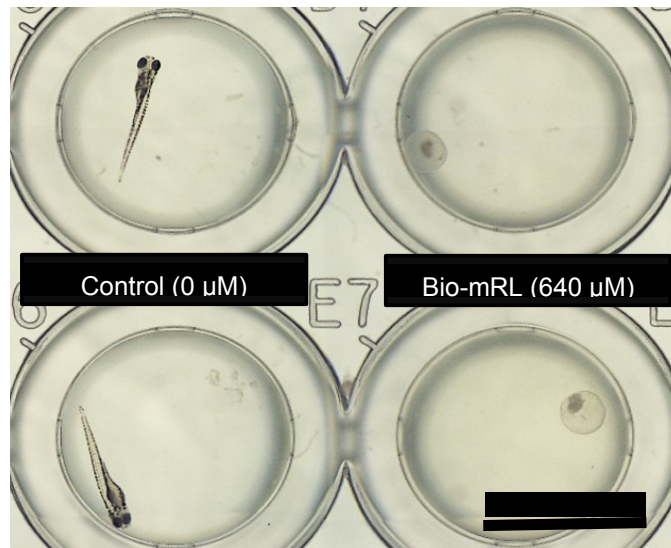


Figure 3.4 Detail of light micrograph showing 120 hpf zebrafish in a 96-well plate. Left wells: control (no monorhamnolipid added); Right wells: bio-mRL (640 μM).

3.4.4. Metal Conditional Stability Constant Assay

The ability of the synthetic and bio-mRL rhamnolipids to bind Pb^{2+} and Cd^{2+} was compared using calculated conditional stability constants ($\log \beta$). The conditional stability constants for Pb^{2+} ranged over four orders of magnitude, from 11.29 to 7.33 decreasing in the order: $S,S \approx S,R > \text{diastereomer mix} > R,S \approx \text{bio-mRL} > R,R$ (Table 3.3). The conditional stability constants for Cd^{2+} ranged over 2.6 orders of magnitude, from 7.49 to 4.85 decreasing in the order: $S,R \approx \text{bio-mRL} > R,S > S,S \approx \text{diastereomer mix} > R,R$ (Table 3.4). The highest stability constants for both metals were observed with the S,R diastereomer and lowest was the R,R diastereomer. However, the order of the remaining monorhamnolipids was metal-dependent.

These experiments also allow calculation of the stoichiometric ratio (χ) of rhamnolipid ligand to metal (Tables 3.3 and 3.4). This ratio varied from 2.1 to 3.0 for Pb^{2+} following the same order as the conditional stability constants. For Cd^{2+} , the ratio did not vary widely for five of the monorhamnolipids tested (1.9 to 2.1). However the R,R diastereomer had a lower ligand to metal ratio of 1.2.

Table 3.3 Conditional stability constants, stoichiometric ratios, and statistical analysis for Pb²⁺ complexes with monorhamnolipid treatments

Monorhamnolipid Treatment	Log β	Std. Error log β	95% Conf. Limits log β		χ	Coefficient of Variation (%)		R ²
			Lower	Upper		Log β	χ	
Bio-mRL	8.95	0.162	8.56	9.38	2.22	1.8	2.3	0.985
Diastereomer <i>R,S</i>	9.00	0.150	8.74	9.32	2.23	1.7	2.2	0.986
Diastereomer <i>R,R</i>	7.33	0.391	6.62	8.00	2.10	5.3	6.1	0.905
Diastereomer <i>S,S</i>	11.29	0.352	10.49	12.10	2.98	3.1	3.9	0.961
Diastereomer <i>S,R</i>	11.15	0.391	10.23	11.81	3.00	3.5	4.3	0.951
Diastereomer Mixture	9.96	0.344	9.12	10.72	2.63	3.5	4.3	0.950

Table 3.4 Conditional stability constants, stoichiometric ratios, and statistical analysis for Cd²⁺ complexes with monorhamnolipid treatments

Monorhamnolipid Treatment	Log β	Std. Error log β	95% Conf. Limits log β		χ	Coefficient of Variation (%)		R ²
			Lower	Upper		Log β	χ	
Bio-mRL	7.45	0.270	6.87	8.22	2.04	3.6	13.2	0.952
Diastereomer <i>R,S</i>	7.29	0.147	6.95	7.62	2.02	2.0	2.4	0.984
Diastereomer <i>R,R</i>	4.85	0.609	3.42	6.08	1.24	12.5	16.2	0.977
Diastereomer <i>S,S</i>	6.91	0.148	6.53	7.23	1.88	2.1	2.6	0.981
Diastereomer <i>S,R</i>	7.49	0.147	7.13	7.79	2.14	2.0	2.3	0.986
Diastereomer Mixture	6.81	0.169	6.41	7.15	2.04	2.5	2.7	0.979

3.5. Discussion

3.5.1. Biodegradability of Synthetic Monorhamnolipids

The Environmental Protection Agency classifies chemicals using the arbitrary classification “readily biodegradable” when the chemicals have passed certain specified screening tests for ultimate biodegradability. Because the screening tests are stringent, the readily biodegradable classification allows one to assume readily biodegradable compounds will rapidly and completely biodegrade in aquatic, aerobic environments.¹⁸³ One way in which readily biodegradable has been quantified is by evaluating mineralization. In this case in order to be considered readily biodegradable, the measured CO₂ must be >60% of the theoretical CO₂ (equal to C_{mRL}) within a 10-day window which begins when measured CO₂ surpasses 10% of theoretical CO₂; the 10-day window must fall within a 28-day study.¹⁸⁷

Mineralization of the monorhamnolipids was evident for all treatments tested with percentages ranging from 42 to 92%. Diastereomer *R,R*, the mixture, and bio-mRL were mineralized to a greater extent than the other treatments and meet the standards for readily biodegradability. Interestingly, bio-mRL had the highest level of mineralization and diastereomer *R,R* was next. These two treatments have the same stereo-orientations which suggests the *R,R* orientation may be more accessible to degrading microorganisms.

We compared rhamnolipid biodegradability to that of COREXIT. The COREXIT dispersants (9500 and 9527) applied to the Deepwater Horizon oil spill in the Gulf of Mexico contained 4 surfactants: anionic bis-(2-ethylhexyl) sulfosuccinate (DOSS), non-ionic sorbitan monooleate (Span 80), non-ionic sorbitan monooleate polyethoxylate (Tween 80), and non-ionic sorbitan trioleate polyethoxylate (Tween 85).¹⁸⁸ Reported

biodegradation values for these compounds, under ideal conditions, by a mixed culture of estuary isolates were ~25% for Tween 80 (14 d), ~65% for Tween 85 (19 d, single isolate), and ~10% for Span 80 (17 d) at 15°C where biodegradation was measured by absorbance shown by surfactant C=C groups or by the absorbance of a colored complex formed during addition of a heteropolyacid.¹⁸⁹ DOSS showed 99% removal (14 d) at 25°C and 98% removal (42 d) at 5°C by a microbial culture collected from the Gulf of Mexico where biodegradation was determined by measuring DOSS concentrations using liquid chromatography mass spectroscopy.¹⁹⁰ These data suggest that the biologically produced and synthetic monorhamnolipids studied here are generally as or more biodegradable than the non-ionic surfactants components of COREXIT and comparably degradable to the anionic DOSS component.

The inherent biodegradability of the monorhamnolipids tested is promising, but further testing under less ideal conditions is required to fully understand the fate of surfactants released to the environment. For example, though DOSS was found to be biodegradable in laboratory settings,¹⁹⁰ samples from the Gulf of Mexico found DOSS in deep-sea sediment and coral communities 6 months after the spill and on Gulf of Mexico beaches nearly 4 years after.¹⁹¹

3.5.2. Toxicity of Synthetic Monorhamnolipids

To determine the risk associated with environmental amendments, a suite of tests are used to develop an ecological effect characterization that describes a substance's toxicity. Characterization tests study substances in the short-term (acute) and long-term (chronic) using a variety of species and measures, e.g., mortality, growth effects, behavioral effects, effect duration, recovery potential, bioaccumulation, etc.¹⁹² In this

study, we use two aquatic toxicity assays to examine monorhamnolipid toxicity:

Microtox and Zebrafish.

3.5.2.1. Microtox

The Microtox assay measures the acute toxicity of toxicants to aquatic prokaryotes using the model bacterium *Vibrio fischeri* by determining the EC₅₀ values where the bacterium's bioluminescence is reduced by half. EC₅₀ values can then be used to categorize materials into one of five EPA ecotoxicity categories for aquatic organism acute exposure concentrations: very highly toxic (<0.1 mg l⁻¹), highly toxic (0.1-1 mg l⁻¹), moderately toxic (>1-10 mg l⁻¹), slightly toxic (>10-100 mg l⁻¹), and practically nontoxic (>100 mg l⁻¹).¹⁹² All of the monorhamnolipid treatments fall into the slightly toxic category (Table 3.5). Table 3.2 shows there were a few statistical differences between the monorhamnolipid treatments, but the classification of all the treatments into the same EPA ecotoxicity category shows there is no practical difference among them.

In comparison to monorhamnolipids, COREXIT 9500 has a Microtox EC₅₀ of 170 mg l⁻¹ (15 min),¹⁹³ and Tween 80, 7000 mg l⁻¹.¹⁹⁴ Thus, monorhamnolipids are more toxic than COREXIT 9500 as a whole and the constituent surfactant Tween 80. No data for DOSS toxicity using Microtox could be found, but when monorhamnolipids are compared to other synthetic anionic surfactants, monorhamnolipid EC₅₀ values are less toxic; sodium dodecyl sulfate (SDS) has a 15 min EC₅₀ of 0.72-1.05 mg l⁻¹,^{195, 196} and linear alkylbenzene sulfates (LAS) have a 30 min EC₅₀ of 5.2-5.5 mg l⁻¹.¹⁹⁷ All of the monorhamnolipids tested herein could be considered less toxic alternatives for SDS and LAS applications, e.g., as soil washing agents or detergents,¹⁶⁰ respectively.

Table 3.5 Bacterial acute toxicity EC₅₀ values at 5, 15, and 30 minutes for Microtox assay (mg l⁻¹)

Monorhamnolipid Treatment	5 minute ^a			15 minute ^a			30 minute ^a					
	(mg l ⁻¹)			(mg l ⁻¹)			(mg l ⁻¹)					
Bio-mRL	40.0	±	5.1	A	25.5	±	4.0	AB	22.7	±	2.4	AB
Diastereomer Mixture	19.7	±	5.2	B	15.8	±	3.5	B	15.8	±	3.0	B
Diastereomer <i>R,S</i>	43.6	±	7.2	A	29.1	±	6.8	A	28.2	±	7.7	A
Diastereomer <i>R,R</i>	39.2	±	2.0	A	26.8	±	1.6	AB	23.5	±	0.6	AB
Diastereomer <i>S,S</i>	32.0	±	4.2	AB	21.2	±	2.2	AB	19.3	±	1.9	AB
Diastereomer <i>S,R</i>	30.8	±	2.3	AB	19.7	±	1.5	AB	18.2	±	1.5	AB

^a Values reported are the means of triplicate trials ± the standard deviations of the mean. Significant treatment differences were determined by one-way ANOVA using the Tukey–Kramer HSD test to compare means ($\alpha = 0.05$). Each column was tested independently. Levels not connected by same letter are significantly different.

In a review of anionic and nonionic surfactant toxicity, Lechuga et al.¹⁹⁸ found chain length of the hydrophobic moiety controls the relative toxicity of surfactants. For example, Microtox data for the alkyl sulfonates C₈, C₁₀, C₁₂, and C₁₄ molecules show 30 min EC₅₀ values of 265, 33, 19, and 66 mg l⁻¹, respectively. Data for the analogous alkyl sulfates were 35.1, 7.0, 0.98, and 34.8 mg l⁻¹, respectively.¹⁹⁷ From these series, chain length is clearly a large contributor to aquatic toxicity with maximum toxicities in the C₁₀₋₁₂ range. This suggests that it may be possible to moderate the acute toxicity of the Rha-C10-C10 by shortening the fatty acid moiety to C₈ or lengthening it to a C₁₄ when selecting a β -hydroxy fatty acid's length during rhamnolipid synthesis.

3.5.2.2. Zebrafish

The zebrafish (*Danio rerio*) is a well-accepted animal model for the *in vivo* testing of chemical ecotoxicity. The assay screens for 22 developmental and neurotoxicity effects of chemicals during embryogenesis. This test was selected because zebrafish have a short generation time, rapid development, and short life cycle during which toxicological effects can be observed.¹⁸⁵ The EPA ecotoxicity categories defined in the previous section are also used to describe zebrafish assay toxicities. All of the treatments, except for diastereomer *R,R*, showed toxic effects resulting in early mortality of Zebrafish embryos at the 640 μM (323 mg l^{-1}) concentration; bio-mRL had the lowest mortality rate of 56%. By the EPA aquatic ecotoxicity measures, *R,R* is practically non-toxic and the bio-mRL, mixture, and *S,R*, classify as slightly toxic. *R,S* and *S,S* cannot be classified since these treatments were found to have significant mortalities at multiple, non-sequential concentrations (Figure 3.3). These results contrast with the results of Johann et al.¹⁹⁹ who report toxicity of 100% mortality at a concentration of 100 mg l^{-1} monorhamnolipids from a recombinant strain of *Pseudomonas putida*. However, both studies agree that monorhamnolipids have low embryotoxic potential overall, and the toxicity appears to manifest as early damage to the embryo. The lack of positive results for measures other than mortality suggests monorhamnolipids have a low ecotoxicity risk, except for very early, vulnerable embryonic stages of growth which are generally more sensitive to chemicals.²⁰⁰

The toxicity of COREXIT 9500 and 9527 have been examined for a variety of early life stages of fish, crustaceans, and mollusks with lethal concentration 50 (LC_{50}) values ranging from 1.6 to $> 100 \text{ mg l}^{-1}$ at 48-96 h—lethal concentration 50 is the

concentration at which a toxicant is lethal for 50% of the organisms in an assay.

Zebrafish were found to have an LC_{50} of 60 mg l^{-1} (slightly toxic) for monorhamnolipids after 48 h¹⁹⁹ and 4.7 mg l^{-1} (moderately toxic) for SDS after 48 h.²⁰¹ Monorhamnolipids are comparably toxic to the COREXIT mixture of surfactants, but less toxic than the anionic surfactant SDS. A direct comparison between monorhamnolipid and DOSS, the only anionic surfactant in COREXIT 9500 and 9527, would be a better comparison than between monorhamnolipids and COREXIT as a whole, but no data for DOSS could be found.

3.5.3. Synthetic Monorhamnolipid and Metal Complexation

Monorhamnolipids were first reported to complex metals in 1994.¹⁹ Subsequent studies have shown that bio-mRLs bind metals of environmental concern (Pb, Zn, Cd)²¹ and rare earth elements²⁰² more strongly than common soil and water cations (Ca, Mg, K). The selectivity of monorhamnolipids for rare earth and toxic elements has engendered interest in these molecules for metal recovery applications,²⁰³ suggesting that we examine the ability of the monorhamnolipid diastereomers to complex metals. The conditional stability constants for the diastereomers with Pb^{2+} and Cd^{2+} differed from bio-mRL with no discernable pattern: some stability constants were larger, some smaller, and some nearly the same with differences changing by up to two orders of magnitude. These differences demonstrate the importance of the hydrophobic moiety during metal complexation by monorhamnolipids. Though the hydrophobic moiety likely takes no active role in the complexation process, the stereo-orientation of the tails would be expected to have a strong effect on the complexation strength. Thus, we hypothesize that the differences in complexation strength are due to interactions among ligands during

multi-ligand complexation of the metal. Namely, reductions in intermolecular steric interference should lead to stronger complexation while increasing steric interference would decrease the complexation strength. Steric hindrance is likely not the only factor, however, because the treatments do not consistently increase or decrease for both metals: diastereomer *S,S* increases for Pb^{2+} but decreases for Cd^{2+} . Another factor like the ion size or molecular conformation, e.g., binding pocket shape of the ligand, must also play a role. The differential changes in metal complexation strength may reveal an opportunity to manipulate the monorhamnolipid structure to create ligands specific for select metals.

3.6. Conclusion

It is important to understand the environmental compatibility of surfactant amendments used in environmental remediation. This study shows that the presence of multiple congeners as well as differences in the stereochemistry of the monorhamnolipid molecule can result in measureable changes in biodegradation, zebrafish toxicity, and metal complexation; no difference was detected for acute aquatic prokaryotic toxicity using the Microtox assay. Because of its recent widespread use and attention, the dispersant COREXIT was compared to monorhamnolipids throughout this paper to demonstrate the importance of evaluating multiple environmental parameters when considering a material as an environmental amendment. It cannot be argued that monorhamnolipids are an environmentally superior material to COREXIT, but by some parameters monorhamnolipids are more environmentally compatible. This work lays a foundation for understanding the environmental compatibility of novel monorhamnolipid diastereomers and provides information regarding their potential as environmental amendments.

CHAPTER 4

REMEDIATING METAL CONTAMINATED WASTEWATERS USING ION FLOTATION WITH MONORHAMNOLIPID COLLECTOR

4.1. Abstract

Water scarcity is a globally recognized issue that is expected to worsen due to global warming and population expansion. To meet future water needs, reclaimed water use will increase to help satiate demand. To prevent risks to human and environmental health, reclaimed water must be free of organic and metal contaminants. Ion flotation using the biosurfactant rhamnolipid, which exhibits metal selectivity for rare earth elements and elements of environmental concern, as a metal collector may offer an environmentally friendly way to remove metal contaminants from water. Thus, monorhamnolipids were examined for their utility as ion flotation collectors for Cs^+ , Cd^{2+} , and La^{3+} . An ion flotation apparatus was designed to test the flotation efficacy of monorhamnolipid at collector to colligend ratios of 2, 5, and 10. Results show that monorhamnolipid forms stable foams and rapidly removes metals from aqueous solution. The collector to colligend ratio and valency of the metal play a large role in determining flotation success. The removal efficiency for the metals when floated individually and at equimolar concentrations was in the order $\text{Cd}^{2+} > \text{La}^{3+} \gg \text{Cs}^+$. The order was $\text{Cd}^{2+} \gg \text{Cs}^+ \gg \text{La}^{3+}$ when the metals were at a ratios of 10:100:1, respectively. Future research should examine parameters including pH and ionic strength that may affect the flotation process as well as actual metal-contaminated waste streams to evaluate the usefulness of this technology.

4.2. Introduction

In light of global climate change and population expansion, water scarcity is a growing problem. The United Nations defines water scarcity as

“the point at which the aggregate impact of all users impinges on the supply or quality of water under prevailing institutional arrangements to the extent that the demand by all sectors, including the environment, cannot be satisfied fully.”²⁰⁴

Water scarcity issues are widely recognized and described in the literature.²⁰⁴⁻²⁰⁸ By 2030, demand for water is expected to reach 6,900 billion m³ (40% above current accessible reliable supplies), and a third of the world population is projected to live in basins where the water deficit is greater than 50%. Water use in 2030 is projected to be 65% agricultural, 22% industrial, 12% domestic.²⁰⁹ In order to close the 40% gap between available and projected water supplies, global scale efforts must be made to reduce water use, improve the efficiency of water use, and reclaim water for re-use. Wastewater reclamation and re-use from industrial and residential sectors is becoming increasingly common. In the arid desert southwest of the United States, reclaimed water is being utilized for industrial processes, groundwater recharge, surface water supply, and recreational and agricultural irrigation.²¹⁰

Before reclaimed water can be used, however, the quality of water must be examined to ensure organic and metal contaminants are sufficiently removed during treatment processes. Metals, in particular, may pose a serious risk to environmental and human health; unlike organic compounds, metals are not biodegraded and are subject to accumulation depending on environmental chemistry and redox reactions which dictate their ultimate fate when released into the environment. Metal contamination has been

found in effluents from mining operations,^{124, 130} industrial processes,¹³³ landfills,¹³⁶ and wastewater treatment facilities.¹³⁵ Risks associated with metal release and accumulation are widely recognized, and many states have implemented regulations regarding acceptable contaminant levels in reclaimed waters.²¹⁰ It is important to identify and treat these effluents to reduce risks associated with reuse and/or environmental release of reclaimed water.

Metalliferous water treatment requires metal capturing compounds selective for metals which pose risks to environmental or human health. The biosurfactant rhamnolipid has shown potential for this purpose.^{19, 21, 74, 202} Biosurfactants are compounds which exhibit surface activity (e.g., reduce surface and interfacial tensions) and are derived from biological sources. They are considered green substances due to their natural derivation, biodegradability, and generally accepted lack of toxicity.²⁰ Monorhamnolipids of *Pseudomonas aeruginosa* (Figure 4.1) are a class of biosurfactant proven to complex metals with a preference for valuable metals (e.g., rare earth elements) and metals of environmental concern (e.g., Cd, Pd, Hg) over common soil and water cations.²⁰²

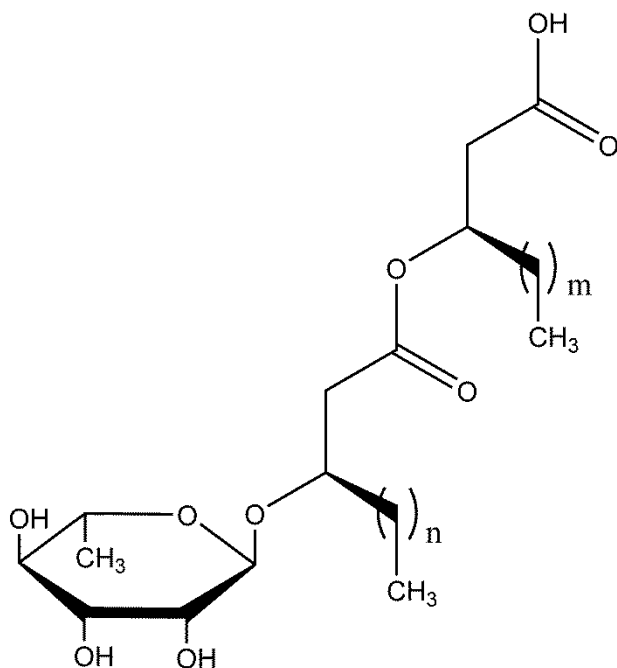


Figure 4.1 Structure of monorhamnolipids utilized in this study. The varying chain lengths of the monorhamnolipid congeners are represented by ‘m’ and ‘n’ which vary from 4 to 12.

Ion flotation is one potential application that can utilize monorhamnolipid-metal binding properties for the removal and recovery of metals from aqueous solutions. Ion flotation was first described by Sebba²¹¹ in 1959. In this process, a dissolved, surface-inactive ion (colligend) is concentrated through complexation with surfactant (collector) and subsequent introduction of air bubbles. The ion-surfactant complexes (sublate) attach to the bubble air/water interfaces and accumulate at the solution surface in collectable foam (foamate).²¹² The remaining solution (raffinate) metal concentration is then reduced and ready for additional treatment or release. Numerous reviews have been published demonstrating the efficacy and optimal operating conditions of ion flotation using a wide variety of collector and colligend pairs.²¹²⁻²¹⁴ When developing a flotation process, the

collector characteristics of collector-colligend selectivity, critical micelle concentration, solubility, toxicity, and biodegradability should be considered. The latter two points are particularly important because some of the collector will be lost in the raffinate, and secondary contamination by a toxic or recalcitrant collector is undesirable.

Despite green characteristics and the ability to preferentially bind valuable and hazardous metals, the use of rhamnolipids in aqueous metal removal technologies has received little attention. Only two studies describing rhamnolipids' utility in aqueous metal remediation applications could be found; the first focused on rhamnolipid use in micellar-enhanced ultrafiltration¹⁰² and the second in ion flotation.¹¹⁴ The latter study showed rhamnolipids could remove Cu, Zn, and Cd from solution, but the description lacked clarity regarding relevant parameters of the experiments such as whether the rhamnolipid used was a mono- or dirhamnolipid or a mixture, and flotation conditions between experiments. Based on their findings and previous metal complexation studies, we sought to further elucidate the operational limits of ion flotation using monorhamnolipid collector. Thus, the objectives of this study were to: 1) design a bench-scale flotation column suitable for use with monorhamnolipid collector, 2) examine collector to colligend ratio effects on metal recovery efficiency, and 3) determine ion flotation efficiencies in mixed metal systems.

4.3. Materials and Methods

4.3.1. Monorhamnolipid Production and Purification

Pseudomonas aeruginosa ATCC 9027 was obtained from the American Type Culture Collection and kept as a glycerol freezer stock at -80° C. This strain is a natural mutant that has been previously shown to exclusively produce monorhamnolipid

congeners^{138, 139}. *P. aeruginosa* was cultured for 24 h at 37° C on a PTYG agar (0.5% protease peptone, 0.5% tryptone, 1% yeast extract, 0.06% MgSO₄•7H₂O, 7x10⁻⁴% CaCl₂•2H₂O, and 1% glucose). The agar culture was transferred to Kay's mineral medium for 24 h growth at 37° C and 200 rpm. Kay's mineral medium contains 100 ml of solution A (0.3% NH₄H₂PO₄, 0.2% K₂HPO₄, and 0.2% glucose), 1 ml solution B (0.025% FeSO₄•7H₂O) and 1 ml solution C (10% MgSO₄•7H₂O). The pre-culture was transferred to a pH 7 minimal salts medium (MSM) with 2% glucose at a ratio of 1 ml pre-culture per 100 ml MSM. MSM is composed of 1 l of solution A (0.25% NaNO₃, 0.04% MgSO₄•7H₂O, 0.1% KCl, 0.1% NaCl, 0.005% CaCl₂•2H₂O, and 0.4% H₃PO₄) mixed with 1 ml of solution B (0.05% FeSO₄•7H₂O, 0.15% ZnSO₄•7H₂O, 0.15% MnSO₄•H₂O, 0.03% H₃BO₃, 0.015% CoCl₂•6H₂O, 0.015% CuSO₄•5H₂O, and 0.01% Na₂MoO₄•2H₂O). The MSM culture is placed in a 37° C gyratory shaker and shaken for 72 h at 200 rpm.

4.3.2. Monorhamnolipid Purification

Monorhamnolipids produced by *Pseudomonas aeruginosa* ATCC 9027 are a congener mixture of up to 30 molecules in which the rhamnose headgroup is preserved but the alkyl chains can vary in chain length and, to a lesser extent, saturation.¹⁴⁰ The protocol used for this work generates a pure native mixture in which the major congener, rhamnosyl-β-hydroxydecanoyl-β-hydroxydecanoate (Rha-C10-C10), typically dominates at 75-85 wt% of the mixture.^{140, 141} This complex assembly of congeners is referred to herein as simply monorhamnolipids.

The monorhamnolipids were concentrated by centrifugation (10,000 rpm for 10 min) to remove cells and cellular debris, followed by removal and acidification of the

supernatant to pH 2 using HCl. Monorhamnolipids have pK_a values of ~ 5.5 , below which they become poorly soluble¹³⁸ and can be collected by centrifugation. Pelleted monorhamnolipids were dissolved in a 9:1 chloroform:methanol mixture and separated from remnant water using a separatory funnel. The solvent was removed by rotoevaporation. The concentrated monorhamnolipids were purified using a solvent mixture of 6:6:6:1:1 (v/v) of hexane:dichloromethane:ethyl acetate:chloroform:methanol (containing 0.1% acetic acid) by elution through a 22 x 300 mm gravity-based, glass chromatography column packed with 45 g of 60-Å-pore silica gel. Monorhamnolipids were collected when column eluent tested positive for rhamnose with anthrone reagent dissolved in H_2SO_4 . The solvent mixture was removed from the monorhamnolipids by rotoevaporation, and purity was determined by reverse phase high performance liquid chromatography on a C18 column.¹³⁸

4.3.3. Metals

$Cs(NO_3)$, $Cd(NO_3)_2 \cdot 4H_2O$, and $La(NO_3)_3 \cdot 6H_2O$ were purchased from Sigma-Aldrich with a purity of $\geq 99\%$ and were used as received. 100% molecular-grade ethanol was purchased from Fisher Scientific and used as received.

4.3.4. Flotation Column Design

A literature review of ion flotation was conducted, and the methodology sections examined for descriptions of flotation column design. Designs were qualitatively compared to determine a design which would be suitable for monorhamnolipid collectors. The design of Thalody and Warr²¹⁵ was selected as the basis for the column design depicted in Figure 4.2. The initial column was made using a glass tube (50 cm tall with a diameter of 5.5 cm) fused to a medium glass frit (Chemglass, 10-15 μm pore size) at the

bottom. The column was equipped with a bulk solution sampling port 5 cm above the frit, and a spout at the top to direct overflow into the foamate collection reservoir.

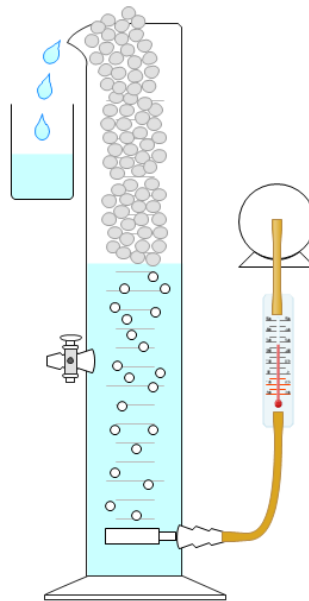


Figure 4.2 Schematic of the initial flotation column design, including the air pump, flow meter, air sparger, sampling port, and foam collection vessel.

Subsequent design improvements led to the lowering of the sampling port to 2 cm above the fritted glass sparger and the incorporation of a removable foam funnel for directing foam to the foamate reservoir. The final column apparatus is shown in Figure 4.3. All glass blowing services were provided by the Department of Chemistry and Biochemistry Glass Shop.

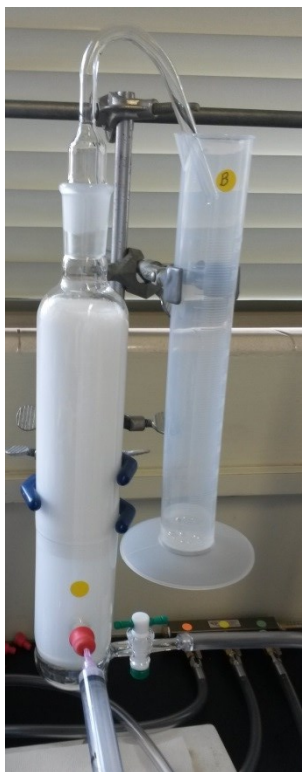


Figure 4.3 Final column apparatus used for flotation experiments in this study.

4.3.5. Ion Flotation Experiments

One previous study¹¹⁴ has examined ion flotation parameters using rhamnolipids as the collector. This study attempted to determine optimal operating parameters for the removal of cadmium from solution including the effects of cadmium concentration, rhamnolipid concentration, pH, frother addition, and type of rhamnolipid (i.e. mono- or dirhamnolipid or a mixture). This study laid the initial foundations for ion flotation using rhamnolipids, but failed to adequately explain the operation parameters or what rhamnolipids were used across experiments, so optimal operating conditions were not established. Their results were used in this study to guide the establishment of initial operating conditions.

All experiments in this study were conducted using a pH of 7, an air flow rate of 50 ml min^{-1} , and an ethanol frother concentration of 0.5 or 0.8% (v/v) based on preliminary experiments (data not shown). pH 7 ensures all of the monorhamnolipids ($\text{pK}_a \approx 5.5^{140}$) are in their anionic form. The air flow rate was determined to be optimal at 50 ml min^{-1} ; faster flow rates caused excessive entrainment of water in the foam, lowering the efficiency of flotation. Frothers are amphiphiles added to flotation processes to improve conditions for bubble and froth formation. As mentioned below, bubble size plays a major role in flotation efficiency. Frothers improve flotation efficiency by facilitating the formation of smaller bubble sizes, preventing coalescence of bubbles, decreasing bubble rise rate thereby increasing the time for substrate attachment to the bubble interface, and increasing the strength of bubbles and stability of foams.²¹⁶ Linear alcohol frothers like ethanol improve foam formation by lowering the air/water interfacial tension enabling smaller bubbles to form and increasing surface area for substrate attachment.^{212, 217} They reduce coalescence and stabilize foams by stabilizing the hydrated layer around the bubble through interactions of their hydrophilic moieties with the aqueous phase. By stabilizing the hydrated layer, it is more difficult to displace the water film surrounding the bubble when bubbles collide, and coalescence is reduced.²¹⁶

Ion flotation is thought to be most efficient at or below the collector's critical micelle concentration (CMC)^{211, 212, 218} because aggregated surfactants compete with interface-attached surfactants for colligend, hindering flotation. Monorhamnolipids have a CMC from ~ 10 to $120 \mu\text{M}$ depending on solution conditions;¹⁴⁰ researchers report CMC values of $50 \mu\text{M}$ at pH 4.0 and 5.0, $150 \mu\text{M}$ at pH 6.5, $100 \mu\text{M}$ at pH 6.8, $180 \mu\text{M}$

at pH 7.0, and 70 μM at pH 7.²¹⁹ All experiments in this study use a monorhamnolipid concentration of 100 μM which lies within the reported CMC values near pH 7.0.

All experiments used 250 ml of solution in the column. Solutions were made using ultrapure water ($\geq 18 \text{ M}\Omega\text{-cm}$) and mixed in acid-washed polypropylene volumetric flasks with magnetic stirring. The pH was adjusted to 7.0 ± 0.1 using 1.0 M NaOH or HCl. Before each experiment, columns were prepared by rinsing with 9:1 chloroform:methanol to ensure that adsorbed rhamnolipid from previous experiments was removed, rinsing 5 times with ultrapure water, and drying by running air through the fritted glass. Columns were not acid-washed between experiments except where noted below. Foamate was collected in acid-washed 250 ml polypropylene graduated cylinders. Foam was broken in the cylinders by an initial addition of 20 ml of 2% nitric acid. Transfer of water from the column to the foamate reservoirs was measured gravimetrically. A compressed air tank (breathing quality UN 1002) was used as the column air supply. Air was supplied at 20 psi via a regulator to a gas manifold with three outlets. Air was supplied to three columns simultaneously immediately after the addition of column solution; air flows were controlled by separate flow meters. Samples were collected via a syringe from the rubber septum sealed sampling port. All samples were collected in metal-free 15 ml centrifuge tubes, diluted in 2% trace metals grade nitric acid (Fisher Scientific), and analyzed by inductively coupled plasma mass spectrometry in the Arizona Laboratory for Emerging Contaminants at the University of Arizona. The operational parameters of all experiments performed are summarized in Table 4.1.

4.3.5.1. Effect of Collector to Colligend Ratio

The collector to colligend ratio (ϕ) was varied to determine the operational limitations of monorhamnolipid collector with a monovalent cation Cs^+ , divalent cation Cd^{2+} , and trivalent cation La^{3+} . Each metal was tested independently at ϕ values of 2, 5, and 10 with an ethanol concentration of 0.8%. Samples from the column were taken at 0, 5, 10, 15, 25, 40, and 60 min. Airflow was stopped at 40 min and the column foam allowed to collapse before sampling the concentration of residual metals in the raffinate at 60 min. The foamate reservoirs were sampled at the end of the experiment to determine metal recovery.

4.3.5.2. Metal Mass Balance

After conducting the collector to colligend ratio experiments, it was determined that insufficient data was available for accurate metal mass tracking. Therefore, the $\phi = 10$ experiments for Cs^+ , Cd^{2+} , and La^{3+} were repeated with additional measurements. The columns were acid washed both before and after the experiment by shaking approximately 100 ml of 10% trace metals grade nitric acid in the column for 2 min followed by a 2 min distilled water rinse. Column samples were collected at 0, 5, 10, 15, 25, 40, and 50 min. Airflow was stopped at 40 min, and the raffinate sampled at 50 min, after foam collapse. The foamate reservoir was sampled for metal recovery. The post-experiment acid rinse was sampled to determine to what degree metals were adsorbing to the glass or complexed to adsorbed rhamnolipids. Sample volumes and dilutions were determined volumetrically to improve accuracy for the metal and water mass balances.

4.3.5.3. La^{3+} Flotation by Foam Fraction

The removal rate for La^{3+} was determined by measuring collected foam fractions for as a function of time. Three columns were run with a ϕ value of 10 and ethanol concentration of 0.5%. Samples were collected from 0-2, 2-4, 4-6, 6-10, 10-15, and 15-20 min where time 0 is the point of first foam collection from the collection funnel. Samples were collected in 50 ml metal-free centrifuge tubes with 4 ml of 2% trace metals grade nitric acid to break the foam. The volume of solution transferred was determined gravimetrically. Sparging was ceased after 20 min of foam production and the foam allowed to collapse before a sample of raffinate was taken for mass balance.

4.3.5.4. Metal Competition

The floatability of a mixed Cs^+ , Cd^{2+} , and La^{3+} solution was tested with the metals at equimolar and order of magnitude different concentrations. In both experiments, the total metal ϕ value was 10. In the former, each metal was at a concentration of 3.3 μM . In the latter experiment, the metals were present at 9, 0.9, and 0.09 μM for Cs^+ , Cd^{2+} , and La^{3+} , respectively. In both experiments, the ethanol concentration was 0.5% and samples were collected at 0, 2.5, 5, 10, 15, 25, and 40 min. Airflow was stopped at 25 min, and raffinate was collected at 40 min. The foamate reservoirs were sampled to determine metal recovery.

Table 4.1 Ion flotation parameters for all experiments in this study

Experiment	Metal	ϕ^a	Metal μM	pH	Airflow Rate ml min^{-1}	Rhamnolipid μM	Ethanol % (v/v)	Number of replicates
Collector to Colligend Ratio	Cs⁺	2	50.0	7.0 ± 0.1	50.0	100.0	0.8	1
		5	20.0	7.0 ± 0.1	50.0	100.0	0.8	1
		10	10.0	7.0 ± 0.1	50.0	100.0	0.8	1
	Cd²⁺	2	50.0	7.0 ± 0.1	50.0	100.0	0.8	1
		5	20.0	7.0 ± 0.1	50.0	100.0	0.8	1
		10	10.0	7.0 ± 0.1	50.0	100.0	0.8	1
	La³⁺	2	50.0	7.0 ± 0.1	50.0	100.0	0.8	1
		5	20.0	7.0 ± 0.1	50.0	100.0	0.8	1
		10	10.0	7.0 ± 0.1	50.0	100.0	0.8	1
Mass Balance	Cs⁺	10	10.0	7.0 ± 0.1	50.0	100.0	0.5	1
	Cd²⁺	10	10.0	7.0 ± 0.1	50.0	100.0	0.5	1
	La³⁺	10	10.0	7.0 ± 0.1	50.0	100.0	0.5	1
Recovery of La³⁺ by Foam Fraction	La³⁺	10	10.0	7.0 ± 0.1	50.0	100.0	0.5	3
Equimolar Mixed Metal	Cs⁺		3.3					
	Cd²⁺	10	3.3	7.0 ± 0.1	50.0	100.0	0.5	3
	La³⁺		3.3					

Table 4.1 Ion flotation parameters for all experiments in this study

Experiment	Metal	ϕ^a	Metal μM	pH	Airflow Rate ml min^{-1}	Rhamnolipid μM	Ethanol % (v/v)	Number of replicates
Order of Magnitude Mixed Metal	Cs⁺		9					
	Cd²⁺	10	0.9	7.0 ± 0.1	50.0	100.0	0.5	3
	La³⁺		0.09					

^a ϕ is the collector to colligend ratio.

4.3.6. Calculations

Multiple measures were used to describe the efficacy of the flotation process. The first is metal removal efficiency (R) which is calculated using Equation 4.1:

$$R = \left(1 - \frac{C}{C_0}\right) \times 100 \quad [4.1]$$

where C is the column solution concentration at time t and C₀ is the column solution concentration at time t=0.^{114, 213, 220} This measure is a traditional method of reporting metal recovery during ion flotation, but it does not take into account the transfer of water from the column to the foamate reservoir. Water removal from the column impacts the efficiency of the flotation processes because it reduces the mass of treated solution, and dilutes the foamate concentrate. To take into account water transfer, an enrichment factor is also reported. The enrichment factor (E) is calculated using Equation 4.2:

$$E = \left(\frac{C_f}{C_0}\right) \quad [4.2]$$

where C_f represents the metal concentration in the foamate.²¹⁸ If E < 1 the colligend is concentrating in the column as bulk water is removed in the foam. If E = 1, there is no retarding or concentrating effect occurring during flotation. If E > 1, the colligend is being concentrated in the foamate. The greater E value, the more concentrated the colligend is and the more efficient the flotation process.

An estimate of the removal kinetics is also reported for each experiment. The kinetics of flotation can be described using the first-order kinetic Equation 4.3:^{213, 221, 222}

$$-\frac{dC}{dt} = kC \quad [4.3]$$

where k is the flotation rate constant. The rate constant k represents a complex function involving many of the flotation variables (air concentration, reagents concentrations, particle and bubble sizes, induction times, flotation cell design, froth removal rate, etc.),

and $\left(\frac{dC}{dt}\right)$ is assumed to remain constant. Integration of Equation 4.3 from C_0 to C yields Equation 4.4:²¹⁵

$$\ln\left(\frac{C}{C_0}\right) = kt \quad [4.4]$$

Since the values of C and C_0 are experimentally determined at a variety of time points, one can plot this equation and determine k from the slope of a linear regression.

4.4. Results and Discussion

4.4.1. Column Design

The initial construction of the flotation columns followed the design shown in Figure 4.2. This design was flawed in a variety of ways. First, the spout at the top of the column was successful in directing the foam during low flow rates, but faster flow rates caused the foam to overflow the sides of the column. Even at slow air flow rates, the directed foam was difficult to collect without loss of material or potential contamination. As a result, the columns were modified to include a narrowing top leading to a glass funnel capable of delivering foam directly into a collection reservoir. The funnel attaches to the column with a ground-glass connection and is removable for column filling and cleaning.

The second design flaw was discovered during preliminary tests of frother addition to the bulk solution. When frother is added, bubble formation increases, and the foam becomes wetter and more voluminous. This resulted in the bulk solution level dropping below the sampling port located 5 cm above the fritted glass. This was corrected by relocating the sampling port to 2 cm above the fritted glass sparging surface. Ideally this port should be located just above the fritted glass, but the port could not be located closer without risking damage to the frit.

Preliminary frothability tests of rhamnolipid showed that rhamnolipid was able to support large heads of foam which filled the columns, especially when column solution included ethanol frother. Upon the addition of metals to the flotation solution, however, foam columns were unable to fill the entire column headspace before collapsing. Initial experiments were conducted with a column solution of 250 ml. Doubling the column solution to 500 ml enabled proper column function and foam collection, but there was insufficient rhamnolipid to support the number of experiments planned for this study. As a result, the column height was reduced to 25 cm, and the column solution was reduced to 250 ml for all experiments. The final column design used for the experiments in this study is shown in Figure 4.3.

During the column and operational modifications described in this chapter, it became clear that finding the optimal combination of operational parameters is a difficult process necessary for each flotation apparatus and solution system. This is because the flotation efficiency and underlying reaction kinetics of ion flotation are reliant on dozens of variables.²²³ Among these variables, the bubble size and initial kinetics should be investigated to improve the ion flotation process with monorhamnolipid collector.

When designing flotation columns, it is important to consider bubble size relative to the sublate size being floated. Aeration of the column solution influences the flotability of different size fractions, with flotation being optimal for small particles with small bubbles and large particles with large bubbles.²²⁴ Ion flotation is thought to occur through two possible processes: 1) the sublate forms in the bulk solution and subsequently attaches to the bubble interface or 2) collector adsorbed to the bubble surface associates with ions but the solid sublate does not form until leaving the solution and becoming

entrained in the foam.²¹² If the former is applicable, flotation efficiency would be increased by minimization of bubble size since monorhamnolipid-metal sublates will be ultrafine particles. If the latter case applies, then it is desirable to have maximal surface area for collector and metal adsorption so bubble size should be minimized. Thus, regardless of the ion flotation process, it is desirable to generate the smallest bubble size possible to improve flotation efficiency.

Bubble size can be controlled by the bubble generation method and chemical amendments such as frothers (discussed above). Bubbles can be created through one of three means: mechanical, pneumatic, and precipitatory.²²⁵ Mechanical bubble generation uses impellers to form bubbles by shearing apart a stream of gas or by causing changes in solution pressures, e.g., precipitation of air bubbles in low pressure cavities resulting from the impellers disturbing the solution. Pneumatic bubble generation can be accomplished by forcing air through porous media such as cloth, glass, or resin. Precipitatory bubble generation uses pressure or vacuum vessels to place a solution under either pressure or vacuum so that when the pressure is reduced, the solution becomes saturated in dissolved gasses which then precipitate out as bubbles.^{213, 225}

The medium frit sparger (pore size of 10-15 μm) used for this experiment is a pneumatic bubble generator. This generator was selected due to the availability of equipment and associated resources. Ethanol was used as a frother to reduce bubble size and prevent coalescence. The flotation efficiency of the experiments discussed below would likely be improved by generating a smaller bubble size using a different generation method. A fine frit sparger, for example, would have a smaller pore size and be able to

generate an overall smaller bubble size. The method of bubble generation should be considered for future column design modifications to improve process efficiency.

Along a similar vein, the initial kinetics of substrate and collector attachment to bubble interfaces should be given more consideration in future column designs. The rate at which bubbles rise through water is a function of bubble size with smaller bubbles rising slower than larger bubbles. In an example provided by Klassen,²¹⁶ a 0.96 mm bubble (radius or diameter was not specified) had a velocity of 19.8 cm s⁻¹ while a 1.54 mm bubble's velocity was 30.2 cm s⁻¹. In a well-mixed system, Morgan et al.²²⁶ estimate it takes 0.1 s for a bubble and collector to reach equilibrium adsorption densities on the bubble interface, but Liu and Doyle²²⁷ show that the time is system specific, reporting times of 0.2, 2, and 8 s for copper flotation with different collectors. To improve the initial flotation kinetics, it is desirable to allow the bubble and reactants to reach adsorption equilibrium densities before entering the foam. To ensure equilibrium is reached, the solution depth of the column should be large enough to allow adsorption equilibrium densities to be attained. To prevent column heights from becoming too large, collectors and frothers can be added to the system to reduce the rise velocity of bubbles and reduce the depth required to reach adsorption equilibrium densities.²¹⁶ For Klassen's bubble size example above, the addition of collectors retarded the rise velocity by 1.7-2.1 times.²¹⁶ Initial kinetics can also be increased by increasing the total bubble surface area (smaller bubbles) as described above, or increasing the flow rate. The latter option increases solution retention in the foam which is undesirable, but this can be compensated for by increasing the time available for foam drainage.²²⁸ Optimizing these initial kinetic

factors is an important step in increasing the overall reaction kinetics of the ion flotation process.

4.4.2. Effect Collector to Colligend Ratio

The effect of collector to colligend ratio (ϕ) on ion flotation was examined for Cs^+ , Cd^{2+} , and La^{3+} individually at ϕ ratios of 2, 5, and 10, and the results are shown in Table 4.2 and Figure 4.4. All three metals were successfully floated and concentrated at ϕ ratios 5 and 10, but only Cs^+ and Cd^{2+} were collected at $\phi = 2$. The efficacy of flotation was assessed using multiple parameters as shown in Table 4.2. Analysis of metal recovery efficiency showed Cd^{2+} was the best floated ion with removal efficiencies from 90.1 to 99.8% and Cs^+ was the least successfully floated with removal efficiencies of 37.1 to 46.2%. Recovery efficiencies appear to increase as the value of ϕ increases. The recovery efficiency calculation is based on column solution concentration without regard to water transferred into the foamate. To account for transfer of water, an enrichment factor—the ratio of foamate concentration to initial solution concentration—is also reported.

All of the treatments showed enrichment of the metals in the foamate, indicating successful flotation, but the degree of enrichment varied greatly. Cd^{2+} had an enrichment factors of 27.2 and 15.4 at $\phi = 2$ and 5, respectively. La^{3+} and Cd^{2+} had lesser enrichment factors with maximums of 6 at $\phi = 5$ and 1.9 at $\phi = 2$, respectively. All of the treatments exhibited decreasing enrichment factors with increasing ϕ . The decrease in enrichment is not surprising because as ϕ increased, so did the entrainment and transfer of water with water transfer of 42, 42, and 30% for Cs^+ , Cd^{2+} , and La^{3+} , respectively, at $\phi = 10$. Metals are sometimes used for foam inhibition because they counteract effects of electrostatic

stabilization and reduce the solubility of ionic surfactants.²¹⁷ Thus, at higher ϕ , there are fewer metals and richer, more stable foam is produced and more water is entrained. For all three metals, coarser foam with larger bubbles was observed for ϕ values of 2 compared to 10 as seen in Figure 4.5. The enrichment factors can be improved by reducing the mass transport of water in the foam. Water entrainment may be reduced by lowering frother concentration or increasing the headspace height to allow additional gravitational drainage.

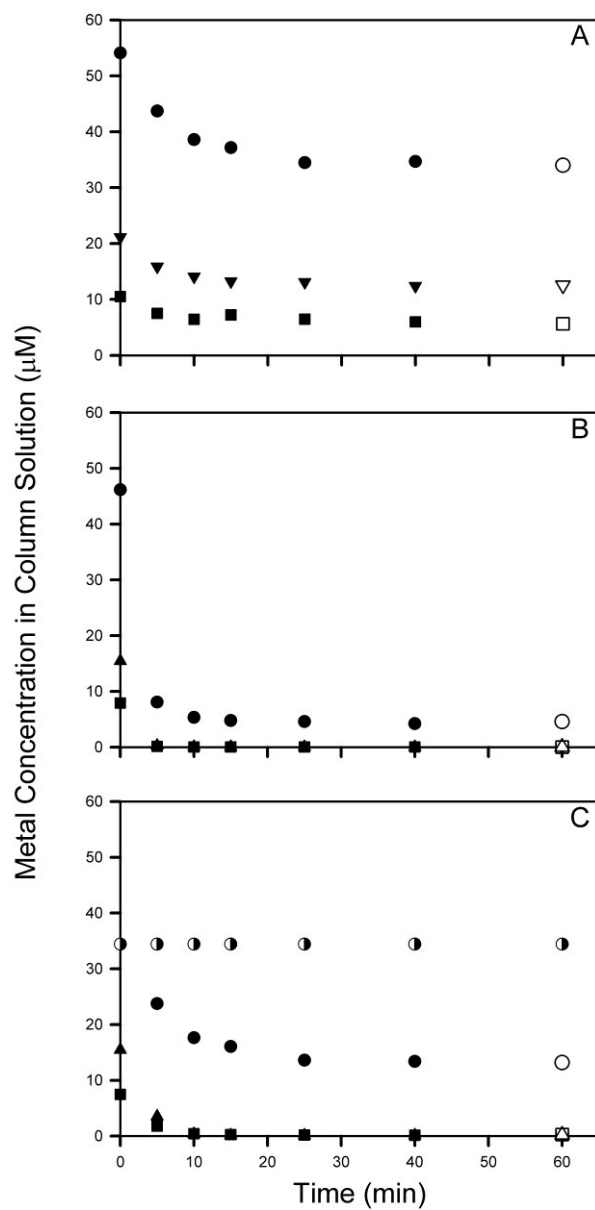


Figure 4.4 Effect of collector to colligend ratio (ϕ) on ion flotation was examined for (A) Cs^+ , (B) Cd^{2+} , and (C) La^{3+} individually at ϕ ratios of 2(\bullet), 5(\blacktriangle), and 10(\blacksquare). The open symbol indicates the raffinate sample collected after column foam was allowed to collapse. In part C, \bullet represents the apparent metal concentration in the column and the half-filled circles represent the actual column metal concentration.

Table 4.2 Results of ion flotation for Cs⁺, Cd²⁺, and La³⁺ at varying collector to colligend ratios

	ϕ^a	Raffinate Concentration	Water Transfer to Foamate	Concentration of Foamate	Metal Removal Efficiency ^b	Enrichment Factor ^c	Flotation Rate Constant ^d
		μM	ml	μM	%		min^{-1}
Cs ⁺	2	34.0	59.9	104.0	37.1	1.9	0.006
	5	12.6	82.8	39.1	40.6	1.8	0.006
	10	5.7	105.9	16.1	46.2	1.5	0.005
Cd ²⁺	2	4.6	6.1	1257.5	90.1	27.2	0.015
	5	0.04	84.3	54.7	99.8	15.4	0.048
	10	0.02	106.2	22.0	99.8	2.8	0.043
La ³⁺	2 ^e	13.2	0.0	--	0.0	0.0	0.015
	5	0.2	45.2	92.8	98.6	6.0	0.060
	10	0.3	73.9	28.5	96.3	3.8	0.072

^a ϕ is the collector to colligend ratio.

^b Calculated using the equation $R = (1-C/C_0) \cdot 100$ where C is the column concentration at time t and C_0 is the initial column concentration.²¹³

^c Calculated using the equation $E = C_f/C_0$ where C_f is the concentration of metal in the foamate and C_0 is the initial column concentration.²¹⁸

^d Estimate calculated using the first-order kinetic equation $(dC/dt) = -kC$ as described by Matis²¹³ and Matis.²²¹

^e No foam was collected from this column due to the formation of a surface scum which could not be collected.



Figure 4.5 Typical appearance of a coarse foam (left) at $\phi = 2$ and a fine foam (right) at $\phi = 10$

La^{3+} at $\phi = 2$ failed to produce any foam and the effective recovery is 0%. A white scum was observed concentrating at the solution surface with some adsorbing onto the glass (Figure 4.6). This scum was a precipitate of monorhamnolipid-La complexes. Because the precipitate was concentrating at the surface, an apparent change in the solution La^{3+} concentration was observed (Figure 4.4C), but no metal was removed from the column. Interestingly, this result demonstrates that ion flotation does not require the formation of foam to be considered successful. Ion flotation causes the formation of a solid particle—consisting of a colligend and collector as chemical constituents—which becomes concentrated on a solution surface as either a foam or scum.^{213, 214} Scum formation in lieu of foam during ion flotation is perfectly acceptable, and may be preferential as scum provides a highly concentrated material that is easily removed from

the surface—the design of the columns used in this study excluded the possibility of collecting the scum for analysis. As an alternative, the precipitate scum could also be floated using additional or alternative collectors in a related process called precipitate flotation.



Figure 4.6 Scum concentrating on the solution surface and adsorbing to the column while floating La^{3+} at $\phi = 2$.

The contrasting results between Cd^{2+} and La^{3+} under the same flotation conditions is intriguing. Both La^{3+} and Cd^{2+} form monorhamnolipid:metal complexes with an average stoichiometry of 2:1.²⁰² All monorhamnolipid monomers should be associated with a metal for both metals at $\phi = 2$. The different behavior of the two metals could be related to either sublimate solubility, or the presence/absence of excess monorhamnolipid monomers. It is possible the Cd^{2+} sublimate is relatively soluble and retains the ability to foam, while the La^{3+} sublimate is much less soluble, inhibiting foam formation. Measurements of residual La^{3+} in the column after precipitate formation showed ~40% of

the metal was still in solution, though it is unknown if this metal was present as an ion or monorhamnolipid complex. If lanthanum was present as the complex, low solubility is the likely explanation. On the other hand, if the lanthanum was present as an ion, it is also possible the monorhamnolipid monomers were depleted, preventing foam formation. If this is true, then the floatability of Cd^{2+} suggests excess surfactant was available and the surfactant:metal stoichiometry was less than two. Future studies should include an examination of the metals' speciation diagrams under this experiment's conditions to resolve this question.

Overall, the results of these colligend to collector ratio experiments show the efficacy and efficiency of ion flotation is reliant on ϕ and the valency of metals. When ϕ is small, the metals are better enriched, but foam quality decreases. At larger ϕ , removal efficiencies increase, but at the cost of greater water transfer and lower metal enrichment. Because the metal sublates are chemical compounds of colligend and collector, flotation requires a specific stoichiometric ϕ for sublata formation. In all ion flotation systems there is an ideal ϕ ratio which is almost always greater than the stoichiometric ratio of the sublata, but varies widely with values ranging from 1 to 44 in early ion flotation studies studies.²¹² The ideal ϕ ratio for monorhamnolipids probably lies between 2 and 5 for the metals and conditions tested herein.

4.4.3. Mass Balance

During analysis of the results from the previous section, it was realized insufficient data was collected to compile an accurate mass balance for the metals. Shortfalls included dilution measurements conducted volumetrically instead of gravimetrically, imprecise tracking of sample volumes removed from the flotation

column, and no pre- and post-experiment acid washing of the flotation column. As a result, the $\phi = 10$ flotation experiments for the three metals were repeated to allow a thorough mass balance analysis with a reduced ethanol frother concentration of 0.5%. The results for the mass balance are reported in Table 4.3 and the results for flotation performance are reported in Table 4.4 and Figure 4.7

Table 4.3 Metal mass balance for ion flotation of Cs^+ , Cd^{2+} , and La^{3+} at a collector to colligend ratio of 10

Metal	Metal Fraction (%)				Total
	Sampling ^a	Residual ^b	Foamate ^c	Acid Wash ^d	
Cs^+	5.0	29.7	52.0	3.8	90.4
Cd^{2+}	1.2	0.1	98.6	0.4	100.3
La^{3+}	1.5	1.3	85.8	1.3	89.9

^a Metal lost due to sampling the column.

^b Metal remaining in the column after flotation has ceased and foam has collapsed.

^c Metal collected in the foamate.

^d Metal collected in the post flotation acid wash of the column.

Table 4.4 Results of ion flotation for Cs⁺, Cd²⁺, and La³⁺ at a collector to colligend ratio of 10

Metal	Raffinate Concentration	Water Transfer to Foamate	Concentration of Foamate	Metal Removal Efficiency^b	Enrichment Factor^c	Flotation Rate Constant^d
	μM	ml	μM	%		min⁻¹
Cs⁺	4.89	80.12	15.94	50.2	1.6	0.011
Cd²⁺	0.02	92.09	19.98	99.8	2.7	0.047
La³⁺	0.21	76.18	24.31	97.6	2.8	0.056

^a ϕ is the collector to colligend ratio.

^b Calculated using the equation $R = (1-C/C_0) \cdot 100$ where C is the column concentration at time t and C_0 is the initial column concentration.²¹³

^c Calculated using the equation $E = C_f/C_0$ where C_f is the concentration of metal in the foamate and C_0 is the initial column concentration.²¹⁸

^d Estimate calculated using the first-order kinetic equation $(dC/dt) = -kC$ as described by Matis²¹³ and Matis.²²¹

^e No foam was collected from this column due to the formation of a surface scum which could not be collected.

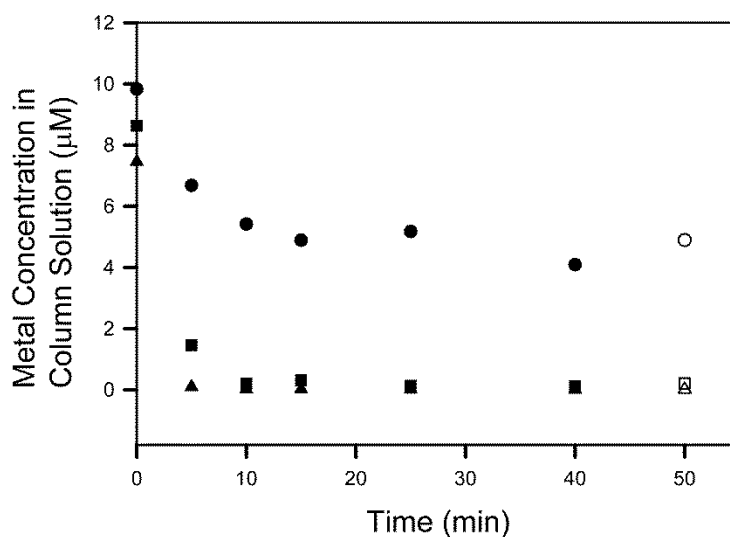


Figure 4.7 Effect of collector to colligend ratio (ϕ) on ion flotation was examined for (●) Cs^+ , (▲) Cd^{2+} , and (■) La^{3+} individually at ϕ ratio 10. The open symbol indicates the raffinate sample collected after column foam was allowed to collapse.

The performance of the second set of $\phi = 10$ experiments were very similar to those described in Table 4.2. Removal efficiencies were in the same order as in the previous experiments ($\text{Cd}^{2+} > \text{La}^{3+} \gg \text{Cs}^+$), with nearly the same values reported for recovery efficiency. The water transfer to the foamate was reduced for Cs^+ (~26 ml) and Cd^{2+} (~14), but increased slightly for La^{3+} (~2). The enrichment factors for Cs^+ and Cd^{2+} were unchanged, and La^{3+} showed a slight decrease. Residual concentrations were nearly the same for all the metals. Flotation rate constants increased for Cs^+ and Cd^{2+} but decreased for La^{3+} . These differences may be the result experimental error, improved metal accounting, changes in frother concentration, or a combination of these effects. The frother concentration was reduced for this experiment and all subsequent experiments in an attempt to reduce the relatively high water transfer rates observed in section 4.4.2.

The metal mass balance (Table 4.3) was able to account for 90.4% of Cs^+ , 100.3% of Cd^{2+} , and 89.9% of La^{3+} . Results show that little metal is lost due to adsorption to the glass column or due to complexation with monorhamnolipid adsorbed to column surfaces. Only minor fractions of the metal were lost due to sampling, and the majority of the metals were located in the raffinate or foamate fractions. The values reported for the foamate in Table 4.3 are directly measured and should be equivalent to the metal recovery efficiency values reported in Table 4.4. A comparison of these values shows some differences which likely arise from the latter not taking into account water transfer from the column solution.

4.4.4. Foam Fraction

During initial experiments, metal concentrations in the column solution dropped rapidly in the first 5-10 minutes. This rapid removal rate is desirable because it reduces the time required to complete the flotation process during batch operations. Due to column design, however, metal removed from solution is not actually removed from the column until the foam reaches the top of the column and is directed into the foamate reservoir. As foam progresses through the column headspace, it is possible for metals to reflux as the foam coalesces and entrained water drains towards the column solution. Thus, it is important to look at the metal content of different fractions of foam as it emerges from the column to better understand metal transport in the foam column. Figure 4.8 shows the La^{3+} content of the foam fractions collected over 20 minutes for triplicate columns with $\phi = 10$. Metal concentrations were greatest in the 4-6 and 6-10 minute fractions, and 90.4% of the La^{3+} was collected in the first 10 min of foam production. A

total of 108% of the metal was collected in the foamate and less than 1% was present in the raffinate.

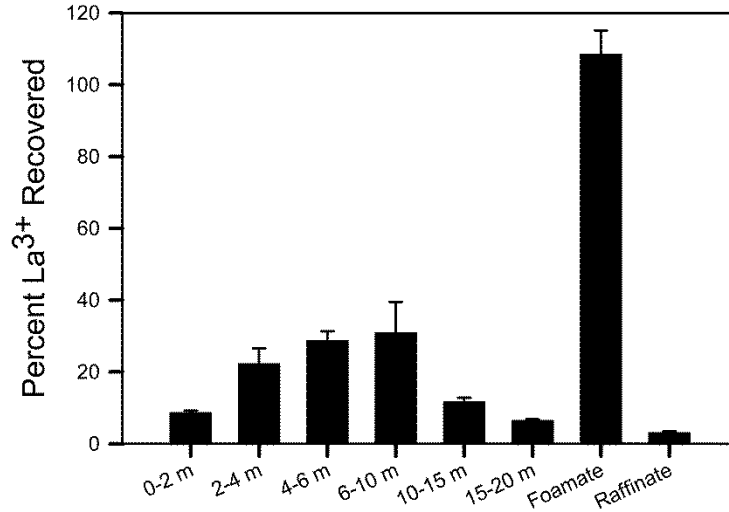


Figure 4.8 Metal recovery during ion flotation of La³⁺ at $\phi = 10$ measured by foam collected during different time frames of foam production. Bars represent averages and standard deviations of triplicate columns.

The 10 min recoveries for La³⁺ ($\phi = 10$) in sections 4.4.2 and 4.4.3 were 94% and 96%, respectively. Because these recoveries were calculated by measuring the column solution and not through direct foam measurements, it was not possible to definitively claim the removed metals would be found in the first ten minutes of foamate. The results of the foam fraction experiment show, in this system, the concentration of metal removed from a solution in a given time frame will be approximately the same as the concentration of metals in an equivalent time frame of foamate, i.e., the metal removed from the column solution in the first 10 min of flotation will be present in the first 10 min of foamate. This observation indicates that metals are not being refluxed inside the column

under these experimental conditions. These results are useful because they provide important information necessary to determine ion flotation process parameters like foamate recovery time required to achieve desired treatment levels of contaminated solutions.

4.4.5. Mixed Metal Ion Flotation

Monorhamnolipids are selective for rare earth elements and elements of environmental concern over common soil and water cations.²⁰² Metals are rarely present as single element solutions, and interest in using ion flotation to selectively concentrate target metals dates back to Sebba's original description of ion flotation.²¹¹ The ability of monorhamnolipid to selectively remove specific metals was tested using mixed metal solution of Cs^+ , Cd^{2+} , and La^{3+} at equimolar concentrations and concentrations different by orders of magnitude.

The efficacy of ion flotation of mixed metal solutions with Cs^+ , Cd^{2+} , and La^{3+} at $3.3 \mu\text{M}$ each (total $\phi = 10$) is summarized in Table 4.5 and Figure 4.9. The order of removal was $\text{Cd}^{2+} > \text{La}^{3+} \gg \text{Cs}^+$ with recoveries of 98.4, 88.1, and 39.4% respectively. The enrichment factor was greatest for Cd^{2+} at 5.1. Inspection of Figure 4.9 shows that Cd^{2+} is almost completely removed from solution by 10 min where it reaches near maximal removal, while La^{3+} reaches a near maximal removal at 15 min. The difference observed in the figure makes it appear as though Cd^{2+} has a faster removal rate than La^{3+} , but a review of the estimated flotation rate constants in Table 4.5 show La^{3+} has the faster rate constant. Though the metals are tested independently in separate columns, these same observations can be made for data in Table 4.3 and Figure 4.7 as well. The cause of this phenomenon is unknown, but from the initial experiments examining collector to

colligend ratios, it was observed La-monorhamnolipid complexes seem to be less soluble than Cd-monorhamnolipid complexes. It is possible Cd^{2+} may appear to have faster removal rates because the mass transfer to the air/water interface is more rapid for dissolved species than for the less soluble species. The conflicting flotation rate constants may be an artifact of poor linear fitting of experimental data into equation 4.4. These flow rate constants are provided primarily as an estimate to provide a general idea of the kinetics monorhamnolipid flotation of metals and could be improved with additional replicate experiments.

The efficacy of ion flotation of mixed metal solutions with Cs^+ , Cd^{2+} , and La^{3+} at 9, 0.9, and 0.09 μM (total $\phi = 10$) is summarized in Table 4.5 and Figure 4.10. Figure 4.10A and Figure 4.10B portray the same data with different y-axis scales. The order of removal for the metals is $\text{Cd}^{2+} \gg \text{Cs}^+ \gg \text{La}^{3+}$. The reported value removal efficiency for La^{3+} is 11.7%, but Figure 4.10A shows an increase in solution concentration at the final time point 40 min. Figure 4.10A also shows the concentration of La^{3+} in solution repeatedly increased and decreased, reaching a minimum at 10 min with a metal recovery efficiency of ~52%. These fluctuating values suggest that La^{3+} is not being fully removed from the column, and may actually be refluxing in the foam column, likely as a fine precipitate.

Table 4.5 Results of ion flotation for mixed metal solutions of Cs⁺, Cd²⁺, and La³⁺ at equimolar and order-of-magnitude difference concentrations

	Metal	Raffinate Concentration		Water Transfer to Foamate		Concentration of Foamate		Metal Removal Efficiency ^b		Enrichment Factor ^c	Flotation Rate Constant ^d
		μM		ml		μM		%			
Equimolar Mixed Metal	Cs ⁺	2.09	± 0.04			7.80	± 0.27	39.4	± 2.7	2.3	0.016
	Cd ²⁺	0.04	± 0.02	54.16	± 7.59	13.19	± 1.62	98.4	± 0.7	5.1	0.070
	La ³⁺	0.32	± 0.05			11.60	± 1.24	88.1	± 2.1	4.3	0.081
Order of Magnitude Mixed Metal	Cs ⁺	5.30	± 0.04			24.91	± 3.45	46.4	± 0.6	2.5	0.020
	Cd ²⁺	0.00	± 0.00	51.51	± 10.58	3.76	± 0.78	99.5	± 0.2	6.4	0.033
	La ³⁺	0.05	± 1.18			1.05	± 0.43	11.7	± 16.0	20.0	0.007

^a ϕ is the collector to colligend ratio.

^b Calculated using the equation $R = (1-C/C_0) \cdot 100$ where C is the column concentration at time t and C_0 is the initial column concentration.²¹³

^c Calculated using the equation $E = C_f/C_0$ where C_f is the concentration of metal in the foamate and C_0 is the initial column concentration.²¹⁴

^d Estimate calculated using the first-order kinetic equation $(dC/dt) = -kC$ as described by Matis²¹³ and Matis²²¹.

^e No foam was collected from this column due to the formation of a surface scum which could not be collected.

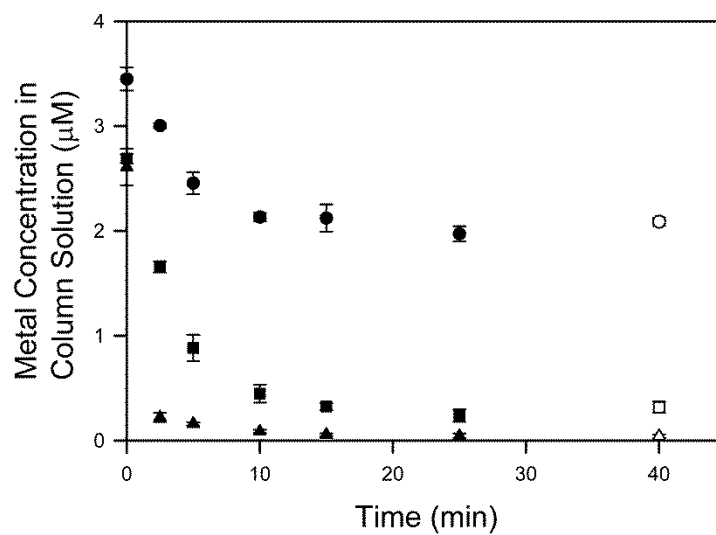


Figure 4.9 Efficacy of ion flotation of mixed metal solutions with (●) Cs⁺, (▲) Cd²⁺, and (■) La³⁺ each 3.3 µM (total $\phi = 10$). The open symbol indicates the raffinate sample collected after column foam was allowed to collapse. Symbols represent mean and standard deviation values from triplicate columns.

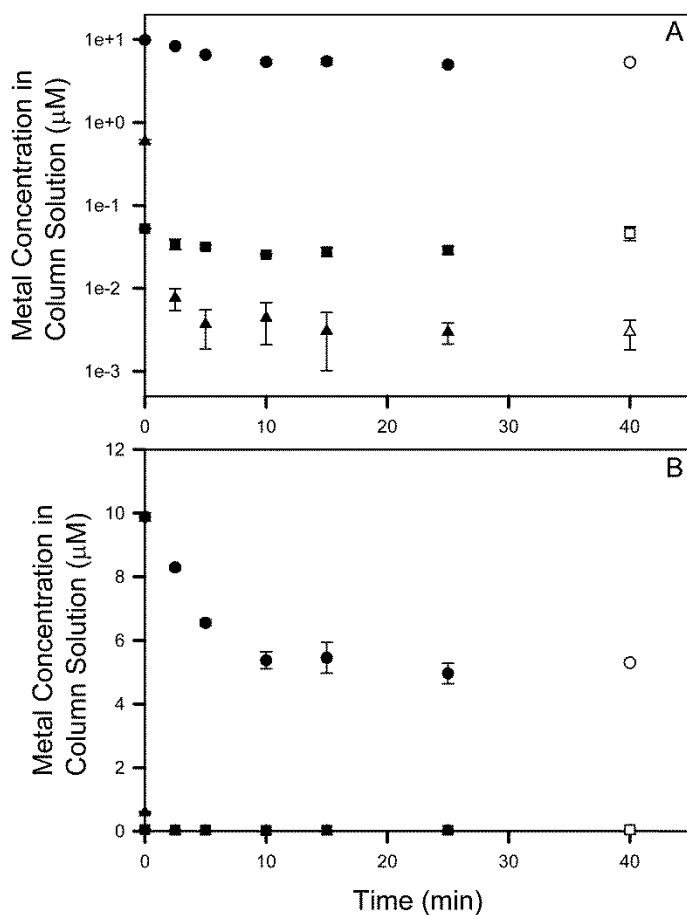


Figure 4.10 Efficacy of ion flotation of mixed metal solutions with (●) Cs⁺, (▲) Cd²⁺, and (■) La³⁺ at 9, 0.9, and 0.009 μM (total $\phi = 10$), respectively. The open symbol indicates the raffinate sample collected after column foam was allowed to collapse. Symbols represent mean and standard deviation values from triplicate columns. The same data is presented on a (A) semi-log graph and (B) linear graph.

With the exception of the mixed metal experiment with metals concentrations differing by orders of magnitude, the flotation removal efficiency order of the metals was $\text{Cd}^{2+} > \text{La}^{3+} \gg \text{Cs}^+$. This result is surprising and unexpected as the stability constants for these metals with monorhamnolipid are $\log \beta = 9.29, 7.17,$ and (3.43) for $\text{La}^{3+}, \text{Cd}^{2+}, \text{Cs}^+$, respectively (see Chapter 2). Based on these stability constants, one would expect La^{3+} removal to exceed Cd^{2+} for all the experiments. The data also shows, however, that at the same concentrations and conditions, the two metals are capable of exhibiting drastically different behaviors, e.g., at $\phi = 2$ Cd^{2+} forms a good foam while La^{3+} forms a scum. The root cause of these differences likely lies in different solubilities of the sublates as described above.

4.5. Conclusion

Monorhamnolipids were examined for their utility as ion flotation collectors for $\text{Cs}^+, \text{Cd}^{2+},$ and La^{3+} . Monorhamnolipids form stable foam during the aeration process, but the stability of the system is highly dependent on the metal and on the stoichiometric ratio of monorhamnolipid to metal. Overall, flotation improved above the estimated stoichiometric ratios of the collector-colligend sublates. Mass balances of the flotation system show minimal losses due to adsorption in the column and sampling, and the majority of the metal was found in the raffinate and foamate fractions. Examination of the foamate fraction shows that metals are rapidly removed, with removal concentrations nearing maximum within 10-15 minutes. When present as mixed metals solutions, metals were not removed as predicted by their stability constants, and metal speciation or sublata solubility issues are likely explanations. Overall, this study shows that monorhamnolipids have potential for use in ion flotation technologies, but determining the optimal operating

conditions for efficient flotation processes is a significant challenge subject to perturbation by even modest changes to single process parameters. Research efforts should be direct towards finding a specific application for monorhamnolipid-based ion flotation and developing application-specific processes for optimal flotation performance.

APPENDIX A

ELABORATION ON SCHUBERT'S METHOD AND ITS RELEVANCE HEREIN

A.1. Introduction

Determination of the stability constant of metal complexes can be accomplished in a variety of ways. A non-exhaustive list of methodologies which have been developed include potentiometry, polarography, amperometry, solubility, phase partitioning, spectrometry, conductivity reaction kinetics, and ion exchange.^{229, 230} The use of ion exchange processes for any purpose was practically non-existent until the creation of synthetic organic ion exchangers in 1935. After their discovery, the utility of ion exchange was rapidly recognized, and ion exchange applications flourished.²³¹ Interest in ion exchange was driven by the unique characteristics of the newly discovered synthetic organic ion exchangers according to Schubert: "high capacity in acid solutions, chemical and physical stability, rapidity and reversibility of the exchange reactions, and the approximate independence of capacity on particle size."²³¹

In 1948, Schubert described an ion exchange methodology for determining the formation constants of complex ions of zero or net negative charge. He summarizes the advantages of his method as 1) only tracer quantities of metal are required (10^{-10} moles), 2) it is suitable for use over a wide range of pH and temperature ranges, 3) it is rapid and simple, and 4) it appears to have good accuracy and precision.¹⁴⁴ Schubert's method was rapidly accepted and utilized for the study of metal complexes. A literature review by Marcus and Kertes²³² identified a total of 28 studies using Schubert's method to study metal complexes with organic and inorganic ligands. In later years, the method was

adapted by researchers studying the metal binding characteristics of humic substances and other environmental organic materials, e.g., poultry liter and wastewater sludges; a literature review by MacCarthy and Mark²³³ list 28 articles using Schubert's method to study organic matter between 1958 and 1975. More recently, Schubert's method has been adapted for the study of metal complexes with biosurfactant ligands.^{21, 74, 202}

A.2. Schubert's Method

A.2.1. Foundation

The adsorption isotherm for a cation and cation-exchanger with a given exchanger weight and solution volume is linear over a wide range of cation concentrations,¹⁴⁴ and this is the basis for Schubert's method. Within the linear range of the adsorption isotherm, the quantity of cations adsorbed on the exchanger, MR (mol kg⁻¹), is proportionate to the quantity of cations in the aqueous phase, M (mol l⁻¹). Thus, the distribution coefficient λ_o (Eq. A.1) within this linear range is constant at equilibrium.^{229,}

231

$$\lambda_o = [MR]/[M] \quad [\text{A.1}]$$

Eq. A.1 describes the distribution coefficient in the absence of a ligand. The distribution coefficient at equilibrium in the presence of ligand is described by Eq. A.2:

$$\lambda = [MR]/[(M + M_c)] \quad [\text{A.2}]$$

M_c is the concentration of complexed metal (mol l⁻¹). Combining Eqs. A.1 and A.2 gives:

$$\lambda_o/\lambda - 1 = [M_c]/[M] \quad [\text{A.3}]$$

which shows $(\lambda_o/\lambda - 1)$ is equal to the ratio of complexed metal to free metal.²³³

λ_o and λ can be experimentally determined by measuring the metal concentration in one or both of the resin and solution phases after the ion exchange reactions have

reached equilibrium. Unknowns can then be determined using mass balance equations. By doing so, this ion exchange method is essentially a technique for measuring and distinguishing between free and complexed metals in solutions.²³³

A.2.2. Determination of Stability Constant

The stability constant is determined using a linear relationship derived from the ligand-metal equilibrium reaction and the distribution coefficients. The equilibrium reaction for the formation of a metal-ligand complex is (charges have been omitted for clarity)



and from the law of mass action, the equilibrium stability constant is then

$$\beta = [ML_{\chi}]/([M][L]^{\chi}) \quad [A.5]$$

In the case of a single complex species in solution, $[M_c]$ from Eq. A.3 equals $[ML_{\chi}]$ and

$$\lambda_o/\lambda - 1 = [ML_{\chi}]/[M] \quad [A.6]$$

If Eq. A.5 is rearranged to

$$(\beta) \cdot ([M][L]^{\chi}) = [ML_{\chi}] \quad [A.7]$$

Eqs. A.6 and A.7 can be combined to obtain

$$\lambda_o/\lambda - 1 = [\beta] \cdot [L]^{\chi} \quad [A.8]$$

Taking the logarithm of both sides results in the linear relationship

$$\log\left(\frac{\lambda_o}{\lambda} - 1\right) = \log([\beta]) + \chi \log([L]) \quad [A.9]$$

originally described by Schubert.²³⁴ This form of Schubert's equation is applicable for only mononuclear complexes,^{143, 233, 235-237} but similar equations have been derived for equilibrium reactions of the general form^{233, 235}



Because monorhamnolipid will form only mononuclear complexes, discussion of polynuclear complexes is beyond the scope of this dissertation and has been omitted.

Using Eq. A.9, metal-ligand stability complexes can be determined if distribution coefficients are measured in a ligand-free system and in a ligand-containing system at two or more ligand concentrations. By plotting $\log([L])$ versus $\log\left(\frac{\lambda_0}{\lambda} - 1\right)$, the slope and intercept will represent the metal to ligand stoichiometry and logarithm of the stability constant, respectively.

A.2.3. Fundamental Assumptions

Underlying Schubert's method are numerous assumptions which must be considered when designing an experiment to determine stability constants by ion exchange. Schubert explicitly states five assumptions that must be met:

1. "The complex-forming ions are 'swamped' by excess neutral salt; the ionic strength remains nearly constant."
2. "The concentration of M^{a+} is negligible as compared to that of the complex-forming anion, A^{-b} ; actually, M^{a+} , is present in radiochemical concentrations ($\sim 10^{-9}$ mole per liter)."
3. "All pairs of solutions which are compared have the same pH, volume of solutions, and weight of adsorbent."
4. "The exchanger used has been previously saturated with the cation component of the bulk electrolyte."
5. "No adsorption of the complex-forming anion or of the complex ion takes place."

Stability constants can be reported as either activity quotients ("thermodynamic" stability constants) or as concentration quotients (stoichiometric stability constants). The former should be independent of ionic media, while the latter are valid in only specific media compositions.²³⁰ Thus,

"[i]f concentration quotients are determined in the presence of a large excess of background salt..., it may be assumed that the activity coefficients are

independent of the concentrations of the reacting species and depend only on the nature and concentration of the bulk electrolyte.”²³⁰

The purpose of Schubert’s first assumption is to ensure the activity coefficients of reacting species remains constant and stoichiometric values can be used instead of activities for the reactants.

Schubert’s second assumption allows for the simplification of calculations during determination of the stability constant. The term $[L]$ in Eq. A.9 is the free, i.e., dissociated, ligand concentration. By having a metal concentration which is negligible (100-fold less than the ligand concentration), the amount of complexed ligand can be considered insignificant and $[L]$ treated as equal to $[L_o]$, the stoichiometric concentration of ligand in the system, for calculations. The low concentrations of cation also ensure that the reaction occurs in the linear region of the adsorption isotherm.²³³ Lastly, for Schubert’s method to work, there must be an analytically detectable difference in the amount of metal in solution when ligand is added at different concentrations. Thus, working within a ligand concentration range which yields large changes in solution metals is desirable. Low concentrations of metals allow a wider range of ligand concentrations to be used such that an optimal range can be utilized.²³⁶

The third assumption of Schubert’s method is to ensure comparable results between complexation reactions. Changing the pH, volume of solution, or weight of adsorbent could change the distribution coefficients, which would in turn, cause error in the calculation of the stability constants.

Assumption four requires the exchanger to be pre-saturated with the cation of the neutral electrolyte. Pre-saturating the exchange resin with the electrolyte serves to pre-condition the resin to experimental conditions. It serves to reduce the transfer of cations

which are not being studied and reduce the error in mass balance calculations by preventing the introduction of unaccounted reactant cations. Lastly, pre-conditioning the resin with the neutral cation ensures that all exchange sites are stripped of H^+ which could affect the pH within and across reactions.²³⁸

The fifth assumption states the resin must not adsorb the ligand or complex ions. This assumption is unique to Schubert's method compared to other ion exchange methods.²³² This assumption is repeatedly made in the literature.^{147, 239-241} Li et al.²³⁹ and Schubert et al.²⁴¹ tested this assumption using radio-labeled acetate and oxalate, respectively, and found neither acetate nor oxalate cation complexes were adsorbed by the resin, thereby confirming the validity of the assumption. These two examples are the exception, however, as few other studies actually test the assumption, despite evidence showing some cation complexes demonstrate affinity for cation exchange resins.²³²

Exchange of positively charged complex species would not be remarkable,²³⁶ but Marcus and Kertes²³² note, "in general, it may be expected that with an anionic ligand L^i , the charge of the cation complexes ML_n^{m-ni} being lower than the uncomplexed metal, M^{m+} , they will have lower affinity to the resin." Galindo and Zunino²³⁶ further elaborate that exchange of positively charged complex species should be expected unless the complex size is so large that steric hindrance could prevent exchange. Complexes which are neutrally charged should have low affinity for the resin unless the conditions of the reaction favor resin infiltration by the complex.²³² Regardless of the charge of the complex species, the validity of this assumption is important: any sorption of complexes to the exchanger will result in lower apparent concentrations of complexes in solution, and error will be introduced into the stability constant determination. It is worth noting

that since Schubert's method was described, alternative ion exchange methods have been developed which are capable of accounting for adsorbed complexes and, thus, are not limited by Schubert's final assumption.^{232, 242}

In addition to Schubert's five assumptions, Zunino et al.²³⁵ list an additional three. First, it is assumed the ion exchange reaction is conducted with a "very high concentration of available cation exchange sites on the resin in relation to the metal-ion concentration in the solution." This assumption is meant to ensure that the adsorption isotherm is linear over a wide range of cation concentrations, and cation adsorption is not limited by limited exchange sites.

The second and third assumptions are "the amount of metal bound to the resin at equilibrium would be the same in the presence or in the absence of the complexant," and "the free metal-ion concentration in solution at equilibrium is the same in the presence or absence of the complexing anion," respectively. Zunino et al. argue that both of these assumptions are clearly erroneous (unless the complexing agent fails to complex the cation), but both wrong assumptions "compensate" each other such that Schubert's method holds true for mononuclear complexes. McCarthy and colleagues^{233, 237, 243} reviewed Schubert's original article¹⁴⁴ to examine the latter two assumptions proposed by Zunino et al.²³⁵ and found Zunino's assumptions were erroneous. MacCarthy found that Zunino's argument were based on misinterpretation of unclear writing and equation misprints in Schubert's paper. MacCarthy and Zunino agree that, as Schubert's equations are written, Schubert's method is valid for only mononuclear complexes, but MacCarthy shows that Schubert's equations would be valid for polynuclear complexes with suitable corrections.²³⁷ Despite Schubert's errors, MacCarthy²³³ further points out that Schubert

makes two unstated assumptions which also make the final equations applicable to only mononuclear complexes:

1. “Schubert assumes that the concentration of the complex in solution is equivalent to the total concentration of complexed metal ion in solution. This is true only for mononuclear complexes....”
2. “It is only in the case of mononuclear complexes that we can express the stability constant of a complex where the free and complexed metal ions are represented only as percentages of the total metal present.”

That is
$$\beta_{mn} = \frac{\%[M_c]}{m\%[M]^m[L]^n} \quad \text{for } m=1 \text{ only.}$$

Because Schubert was primarily interested in ligands which formed mononuclear complexes only, he likely overlooked these errors and assumptions in his original paper.²³³

A.3. Examination of Schubert’s Method as Used Herein

A.3.1. Chapters 2 and 3: Conformity to Schubert’s Assumption

Upon review of the methodologies described in Chapters 2 and 3 of this dissertation, it was determined that the conditions utilized did not fully satisfy the six assumptions required for Schubert’s method to be valid. The conditions which were employed and the degree to which they satisfy Schubert’s assumptions are described:

1. The reactants must be swamped by excess neutral salt:

The ion exchange reactions contained monorhamnolipid from 0.1 to 4 mM, metal at 0.5 mM, and 0.01 M of the neutral salt piperazine-N,N'-bis(2-ethanesulfonic acid (PIPES). To satisfy Schubert’s assumptions, the neutral salt must “swamp” the reactants. “Swamped” is defined as a 100-fold difference in concentration. The concentration of PIPES exceeded monorhamnolipid by 2.5 to 100 times. PIPES exceeded the metal

concentration by 20 times. These conditions do not fully satisfy this Schubert assumption.

2. The cation concentration is negligible compared to that of the anion:

The ion exchange reactions contained monorhamnolipid from 0.1 to 4 mM and metal at 0.5 mM. To be considered “negligible”, a material must have a 100-fold lower concentration than the material to which it is being compared. The monorhamnolipid concentration ranged from 0.2 to 8 times the metal concentration. These conditions do not fully satisfy this Schubert assumption.

3. All pairs of reactions to be compared have equivalent pH, resin weight, and solution volume:

All ion exchange reactions were conducted at pH 6.9 in 10 mL of solution, with 100 mg of resin. These conditions meet Schubert’s assumption.

4. The resin was pre-saturated with the cation of the neutral salt:

SP Sephadex C25 resin is manufactured with Na^+ as the counter-ion in the exchanger and was the resin utilized for all reactions. The resin was initially prepared by overnight soak in deionized water. The hydrated resin was rinsed with 1 l of deionized water, and mixed with enough pH 6.9 PIPES- Na_2 buffer to exceed the exchange site capacity of the resin with Na^+ . The resin was then dried for use in the ion exchange reactions. During the experiment, the acid form of PIPES was used as the neutral electrolyte buffer. Though Na^+ was not the cation of the neutral electrolyte, saturating the resin with Na^+ instead of H^+ was required to prevent resin H^+ from changing the reaction pH.²³⁸ These conditions do not technically meet Schubert’s assumption, but the conditions

were selected to meet the needs of the experiment and were supported by published protocols in the literature.²³⁸

5. The anion nor any complex species adsorb to the resin.

Previous research has shown monorhamnolipids do not adsorb to the resin.⁷⁴ No method was used to verify whether monorhamnolipid-metal complexes were adsorbing to the resin herein. Equilibrium first principles calculations (discussed in Chapter 2) show less metal is found in solution than is predicted by the stability constants (Table 2.2). This suggests some metal may be forming cationic 1:1 complexes with monorhamnolipid and being retained on the resin. Thus, the conditions used may not satisfy this Schubert assumption.

6. The number of cation exchange sites must be in excess of the cation concentration.

SP Sephadex C25 resin has a total ionic capacity of 2-2.6 mmols g⁻¹ dry resin. Assuming the lower limit, 0.2 mmols of ionic capacity was available in each reaction. The reactions contained 0.005, 0.01, and 0.015 mmols of charge for the mono-, di-, and trivalent metals, respectively. The resin had at least 13 to 40 times the capacity required by the metal concentrations in the reaction.

These conditions meet this Schubert assumption.

Because the conditions utilized in Chapters 2 and 3 did not fully satisfy Schubert's assumptions, a revised experiment was devised to examine monorhamnolipid complexation of Pb²⁺ and La³⁺ in conditions which satisfy Schubert's assumptions.

A.3.2. Revised Experimental Materials and Methods

A.3.2.1. Monorhamnolipid Production

Pseudomonas aeruginosa ATCC 9027 was obtained from the American Type Culture Collection and kept as a glycerol freezer stock at -80° C. This strain is a natural mutant that has been previously shown to exclusively produce monorhamnolipid congeners.^{138, 139} *P. aeruginosa* was cultured for 24 h at 37° C on a PTYG agar (0.5% protease peptone, 0.5% tryptone, 1% yeast extract, 0.06% MgSO₄•7H₂O, 7x10⁻⁴% CaCl₂•2H₂O, and 1% glucose). The agar culture was transferred to Kay's mineral medium for 24 h growth at 37° C and 200 rpm. Kay's mineral medium contains 100 ml of solution A (0.3% NH₄H₂PO₄, 0.2% K₂HPO₄, and 0.2% glucose), 1 ml solution B (0.025% FeSO₄•7H₂O) and 1 ml solution C (10% MgSO₄•7H₂O). The pre-culture was transferred to a pH 7 minimal salts medium (MSM) with 2% glucose at a ratio of 1 ml pre-culture per 100 ml MSM. MSM is composed of 1 l of solution A (0.25% NaNO₃, 0.04% MgSO₄•7H₂O, 0.1% KCl, 0.1% NaCl, 0.005% CaCl₂•2H₂O, and 0.4% H₃PO₄) mixed with 1 ml of solution B (0.05% FeSO₄•7H₂O, 0.15% ZnSO₄•7H₂O, 0.15% MnSO₄•H₂O, 0.03% H₃BO₃, 0.015% CoCl₂•6H₂O, 0.015% CuSO₄•5H₂O, and 0.01% Na₂MoO₄•2H₂O). The MSM culture is placed in a 37° C gyratory shaker and shaken for 72 h at 200 rpm.

A.3.2.2. Monorhamnolipid Purification

Monorhamnolipids produced by *Pseudomonas aeruginosa* ATCC 9027 are a congener mixture of up to 30 molecules in which the rhamnose headgroup is preserved but the alkyl chains can vary in chain length and, to a lesser extent, saturation.¹⁴⁰ The protocol used for this work generates a pure native mixture in which the major congener, rhamnosyl-β-hydroxydecanoyl-β-hydroxydecanoate (Rha-C10-C10), typically dominates

at 75-85 wt% of the mixture.^{140, 141} This complex assembly of congeners is referred to herein as either the native monorhamnolipid mixture or simply monorhamnolipids.

The native monorhamnolipid mixture was concentrated by centrifugation (10,000 rpm for 10 min) to remove cells and cellular debris, followed by removal and acidification of the supernatant to pH 2 using HCl. Monorhamnolipids have pK_a values of ~5.5, below which they become poorly soluble¹³⁸ and can be collected by centrifugation. Pelleted monorhamnolipids were dissolved in a 9:1 chloroform:methanol mixture and separated from remnant water using a separatory funnel. The solvent was removed by rotoevaporation. The concentrated monorhamnolipids were purified using a solvent mixture of 6:6:6:1:1 (v/v) of hexane:dichloromethane:ethyl acetate:chloroform:methanol (containing 0.1% acetic acid) by elution through a 22 x 300 mm gravity-based, glass chromatography column packed with 45 g of 60-Å-pore silica gel. Monorhamnolipids were collected when column eluent tested positive for rhamnose with anthrone reagent dissolved in H₂SO₄. The solvent mixture was removed from the monorhamnolipids by rotoevaporation, and purity is checked by reversed phase high performance liquid chromatography on a C18 column.¹³⁸

A.3.2.3. Metals

Pb(NO₃)₂ and La(NO₃)₃•6H₂O were purchased from Sigma-Aldrich with a purity of ≥99% and were used as received.

A.3.2.4. Ion Exchange Reactions

The ion exchange resin SP Sephadex C25 (GE Healthcare) was prepared by soaking in ultrapure water (≥18 MΩ-cm) overnight. The hydrated resin was washed with equal parts ultrapure water, then pH 6.9 PIPES-Na₂ buffer, and air-dried; sufficient buffer

was used to saturate the resin with Na^+ . Ion exchange reactions were conducted in 15-ml metal-free centrifuge tubes. Each reaction contained 10 mg of prepared resin, a volume of 10 ml, a pH of 6.9, and final concentrations of 50 nM metal, 0.01 M PIPES- Na_2 buffer, 0.1 M NaNO_3 , and 0, 10, 20, 30, or 40 μM of the native monorhamnolipid mixture. NaCl was tested for use as the neutral electrolyte, but it was found to be unsuitable due to precipitate formation with the test metals. 10 mM monorhamnolipid solution was generated in a Teflon container using a molecular weight of 504 g mol^{-1} for the native monorhamnolipid mixture. Monorhamnolipids were measured gravimetrically, dissolved in the reaction buffer (0.1 M NaNO_3 and 0.01 M PIPES- Na_2), and the solution adjusted to pH 6.9. 0.5 mM metal solutions were mixed with the same reaction buffer 0.5 h before use. Reactions were mixed horizontally on a platform rotator for 2 h, allowed to settle vertically for a minimum of 1 h, and then a sample of supernatant was removed and diluted in 2% HNO_3 . To determine a metal mass balance, the remaining supernatant was decanted from the resin, and the resin was oven dried at 60° for 4 days. Both the supernatant and resin samples were sent to the Arizona Laboratory for Emerging Contaminants (ALEC) at the University of Arizona for metals analysis by inductively coupled plasma mass spectrometry. Metal analysis of the resin samples included a nitric acid and microwave digestion procedure performed by ALEC personnel.

A.3.3. Revised Experiment's Conformity to Schubert's Assumptions

The degree to which the conditions outlined in section A.3.2 satisfy Schubert's assumptions are described:

1. The reactants must be swamped by excess neutral salt:

The ion exchange reactions contained monorhamnolipid from 10 to 40 μM ,

metal at 50 nM, and 0.1 M of the neutral salt NaNO₃. To satisfy Schubert's assumptions, the neutral salt must "swamp" the reactants. "Swamped" is defined as a 100-fold difference in concentration. The concentration of NaNO₃ exceeded monorhamnolipid by 2500 to 10,000 times. PIPES exceeded the metal concentration by two million times. These conditions satisfy this Schubert assumption.

2. The cation concentration is negligible compared to that of the anion:

The ion exchange reactions contained monorhamnolipid from 10 to 40 μM and metal at 50 nM. To be considered "negligible", a material must have a 100-fold lower concentration than the material to which it is being compared. The monorhamnolipid concentration ranged from 200 to 800 times the metal concentration. These conditions satisfy this Schubert assumption.

3. All pairs of reactions to be compared have equivalent pH, resin weight, and solution volume:

All ion exchange reactions were conducted at pH 6.9 in 10 mL of solution with 10 mg of resin. These conditions satisfy Schubert's assumption.

4. The resin was pre-saturated with the cation of the neutral salt:

SP Sephadex C25 resin is manufactured with Na⁺ as the counter-ion in the exchanger and was the resin utilized for all reactions. The resin was initially prepared by overnight soak in deionized water. The hydrated resin was rinsed with 1 l of deionized water, and mixed with enough pH 6.9 PIPES-Na₂ buffer to exceed the exchange site capacity of the resin with Na⁺. The resin was then dried for use in the ion exchange reactions. During the experiment, a NaNO₃

and PIPES- Na_2 buffer were used as the neutral electrolyte. Since both the buffer and resin utilized Na^+ as the neutral electrolyte cation, these conditions satisfy this Schubert assumption.

5. The anion nor any complex species adsorb to the resin.

The resin was not directly measured for adsorbed monorhamnolipids, nor was the supernatant measured to determine the monorhamnolipid distribution in the ion exchange reactions. Direct quantitative measurement of the monorhamnolipids used in this experiment would be difficult due to the mass of monorhamnolipids used: 50-200 μg per reaction. Based on the large stability constants determined in Chapter 2 and given the large excess of ligand compared to cation, it is assumed all metal in the reaction is complexed to some degree with the monorhamnolipid ligand and no free metal exists. Thus, any metal found adsorbed to the resin is assumed to be part of a metal-ligand complex. While evidence is collected to determine whether this assumption is satisfied, the conditions used in the revised experiment do not directly address this Schubert assumption.

6. The number of cation exchange sites must be in excess of the cation concentration.

SP Sephadex C25 resin has a total ionic capacity of 2.-2.6 mmols g^{-1} dry resin. Assuming the lower limit, 0.02 mmols of ionic capacity was available in each reaction. The reactions contained 1 or 1.5 nmols of charge for the Pb^{2+} and La^{3+} , respectively. The resin had at least 13,333 to 20,000 times the capacity

required by the metal concentration in the reactions. These conditions meet this Schubert assumption.

A.3.4. Results and Discussion

The metals lead and lanthanum were reacted with monorhamnolipid to determine the conditional stability constants and stoichiometry of monorhamnolipid:metal complexes using Schubert's ion exchange technique.¹⁴⁴ Figure A.1A shows the change in solution metal content as the monorhamnolipid concentration is increased. Solution La^{3+} increased from 9% of added metal in the ligand free control to 16% at the highest monorhamnolipid concentration of 40 μM . The solution Pb^{2+} content remained effectively constant at all of the monorhamnolipid concentrations tested. These results starkly contrast the results for Pb^{2+} and La^{3+} using the experimental conditions outlined in Chapter 2 (Figure A.1B) where 97% and 84% of the added metals were found in solution at the highest monorhamnolipid concentration, respectively. Even when no ligand is present in either metal system, the adsorption of Pb^{2+} and La^{3+} are dramatically different between the experimental conditions of Appendix A and Chapter 2. In the former, Pb^{2+} and La^{3+} are 59% and 9% in solution versus <1% in solution for both in the latter set of conditions. λ_o values decrease for both metals. La^{3+} decreased from 3330 to 9.8 and Pb^{2+} decreased from 166 to 0.7.

Solution metal concentrations were used to determine the conditional stability constants and complex stoichiometry using Eq. A.9. Figure A.2 shows a plot of $\log\left(\frac{\lambda_o}{\lambda} - 1\right)$ as a function of $\log(L)$ for La^{3+} , from which the conditional stability constant and complex stoichiometry can be determined using the linear regression shown. The conditional stability constant ($\log \beta$) is 4.56 and the complex stoichiometry (χ) is 1.06 for

La^{3+} interacting with monorhamnolipids under conditions which meet the Schubert method's assumptions. These values are significantly lower than those reported in Table 2.1 from Chapter 2: $\log(\beta) = 9.29$ and $\chi = 2.07$. Because Pb^{2+} showed no increase in solution metal with increasing monorhamnolipid concentration, Schubert's method could not be used for the determination of the monorhamnolipid-metal stability constant under these conditions.

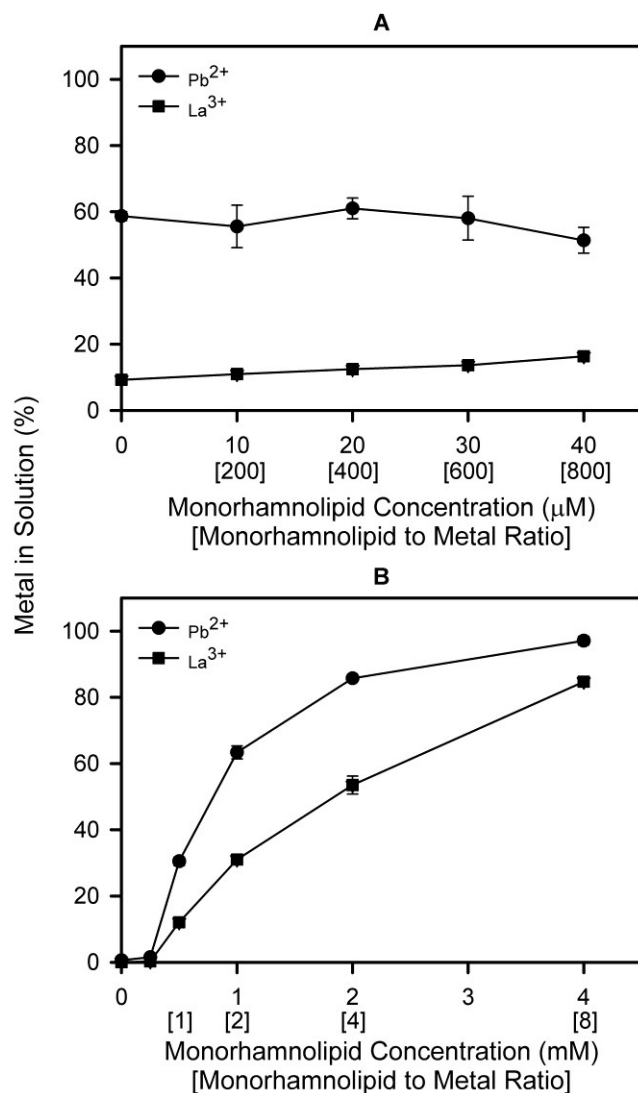


Figure A.1 (A) Effect of monorhamnolipid concentration on the complexation of Pb^{2+} and La^{3+} under conditions which meet the Schubert method assumptions. Each point represents the mean and standard deviation of 3 replicates. **(B)** Effect of monorhamnolipid concentration on the complexation of Pb^{2+} and La^{3+} under the original conditions of Chapter 2. Each point represents the mean and standard deviation of 6 replicates.

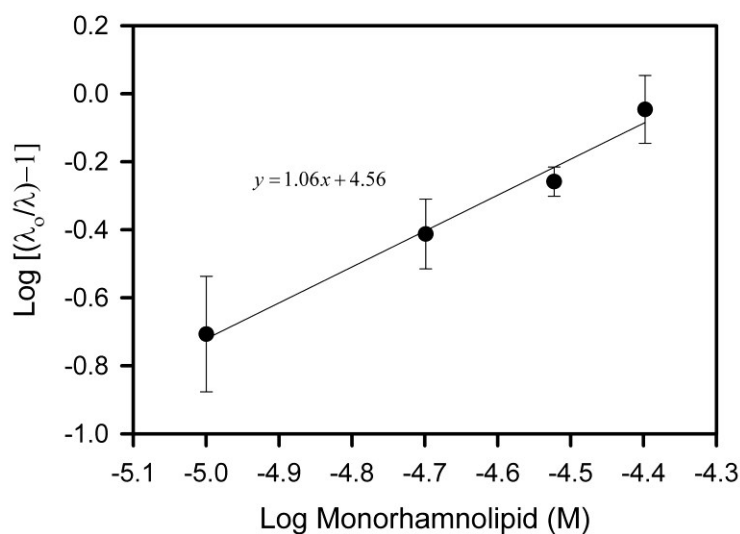


Figure A.2 Determination of the conditional stability constant and stoichiometry of monorhamnolipid:metal complexes by ion-exchange equilibrium method for La^{3+} under conditions which meet the Schubert method assumptions. Each point represents the mean and standard deviation of 3 replicates.

These results demonstrate that when the conditions under which the Schubert methodology is conducted are changed, there are dramatic shifts in the behavior of the system as a whole. The purpose of this appendix is to examine these differences and determine what impact changing the experimental conditions to meet Schubert's assumptions would have on the complexation data presented in Chapters 2 and 3. Unfortunately, the changes to the conditions were so drastic that the experimental methodologies created two completely different systems, and it is difficult, if not impossible, to determine the cause of differences in results between the two methodologies. For the purpose of subsequent discussion, the methodology described in Chapters 2 and 3 will be referred to the "original methodology" and the methodology

described in Appendix A will be referred to as the “modified methodology”. Table A.1 summarizes the experimental conditions used for these methods.

Table A.1 Summary of experimental conditions for the original (chapter 2 & 3) and modified (appendix A) methodologies

	Methodology	
	Original	Modified
NaNO₃ (mM)	0	100
PIPES (mM)	10	10
Monorhamnolipid (μM)	0, 100, 500, 1000, 2000, 4000	0, 10, 20, 30, 40
Metal (nM)	500000	50
Resin (mg)	100	10
Volume (ml)	10	10
pH	6.9	6.9

To illustrate the difficulty in comparing results between the methodologies, consider the conditional stability constant of La³⁺. Using the original methodology, the conditional stability constant of La³⁺ was $\log(\beta) = 9.13$, while the modified method yielded $\log(\beta) = 4.56$. The difference of 4.57 could be the result of the latter experiment conforming to the Schubert assumptions, but there are numerous factors which are likely causes of the disagreement. For example, changing the ionic strength of the solution in an ion exchange experiment can cause order of magnitude stability constant differences in otherwise identical systems. This was demonstrated in a study that examined changing the ionic strength from 0.0 to 0.15. Increased ionic strength caused $\log(\beta)$ values to

decrease linearly in metal-fulvic acid systems for all 10 metals tested.¹⁴² The degree of change was dependent on the metal, but differences were on the scale of one or more orders of magnitude.¹⁴² The same trend was observed for a strontium and citrate system.²⁴⁴ These two studies show the differences in stability constant with changing ionic strength are characteristic of a ligand and metal pair. In the experiments reported herein, the difference in ionic strength was about 0.1 M, and the ~4 order of magnitude difference could be the result of differences in ionic strength.

The monorhamnolipid concentrations were also changed by two orders of magnitude. The monorhamnolipid concentration was changed from well above the critical micelle concentration to a concentration near the critical micelle concentration. It is unknown what effect the presence or absence of monorhamnolipid aggregates would have on the conditional stability constant determined by Schubert's method. Furthermore, the reduction of the monorhamnolipid concentration to 10-40 μM from 0.1-4 mM, raises concerns of monorhamnolipid loss due to adsorption to the reaction vessel. At the 10-40 μM range, the 15-ml centrifuge tubes have enough surface area to adsorb 2.5 to 10% of the added monorhamnolipid, respectively (calculations not shown). Loss of this much monorhamnolipid from the system could be a potential explanation of lower stability constants using the modified methodology. In the 0.1-4 mM concentration range, monorhamnolipid loss due to adsorption can be considered negligible. These calculations do not include the surface area added by the resin, but it has been shown that there is no measureable loss of monorhamnolipid due to resin adsorption at a concentration range of 0-4.2 mM.⁷⁴ Because of the much smaller concentration range, it is feasible that

adsorption of monorhamnolipid to resin may not be negligible for μM concentrations, thus, potentially reducing the stability constant further.

Other considerations for the difference in stability constants should include the addition of large quantities of neutral electrolyte and the reduction of resin weight in the modified methodology. The results show that the large difference in background cation concentration and reduction in resin weight reduced the ligand-free distribution coefficient, λ_o , for both metals with unknown effect on stability constant determinations. The use of Eq. A.9 assumes no other ligands complex the metal. This is not always true and other equations are required to describe more complicated systems where this is occurring.²⁴⁴ NO_3^- concentrations increased by nearly three orders of magnitude in the modified methodology, and it is unknown the degree to which NO_3^- is interacting with the metals or how it may be affecting the stability constant determination. In the original method, NO_3^- is present at the same concentration as the metal because nitrate metal salts were used.

As a final illustration of the difficulty in comparing differences of the results from Appendix A and Chapters 2 and 3, consider the monorhamnolipid to metal ratios in Figure A.1 where Figure A.1A is data collected using the modified methodology, and Figure A.1B is data collected using the original methodology. During the discussion of first principle calculations versus observed results in section 2.4.2, it was noted that calculated estimates of metal complexation differed from observed data. The difference was attributed to positively charged complex species adsorbing to the resin. Assume this is true. Figure A.1B shows that as the monorhamnolipid to metal ratio increases from 1 to 8, the amount of complexed metal (indicated by the presence of metal in solution)

increases from 1.5% to 97% for Pb^{2+} and from ~0.25% to 85% for La^{3+} . The increase in solution metal is expected because, as the ligand to metal ratio increases, there is additional ligand available for the formation of ML_n species with higher 'n' values. As 'n' increases, so does the number of neutrally or negatively charged species in solution.

Contrast this data to the data in Figure A.1A where the monorhamnolipid to metal ratio increases from 200 to 800. Despite the ligand being in great excess where 'n' should be at a maximum, Pb^{2+} shows no increase in the reaction solution. If our assumption above is true, then this can be attributed to either the formation of only positively charged complexes or no complexation of lead with monorhamnolipid. The former explanation is contradictory to the results of Figure A.1B since neutral or negatively charged lead-monorhamnolipid species are evident at the much lower monorhamnolipid to metal ratios, and the latter case is clearly erroneous as there is plentiful evidence of monorhamnolipid binding of lead.²⁰³ Examination of La^{3+} in Figure A.1 shows a similar divergence where at lower monorhamnolipid to metal ratios, there is a substantial degree of neutral or negatively charged species in solution (Figure A.1B), while at the much high monorhamnolipid to metal ratios there is relatively little formation of such complex species. These differences are evidence that the two methodologies have resulted in two systems so vastly different, that comparison of the two systems for the purpose of understanding the effects of Schubert's assumptions is not feasible. The difference in conditional stability constants between the two methods is certainly a function of meeting Schubert's assumptions, but due to the compounding issues highlighted above, understanding the effects Schubert's assumptions requires a significant amount of additional research to manage, understand, or eliminate other variables.

A.4. Conclusion

The underlying principle of the conditional stability constant is that, during analysis, the concentration of the anticipated or desired analyte is of the utmost importance and other species are of lesser importance.^{245, 246} By approaching the determination of stability constants in this way, the stability constant is *conditional* on the prevailing conditions in which it was determined.²⁴⁵ In this dissertation, there is no question, the methodology of Chapters 2 and 3 do not fully satisfy the assumptions underlying Schubert's method, but they do provide a measure of the analyte of interest: monorhamnolipid complexed metal. Schubert's method is intended to determine the stoichiometric stability constant of metal ligand complexes; the work in this dissertation and by others^{21, 74} has adapted Schubert's method for the determination of *conditional* stability constants so that an understanding of the relative binding strengths of monorhamnolipid with a variety of metals could be developed. Even Schubert has used a similar approach which did not meet his assumptions to determine the relative influence of factors such as temperature, ionic strength, and presence of formaldehyde on stability constants: "[Eq. A.9] is valid for the conditions employed even when the complex ion is itself adsorbed, *i.e.*, has a net positive charge."²⁴⁴ The suitability of this approach is supported by the results of mixed metals studies in this dissertation (Chapters 2 & 4) and the literature.^{73-77, 79, 80, 82, 102}

At the outset of the work covered in this dissertation, it was never the goal to establish exact stoichiometric stability constants for metal-monorhamnolipid complexes. Rather, I sought to assess the relative binding strength of monorhamnolipids with a variety of metals to determine which metals are preferentially bound by

monorhamnolipid. The information gleaned from this research would then become the foundation on which monorhamnolipid-based technologies could be developed for the recovery of target metals from metalliferous aqueous media, whether for economic gain or environmental protection. I strongly believe that the work contained within this dissertation accomplished this goal, generated reliable data using appropriate methods, and contributed valuable information to the scientific community.

If the specific stoichiometric stability constant and step-wise stability constants of monorhamnolipid with metals are of future research interest, the method of Schubert may be utilized. The assumptions on which the method is based can be satisfied, but careful research will be required to determine optimal reaction conditions; a review of the literature related to Schubert's method will yield numerous papers which provide guidance on what conditions and mathematical treatments should be utilized to generate reliable data with little error.^{230, 232, 233, 235, 236, 244, 244, 247} If challenges remain, such as adsorption of ligand to the resin, other methodologies may prove to be more successful approaches.^{230, 232}

REFERENCES

1. Nriagu, J.O. A history of global metal pollution. *Science* **1996**, 272 (5259), 223-223;
10.1126/science.272.5259.223.
2. Kotz, J.C.; Treichel, P.; Weaver, G.C. *Chemistry & chemical reactivity*. Thomson
Brooks/Cole: Belmont, CA, 2006.
3. Essington, M.E. *Soil and water chemistry: an integrative approach*. CRC Press: Boca
Raton, 2004.
4. Callender, E. 9.03 - Heavy metals in the environment—historical trends, In *Treatise on
Geochemistry*, Editors-in-Chief: Heinrich D. Holland; Karl K. Turekian, Eds.;
Pergamon: Oxford, 2003; pp. 67-105.
5. Csavina, J.; Landazuri, A.; Rheinheimer, P.; Saez, A.E.; Wonaschutz, A.; Rine, K.;
Barbaris, B.; Conant, W.; Betterton, E.A. Metal and metalloid contaminants in
atmospheric aerosols from mining operations. *Water Air Soil Pollut. Water, Air,
and Soil Pollution* **2011**, 221 (1-4), 145-157.
6. Maier, R.M.; Pepper, I.L.; Gerba, C.P. *Environmental microbiology*.
Elsevier/Academic Press: Amsterdam; Boston, 2009.
7. Nriagu, J.O. A global assessment of natural sources of atmospheric trace-metals.
Nature **1989**, 338 (6210), 47-49; 10.1038/338047a0.

8. Nriagu, J.O.; Pacyna, J.M. Quantitative assessment of worldwide contamination of air, water and soils by trace-metals. *Nature* **1988**, *333* (6169), 134-139;
10.1038/333134a0.
9. Pacyna, J.M.; Pacyna, E.G. An assessment of global and regional emissions of trace metals to the atmosphere from anthropogenic sources worldwide. *Env. Rev.* **2001**, *9* (4), 269.
10. Nriagu, J.O. Global metal pollution: poisoning the biosphere? *Environment: Science and Policy for Sustainable Development* **1990**, *32* (7), 7-33;
10.1080/00139157.1990.9929037.
11. Wuana, R.A.; Okieimen, F.E. Heavy metals in contaminated soils: a review of sources, chemistry, risks and best available strategies for remediation. *ISRN Ecology ISRN Ecology* **2011**, *2011* (4), 1-20.
12. Pacyna, J.M.; Scholtz, M.T.; Li, Y.F. Global budget of trace metal sources. *Environ.Rev.Environmental Reviews* **1995**, *3* (2), 145-159.
13. Bodour, A.A.; Guerrero-Barajas, C.; Jiorle, B.V.; Malcomson, M.E.; Paull, A.K.; Somogyi, A.; Trinh, L.N.; Bates, R.B.; Maier, R.M. Structure and characterization of flavolipids, a novel class of biosurfactants produced by *Flavobacterium* sp. strain MTN11. *Applied and Environmental Microbiology* **2004**, *70* (1), 114-120;
10.1128/AEM.70.1.114-120.2004.

14. Lang, S. Biological amphiphiles (microbial biosurfactants). *Current Opinion in Colloid & Interface Science* **2002**, 7 (1-2), 12-20; 10.1016/S1359-0294(02)00007-9.
15. Singh, A.; Van Hamme, J.D.; Ward, O.P. Surfactants in microbiology and biotechnology: part 2. application aspects. *Biotechnol. Adv.* **2007**, 25 (1), 99-121; 10.1016/j.biotechadv.2006.10.004.
16. Van Hamme, J.D.; Singh, A.; Ward, O.P. Physiological aspects - part 1 in a series of papers devoted to surfactants in microbiology and biotechnology. *Biotechnol. Adv.* **2006**, 24 (6), 604-620; 10.1016/j.biotechadv.2006.08.001.
17. Thimon, L.; Peypoux, F.; Michel, G. Interactions of surfactin, a biosurfactant from *Bacillus subtilis*, with inorganic cations. *Biotechnol. Lett.* **1992**, 14 (8), 713-718; 10.1007/BF01021648.
18. Thimon, L.; Peypoux, F.; Wallach, J.; Michel, G. Ionophorous and sequestering properties of surfactin, a biosurfactant from *Bacillus subtilis*. *Colloids and Surfaces B: Biointerfaces* **1993**, 1 (1), 57-62; 10.1016/0927-7765(93)80018-T.
19. Tan, H.; Champion, J.T.; Artiola, J.F.; Brusseau, M.L.; Miller, R.M. Complexation of cadmium by a rhamnolipid biosurfactant. *Environ. Sci. Technol.* **1994**, 28 (13), 2402-2406; 10.1021/es00062a027.

20. Abdel-Mawgoud, A.M.; Lepine, F.; Deziel, E. Rhamnolipids: diversity of structures, microbial origins and roles. *Appl. Microbiol. Biotechnol.* **2010**, *86* (5), 1323-1336; 10.1007/s00253-010-2498-2.
21. Ochoa-Loza, F.J.; Artiola, J.F.; Maier, R.M. Stability constants for the complexation of various metals with a rhamnolipid biosurfactant. *J. Environ. Qual.* **2001**, *30* (2), 479-485.
22. Schalnat, T.A. Metal complexation and interfacial behavior of the microbially-produced surfactant monorhamnolipid by *Pseudomonas aeruginosa* ATCC 9027. Ph.D. Dissertation, University of Arizona, 2012.
23. Bodor, A.; Banyai, I.; Toth, I. H-1- and C-13-NMR as tools to study aluminium coordination chemistry - aqueous Al(III)-citrate complexes. *Coord. Chem. Rev.* **2002**, *228* (2), 175-186; 10.1016/S0010-8545(02)00039-5.
24. Ferrari, E.; Grandi, R.; Lazzari, S.; Saladini, M. Hg(II)-coordination by sugar-acids: role of the hydroxy groups. *J. Inorg. Biochem.* **2005**, *99* (12), 2381-2386; 10.1016/j.jinorgbio.2005.09.005.
25. Rondeau, P.; Sers, S.; Jhurry, D.; Cadet, F. Sugar interaction with metals in aqueous solution: Indirect determination from infrared and direct determination from nuclear magnetic resonance spectroscopy. *Appl. Spectrosc.* **2003**, *57* (4), 466-472; 10.1366/00037020360626023.

26. Pankiewicz, R.; Schroeder, G.; Brzezinski, B.; Bartl, F. NMR, FT-IR and ESI-MS study of new lasalocid ester with 2-(hydroxymethyl)-12-crown-4 and its complexes with monovalent cations. *J. Mol. Struct.* **2005**, *749* (1-3), 128-137; 10.1016/j.molstruc.2005.03.039.
27. Karkhaneei, E.; Zebarjadian, M.H.; Shamsipur, M. Complexation of Ba²⁺, Pb²⁺, Cd²⁺, and UO₂²⁺ ions with 18-crown-6 and dicyclohexyl-18-crown-6 in nitromethane and acetonitrile solutions by a competitive NMR technique using the Li⁻⁷ nucleus as a probe. *Journal of Solution Chemistry* **2001**, *30* (4), 323-333; 10.1023/A:1010323106004.
28. Rouhollahi, A.; Amini, M.K.; Shamsipur, M. NMR-study of the stoichiometry, stability and exchange kinetics of complexation reaction between Pb²⁺ ion and 18-crown-6 in binary acetonitrile-water mixtures. *Journal of Solution Chemistry* **1994**, *23* (1), 63-74; 10.1007/BF00972608.
29. Colthup, N.B.; Daly, L.H.; Wiberley, S.E. *Introduction to infrared and raman spectroscopy*. Academic Press: Boston, 1990.
30. Mehrotra, R.C.; Bohra, R. *Metal carboxylates*. Academic Press: London; New York, 1983.
31. Palacios, E.G.; Juarez-Lopez, G.; Monhemius, A.J. Infrared spectroscopy of metal carboxylates - II. analysis of Fe(III), Ni and Zn carboxylate solutions. *Hydrometallurgy* **2004**, *72* (1-2), 139-148; 10.1016/S0304-386X(03)00137-3.

32. Strathmann, T.J.; Myneni, S.C.B. Speciation of aqueous Ni(II)-carboxylate and Ni(II)-fulvic acid solutions: combined ATR-FTIR and XAFS analysis. *Geochim. Cosmochim. Acta* **2004**, *68* (17), 3441-3458; 10.1016/j.gca.2004.01.012.
33. Tajmir-Riahi, H. Sugar complexes with alkaline earth metal ions: synthesis, structure, and spectroscopic studies of Mg(II), Sr(II), and Ba(II) complexes of d-glucuronic acid. *J. Inorg. Biochem.* **1985**, *24* (2), 127-136; 10.1016/0162-0134(85)80004-0.
34. Tajmir-Riahi, H. Carbohydrate complexes with lead(II) ion: interaction of Pb(II) with Beta-D-glucurono-6,3-lactone, D-glucono-1,5-lactone, and their acid anions and the effects of metal ion binding on the sugar hydrolysis. *Bull. Chem. Soc. Jpn.* **1989**, *62* (4), 1281-1286; 10.1246/bcsj.62.1281.
35. Tian, W.; Yang, L.M.; Xu, Y.Z.; Weng, S.F.; Wu, J.G. Sugar interaction with metal ions: FT-IR study on the structure of crystalline galactaric acid and its K^+ , NH_4^+ , Ca^{2+} , Ba^{2+} , and La^{3+} complexes. *Carbohydr. Res.* **2000**, *324* (1), 45-52; 10.1016/S0008-6215(99)00276-1.
36. Campbell, S.; Rodgers, M.T.; Marzluff, E.M.; Beauchamp, J.L. Structural and energetic constraints on gas-phase hydrogen-deuterium exchange-reactions of protonated peptides with D_2O , CD_3OD , CD_3CO_2D , and ND_3 . *J. Am. Chem. Soc.* **1994**, *116* (21), 9765-9766; 10.1021/ja00100a058.
37. Campbell, S.; Rodgers, M.T.; Marzluff, E.M.; Beauchamp, J.L. Deuterium exchange reactions as a probe of biomolecule structure. Fundamental studies of gas phase H/D exchange reactions of protonated glycine oligomers with D_2O , CD_3OD ,

CD₃CO₂D, and ND₃. *J. Am. Chem. Soc.* **1995**, *117* (51), 12840-12854;
10.1021/ja00156a023.

38. Green, M.K.; Gard, E.; Bregar, J.; Lebrilla, C.B. H-D exchange kinetics of alcohols and protonated peptides - effects of structure and proton affinity. *Journal of Mass Spectrometry* **1995**, *30* (8), 1103-1110; 10.1002/jms.1190300807.
39. Neilson, J.W.; Zhang, L.; Veres-Schalnat, T.A.; Chandler, K.B.; Neilson, C.H.; Crispin, J.D.; Pemberton, J.E.; Maier, R.M. Cadmium effects on transcriptional expression of rhlB/rhlC genes and congener distribution of monorhamnolipid and dirhamnolipid in *Pseudomonas aeruginosa* IGB83. *Appl. Microbiol. Biotechnol.* **2010**, *88* (4), 953-963; 10.1007/s00253-010-2808-8.
40. Maslin, P.; Maier, R.M. Rhamnolipid-enhanced mineralization of phenanthrene in organic-metal co-contaminated soils. *Bioremediation J.* **2000**, *4* (4), 295-308.
41. Guerrasantos, L.; Kappeli, O.; Fiechter, A. *Pseudomonas aeruginosa* biosurfactant production in continuous culture with glucose as carbon source. *Appl. Environ. Microbiol.* **1984**, *48* (2), 301-305.
42. Ramana, K.V.; Karanth, N.G. Factors affecting biosurfactant production using *Pseudomonas aeruginosa* Cftr-6 under submerged conditions. *Journal of Chemical Technology and Biotechnology* **1989**, *45* (4), 249-257.
43. Deziel, E.; Lepine, F.; Milot, S.; Villemur, R. rhlA is required for the production of a novel biosurfactant promoting swarming motility in *Pseudomonas aeruginosa*: 3-

- (3-hydroxyalkanoyloxy)alkanoic acids (HAAs), the precursors of rhamnolipids. *Microbiology-(UK)* **2003**, *149*, 2005-2013; 10.1099/mic.0.26154-0.
44. Glick, R.; Gilmour, C.; Tremblay, J.; Satanower, S.; Avidan, O.; Deziel, E.; Greenberg, E.P.; Poole, K.; Banin, E. Increase in rhamnolipid synthesis under iron-limiting conditions influences surface motility and biofilm formation in *Pseudomonas aeruginosa*. *J. Bacteriol.* **2010**, *192* (12), 2973-2980; 10.1128/JB.01601-09.
45. Guerrasantos, L.; Kappeli, O.; Fiechter, A. Dependence of *Pseudomonas aeruginosa* continuous culture biosurfactant production on nutritional and environmental factors. *Appl. Microbiol. Biotechnol.* **1986**, *24* (6), 443-448.
46. Saini, H.S.; Barragan-Huerta, B.E.; Lebron-Paler, A.; Pemberton, J.E.; Vazquez, R.R.; Burns, A.M.; Marron, M.T.; Seliga, C.J.; Gunatilaka, A.A.L.; Maier, R.M. Efficient purification of the biosurfactant viscosin from *Pseudomonas libanensis* strain M9-3 and its physicochemical and biological properties. *J. Nat. Prod.* **2008**, *71* (6), 1011-1015; 10.1021/np800069u.
47. Dejugnat, C.; Diat, O.; Zemb, T. Surfactin self-assembles into direct and reverse aggregates in equilibrium and performs selective metal cation extraction. *ChemPhysChem* **2011**, *12* (11), 2138-2144; 10.1002/cphc.201100094.
48. Bonmatin, J.M.; Genest, M.; Labbe, H.; Ptak, M. Solution 3-dimensional structure of surfactin - a cyclic lipopeptide studied by H-1-Nmr, distance geometry, and

molecular-dynamics. *Biopolymers* **1994**, *34* (7), 975-986;
10.1002/bip.360340716.

49. Shen, H.; Lin, T.; Thomas, R.K.; Taylor, D.J.F.; Penfold, J. Surfactin structures at interfaces and in solution: the effect of pH and cations. *J Phys Chem B* **2011**, *115* (15), 4427-4435; 10.1021/jp109360h.
50. Grangemard, I.; Wallach, J.; Maget-Dana, R.; Peypoux, F. Lichenysin - a more efficient cation chelator than surfactin. *Appl. Biochem. Biotechnol.* **2001**, *90* (3), 199-210; 10.1385/ABAB:90:3:199.
51. Sheppard, J.D.; Jumarie, C.; Cooper, D.G.; Laprade, R. Ionic channels induced by surfactin in planar lipid bilayer membranes. *Biochim. Biophys. Acta* **1991**, *1064* (1), 13-23; 10.1016/0005-2736(91)90406-X.
52. Cooper, D.G.; Macdonald, C.R.; Duff, S.J.B.; Kosaric, N. Enhanced production of surfactin from *Bacillus subtilis* by continuous product removal and metal cation additions. *Appl. Environ. Microbiol.* **1981**, *42* (3), 408-412.
53. Makkar, R.S.; Cameotra, S.S. Effects of various nutritional supplements on biosurfactant production by a strain of *Bacillus subtilis* at 45 degrees C. *J. Surfactants Deterg.* **2002**, *5* (1), 11-17; 10.1007/s11743-002-0199-8.
54. Herrera-Martinez, A.; McBride M.J.; Legatzki A.; Hunnicut D.W.; Wolfe G.; Bates R.B.; Pemberton, J.E.; Maier R.M. *Pedobacter* sp. MTN11 *iucC* and *iucD* genes required for production of the biosurfactant siderolipid. **In Review.**

55. Palme, O.; Moszyk, A.; Iphoefer, D.; Lang, S. Selected microbial glycolipids: production, modification and characterization. *Adv. Exp. Med. Biol.* **2010**, *672*, 185-202.
56. Aniszewski, E.; Peixoto, R.S.; Mota, F.F.; Leite, S.G.F.; Rosado, A.S. Bioemulsifier production by *Microbacterium* sp. strains isolated from mangrove and their application to remove cadmium and zinc from hazardous industrial residue. *Brazilian J. Microbiol.* **2010**, *41* (1), 235-245; 10.1590/S1517-83822010000100033.
57. Hong, K.J.; Tokunaga, S.; Ishigami, Y.; Kajiuchi, T. Extraction of heavy metals from MSW incinerator fly ash using saponins. *Chemosphere* **2000**, *41* (3), 345-352; 10.1016/S0045-6535(99)00489-0.
58. Gusiatin, Z.M.; Klimiuk, E. Metal (Cu, Cd and Zn) removal and stabilization during multiple soil washing by saponin. *Chemosphere* **2012**, *86* (4), 383-391; 10.1016/j.chemosphere.2011.10.027.
59. Van Bogaert, I.N.A.; Zhang, J.; Soetaert, W. Microbial synthesis of sophorolipids. *Process Biochem.* **2011**, *46* (4), 821-833; 10.1016/j.procbio.2011.01.010.
60. Kasture, M.B.; Patel, P.; Prabhune, A.A.; Ramana, C.V.; Kulkarni, A.A.; Prasad, B.L.V. Synthesis of silver nanoparticles by sophorolipids: effect of temperature and sophorolipid structure on the size of particles. *J. Chem. Sci.* **2008**, *120* (6), 515-520; 10.1007/s12039-008-0080-6.

61. Ishigami, Y.; Zhang, Y.J.; Ji, F.X. Spiculisporic acid. Functional development of biosurfactant. *Chim. Oggi-Chem. Today* **2000**, *18* (7-8), 32-34.
62. Ishigami, Y.; Yamazaki, S.; Gama, Y. Surface active properties of biosoap from spiculisporic acid. *J. Colloid Interface Sci.* **1983**, *94* (1), 131-139; 10.1016/0021-9797(83)90242-4.
63. Choi, Y.K.; Lee, C.H.; Takizawa, Y.; Gama, Y.; Ishigami, Y. Tricarboxylic acid biosurfactant derived from spiculisporic acid. *Journal of Japan Oil Chemists' Society* **1993**, *42* (2), 95 <last_page> 99; 10.5650/jos1956.42.95.
64. Hong, J.; Yang, S.M.; Lee, C.H.; Choi, Y.K.; Kajiuchi, T. Ultrafiltration of divalent metal cations from aqueous solution using polycarboxylic acid type biosurfactant. *J. Colloid Interface Sci.* **1998**, *202* (1), 63-73; 10.1006/jcis.1998.5446.
65. Hong, J.; Yang, S.; Choi, Y.; Lee, C. Precipitation of tricarboxylic acid biosurfactant derived from spiculisporic acid with metal ions in aqueous solution. *J. Colloid Interface Sci.* **1995**, *173* (1), 92-103; 10.1006/jcis.1995.1301.
66. Miller, R.M. Biosurfactant-facilitated remediation of metal-contaminated soils. *Environ. Health Perspect.* **1995**, *103*, 59-62; 10.2307/3432014.
67. Wen, J.; Stacey, S.P.; McLaughlin, M.J.; Kirby, J.K. Biodegradation of rhamnolipid, EDTA and citric acid in cadmium and zinc contaminated soils. *Soil Biol. Biochem.* **2009**, *41* (10), 2214-2221; 10.1016/j.soilbio.2009.08.006.

68. Lestan, D.; Luo, C.; Li, X. The use of chelating agents in the remediation of metal-contaminated soils: a review. *Environ. Pollut.* **2008**, *153* (1), 3-13; 10.1016/j.envpol.2007.11.015.
69. Neilson, J.W.; Artiola, J.F.; Maier, R.M. Characterization of lead removal from contaminated soils by nontoxic soil-washing agents. *J. Environ. Qual.* **2003**, *32* (3), 899-908.
70. Torres, L.G.; Lopez, R.B.; Beltran, M. Removal of As, Cd, Cu, Ni, Pb, and Zn from a highly contaminated industrial soil using surfactant enhanced soil washing. *Phys. Chem. Earth* **2012**, *37-39*, 30-36; 10.1016/j.pce.2011.02.003.
71. Malandrino, M.; Abollino, O.; Giacomino, A.; Aceto, M.; Mentasti, E. Adsorption of heavy metals on vermiculite: influence of pH and organic ligands. *J. Colloid Interface Sci.* **2006**, *299* (2), 537-546; 10.1016/j.jcis.2006.03.011.
72. Mulligan, C.N.; Yong, R.N.; Gibbs, B.F.; James, S.; Bennett, H.P.J. Metal removal from contaminated soil and sediments by the biosurfactant surfactin. *Environ. Sci. Technol.* **1999**, *33* (21), 3812-3820; 10.1021/es9813055.
73. Mulligan, C.N.; Yong, R.N.; Gibbs, B.F. Heavy metal removal from sediments by biosurfactants. *J. Hazard. Mater.* **2001**, *85* (1-2), 111-125; 10.1016/S0304-3894(01)00224-2.

74. Herman, D.C.; Artiola, J.F.; Miller, R.M. Removal of cadmium, lead, and zinc from soil by a rhamnolipid biosurfactant. *Environ. Sci. Technol.* **1995**, *29* (9), 2280-2285; 10.1021/es00009a019.
75. Parthasarathi, R.; Sivakumaar, P.K. Biosurfactant mediated remediation process evaluation on a mixture of heavy metal spiked topsoil using soil column and batch washing methods. *Soil Sed. Contam.* **2011**, *20* (8), 892-907; 10.1080/15320383.2011.620043.
76. Juwarkar, A.A.; Nair, A.; Dubey, K.V.; Singh, S.K.; Devotta, S. Biosurfactant technology for remediation of cadmium and lead contaminated soils. *Chemosphere* **2007**, *68* (10), 1996-2002; 10.1016/j.chemosphere.2007.02.027.
77. Wang, S.; Mulligan, C.N. Rhamnolipid foam enhanced remediation of cadmium and nickel contaminated soil. *Water Air and Soil Pollution* **2004**, *157* (1-4), 315-330; 10.1023/B:WATE.0000038904.91977.f0.
78. Hong, K.J.; Tokunaga, S.; Kajiuchi, T. Evaluation of remediation process with plant-derived biosurfactant for recovery of heavy metals from contaminated soils. *Chemosphere* **2002**, *49* (4), 379-387; 10.1016/S0045-6535(02)00321-1.
79. Slizovskiy, I.B.; Kelsey, J.W.; Hatzinger, P.B. Surfactant-facilitated remediation of metal-contaminated soils: efficacy and toxicological consequences to earthworms. *Environ. Toxicol. Chem.* **2011**, *30* (1), 112-123; 10.1002/etc.357.

80. Dahrazma, B.; Mulligan, C.N. Investigation of the removal of heavy metals from sediments using rhamnolipid in a continuous flow configuration. *Chemosphere* **2007**, *69* (5), 705-711; 10.1016/j.chemosphere.2007.05.037.
81. Wang, S.; Mulligan, C.N. Arsenic mobilization from mine tailings in the presence of a biosurfactant. *Appl. Geochem.* **2009**, *24* (5), 928-935; 10.1016/j.apgeochem.2009.02.017.
82. Wang, S.; Mulligan, C.N. Rhamnolipid biosurfactant-enhanced soil flushing for the removal of arsenic and heavy metals from mine tailings. *Process Biochemistry* **2009**, *44* (3), 296-301; 10.1016/j.procbio.2008.11.006.
83. Gao, L.; Kano, N.; Sato, Y.; Li, C.; Zhang, S.; Imaizumi, H. Behavior and distribution of heavy metals including rare earth elements, thorium, and uranium in sludge from industry water treatment plant and recovery method of metals by biosurfactants application. *Bioinorg. Chem. Appl.* **2012**, 10.1155/2012/173819.
84. Ochoa-Loza, F.J.; Noordman, W.H.; Janssen, D.B.; Brusseau, M.L.; Maier, R.M. Effect of clays, metal oxides, and organic matter on rhamnolipid biosurfactant sorption by soil. *Chemosphere* **2007**, *66* (9), 1634-1642; 10.1016/j.chemosphere.2006.07.068.
85. Chen, W.; Hsia, L.; Chen, K.K. Metal desorption from copper(II)/nickel(II)-spiked kaolin as a soil component using plant-derived saponin biosurfactant. *Process Biochemistry* **2008**, *43* (5), 488-498; 10.1016/j.procbio.2007.11.017.

86. Asci, Y.; Nurbas, M.; Acikel, Y.S. A comparative study for the sorption of Cd(II) by soils with different clay contents and mineralogy and the recovery of Cd(II) using rhamnolipid biosurfactant. *J. Hazard. Mater.* **2008**, *154* (1-3), 663-673; 10.1016/j.jhazmat.2007.10.078.
87. Asci, Y.; Nurbas, M.; Acikel, Y.S. Investigation of sorption/desorption equilibria of heavy metal ions on/from quartz using rhamnolipid biosurfactant. *J. Environ. Manage.* **2010**, *91* (3), 724-731; 10.1016/j.jenvman.2009.09.036.
88. Asci, Y.; Nurbas, M.; Acikel, Y.S. Sorption of Cd(II) onto kaolin as a soil component and desorption of Cd(II) from kaolin using rhamnolipid biosurfactant. *J. Hazard. Mater.* **2007**, *139* (1), 50-56; 10.1016/j.jhazmat.2006.06.004.
89. Torrens, J.L.; Herman, D.C.; Miller-Maier, R.M. Biosurfactant (rhamnolipid) sorption and the impact on rhamnolipid-facilitated removal of cadmium from various soils under saturated flow conditions. *Environ. Sci. Technol.* **1998**, *32* (6), 776-781; 10.1021/es970285o.
90. Jordan, F.L.; Robin-Abbott, M.; Maier, R.M.; Glenn, E.P. A comparison of chelator-facilitated metal uptake by a halophyte and a glycophyte. *Environ. Toxicol. Chem.* **2002**, *21* (12), 2698-2704; 10.1897/1551-5028(2002)021<2698:ACOCFM>2.0.CO;2.
91. Johnson, A.; Gunawardana, B.; Singhal, N. Amendments for enhancing copper uptake by *Brassica juncea* and *Lolium perenne* from solution. *Int. J. Phytoremediation* **2009**, *11* (3), 215-234; 10.1080/15226510802429633.

92. Wen, J.; McLaughlin, M.J.; Stacey, S.P.; Kirby, J.K. Is rhamnolipid biosurfactant useful in cadmium phytoextraction? *Journal of Soils and Sediments* **2010**, *10* (7), 1289-1299; 10.1007/s11368-010-0229-z.
93. Gunawardana, B.; Singhal, N.; Johnson, A. Amendments and their combined application for enhanced copper, cadmium, lead uptake by *Lolium perenne*. *Plant Soil* **2010**, *329* (1-2), 283-294; 10.1007/s11104-009-0153-4.
94. Stacey, S.P.; McLaughlin, M.J.; Cakmak, I.; Hetitiarachchi, G.M.; Scheckel, K.G.; Karkkainen, M. Root uptake of lipophilic zinc-rhamnolipid complexes. *J. Agric. Food Chem.* **2008**, *56* (6), 2112-2117; 10.1021/jf0729311.
95. Sandrin, T.R.; Chech, A.M.; Maier, R.M. A rhamnolipid biosurfactant reduces cadmium toxicity during naphthalene biodegradation. *Appl. Environ. Microbiol.* **2000**, *66* (10), 4585-4588; 10.1128/AEM.66.10.4585-4588.2000.
96. Sandrin, T.R.; Maier, R.M. Impact of metals on the biodegradation of organic pollutants. *Environ. Health Perspect.* **2003**, *111* (8), 1093-1101; 10.1289/ehp.5840.
97. Zhang, Y.; Miller, R. Enhanced octadecane dispersion and biodegradation by a *Pseudomonas* rhamnolipid surfactant (biosurfactant). *Appl. Environ. Microbiol.* **1992**, *58* (10), 3276-3282.

98. Song, S.; Zhu, L.; Zhou, W. Simultaneous removal of phenanthrene and cadmium from contaminated soils by saponin, a plant-derived biosurfactant. *Environmental Pollution* **2008**, *156* (3), 1368-1370; 10.1016/j.envpol.2008.06.018.
99. Lima, T.M.S.; Procopio, L.C.; Brandao, F.D.; Carvalho, A.M.X.; Totola, M.R.; Borges, A.C. Simultaneous phenanthrene and cadmium removal from contaminated soil by a ligand/biosurfactant solution. *Biodegradation* **2011**, *22* (5), 1007-1015; 10.1007/s10532-011-9459-z.
100. Ozdemir, G.; Yapar, S. Adsorption and desorption behavior of copper ions on Na-montmorillonite: effect of rhamnolipids and pH. *J. Hazard. Mater.* **2009**, *166* (2-3), 1307-1313; 10.1016/j.jhazmat.2008.12.059.
101. Fillipi, B.R.; Brant, L.W.; Scamehorn, J.F.; Christian, S.D. Use of micellar-enhanced ultrafiltration at low surfactant concentrations and with anionic-nonionic surfactant mixtures. *J. Colloid Interface Sci.* **1999**, *213* (1), 68-80; 10.1006/jcis.1999.6092.
102. El Zeftawy, M.A.M.; Mulligan, C.N. Use of rhamnolipid to remove heavy metals from wastewater by micellar-enhanced ultrafiltration (MEUF). *Separation and Purification Technology* **2011**, *77* (1), 120-127; 10.1016/j.seppur.2010.11.030.
103. Chen, H.; Chen, C.; Reddy, A.S.; Chen, C.; Li, W.R.; Tseng, M.; Liu, H.; Pan, W.; Maity, J.P.; Atla, S.B. Removal of mercury by foam fractionation using surfactin, a biosurfactant. *Int. J. Mol. Sci.* **2011**, *12* (11), 8245-8258; 10.3390/ijms12118245.

104. Yuan, X.Z.; Meng, Y.T.; Zeng, G.M.; Fang, Y.Y.; Shi, J.G. Evaluation of tea-derived biosurfactant on removing heavy metal ions from dilute wastewater by ion flotation. *Colloid Surf. A-Physicochem. Eng. Asp.* **2008**, *317* (1-3), 256-261; 10.1016/j.colsurfa.2007.10.024.
105. Menezes, C.T.B.; Barros, E.C.; Rufino, R.D.; Luna, J.M.; Sarubbo, L.A. Replacing synthetic with microbial surfactants as collectors in the treatment of aqueous effluent produced by acid mine drainage, using the dissolved air flotation technique. *Appl. Biochem. Biotechnol.* **2011**, *163* (4), 540-546; 10.1007/s12010-010-9060-7.
106. Zouboulis, A.I.; Matis, K.A.; Lazaridis, N.K.; Golyshin, P.N. The use of biosurfactants in flotation: application for the removal of metal ions. *Minerals Eng* **2004**, *17* (1), 105-105; 10.1016/j.mineng.2003.11.017.
107. Mulligan, C.N.; Sharma, S.K.; Mudhoo, A. *Biosurfactants: research trends and applications*. CRC Press: 2014.
108. Khan, M.Y.; Swapna, T.; Hameeda, B.; Reddy, G. Bioremediation of heavy metals using biosurfactants. *Advances in Biodegradation and Bioremediation of Industrial Waste* **2015**, , 381.
109. Pradhan, A.K.; Pradhan, N. Microbial biosurfactant for hydrocarbons and heavy metals bioremediation, In *Environmental Microbial Biotechnology*. Springer: **2015**; pp. 91-104.

110. Franzetti, A.; Tamburini, E.; Banat, I.M. Applications of biological surface active compounds in remediation technologies. *Biosurfactants* **2010**, *672*, 121-134.
111. Sarubbo, L.; Rocha Jr, R.; Luna, J.; Rufino, R.; Santos, V.; Banat, I. Some aspects of heavy metals contamination remediation and role of biosurfactants. *Chem. Ecol.* **2015**, *31* (8), 707-723.
112. Ławniczak, Ł.; Marecik, R.; Chrzanowski, Ł. Contributions of biosurfactants to natural or induced bioremediation. *Appl. Microbiol. Biotechnol.* **2013**, *97* (6), 2327-2339.
113. Abyaneh, A.S.; Fazaelpoor, M.H. Evaluation of rhamnolipid (RL) as a biosurfactant for the removal of chromium from aqueous solutions by precipitate flotation. *J. Environ. Manage.* **2016**, *165*, 184-187.
114. Bodagh, A.; Khoshdast, H.; Sharafi, H.; Zahiri, H.S.; Noghabi, K.A. Removal of cadmium(II) from aqueous solution by ion flotation using rhamnolipid biosurfactant as an ion collector. *Ind Eng Chem Res* **2013**, *52* (10), 3910-3917; 10.1021/ie400085t.
115. Luna, J.M.; Rufino, R.D.; Sarubbo, L.A. Biosurfactant from *Candida sphaerica* UCP0995 exhibiting heavy metal remediation properties. *Process Saf. Environ. Prot.* **2016**, *102*, 558-566.

116. Haryanto, B.; Chang, C. Foam-enhanced removal of adsorbed metal ions from packed sands with biosurfactant solution flushing. *Journal of the Taiwan Institute of Chemical Engineers* **2014**, *45* (5), 2170-2175.
117. Singh, A.K.; Cameotra, S.S. Efficiency of lipopeptide biosurfactants in removal of petroleum hydrocarbons and heavy metals from contaminated soil. *Environmental Science and Pollution Research* **2013**, *20* (10), 7367-7376.
118. U.S. National Research Council *Minerals, critical minerals, and the U.S. economy*. National Academies Press: Washington, D.C., 2008.
119. Binnemans, K.; Jones, P.; Blanpain, B.; Gerven, T.; Yang, Y.; Walton, A.; Buchert, M. Recycling of rare earths: a critical review. *J. Clean. Prod.* **2013**, *51*, 1-22; <http://dx.doi.org/10.1016/j.jclepro.2012.12.037>.
120. *International strategic minerals inventory summary report; rare-earth oxides*; U.S. Geological Survey: <http://pubs.er.usgs.gov/publication/cir930N>.
121. *Financial assistance funding opportunity announcement: Eenergy innovation hub – critical materials*; U.S. Department of Energy; <https://eere-exchange.energy.gov/#FoalId71ef57c0-ce63-4f56-865c-76ff132eaf21>.
122. *Critical raw materials for the EU*; European Commission; http://ec.europa.eu/enterprise/policies/raw-materials/critical/index_en.htm.
123. *Rare earth elements: the global supply chain*; Congressional Research Service: www.fas.org; <http://www.fas.org/sgp/crs/natsec/R41347.pdf>.

124. Merten, D.; Buchel, G. Determination of rare earth elements in acid mine drainage by inductively coupled plasma mass spectrometry. *Microchimica Acta* **2004**, *148* (3/4), 163-170.
125. Protano, G.; Riccobono, F. High contents of rare earth elements (REEs) in stream waters of a Cu–Pb–Zn mining area. *Environmental Pollution* **2002**, *117* (3), 499-514.
126. Borrego, J.; Carro, B.; Lopez-Gonzalez, N.; de la Rosa, J.; Grande, J.; Gomez, T.; de la Torre, M. Effect of acid mine drainage on dissolved rare earth elements geochemistry along a fluvial-estuarine system: the Tinto-Odiel Estuary (SW Spain). *Hydrology Research* **2012**, *43* (3), 262-274.
127. Gammons, C.H.; Wood, S.A.; Jonas, J.P.; Madison, J.P. Geochemistry of the rare-earth elements and uranium in the acidic Berkeley Pit lake, Butte, Montana. *Chem. Geol.* **2003**, *198* (3–4), 269-288; [http://dx.doi.org/10.1016/S0009-2541\(03\)00034-2](http://dx.doi.org/10.1016/S0009-2541(03)00034-2).
128. Fernandez-Caliani J.C.; De la Rosa J.D.; Barba-Brioso C. Mobility and speciation of rare earth elements in acid minesoils and geochemical implications for river waters in the southwestern Iberian margin. *Geoderma Geoderma* **2009**, *149* (3-4), 393-401.
129. Miekeley, N.; Coutinho de Jesus, H.; Porto da Silveira, C.L.; Linsalata, P.; Morse, R. Rare earth elements in groundwaters from the Osamu Utsumi mine and Morro

- do Ferro analogue study sites, Poços de Caldas, Brazil. *J. Geochem. Explor.* **1992**, 45 (1–3), 365-387; [http://dx.doi.org/10.1016/0375-6742\(92\)90131-Q](http://dx.doi.org/10.1016/0375-6742(92)90131-Q).
130. Cravotta, C.A. Dissolved metals and associated constituents in abandoned coal-mine discharges, Pennsylvania, USA. Part 1: Constituent quantities and correlations. *Applied geochemistry : journal of the International Association of Geochemistry and Cosmochemistry.* **2008**, 23 (2), 166-202.
131. Zhao, F.; Cong, Z.; Sun, H.; Ren, D. The geochemistry of rare earth elements (REE) in acid mine drainage from the Sitai coal mine, Shanxi Province, North China. *International Journal of Coal Geology* **2007**, 70 (1–3), 184-192; <http://dx.doi.org/10.1016/j.coal.2006.01.009>.
132. Worrall, F.; Pearson, D.G. Water-rock interaction in an acidic mine discharge as indicated by rare earth element patterns. *Geochim. Cosmochim. Acta* **2001**, 65 (18), 3027-3040; [http://dx.doi.org/10.1016/S0016-7037\(01\)00662-7](http://dx.doi.org/10.1016/S0016-7037(01)00662-7).
133. Fu, F.; Wang, Q. Removal of heavy metal ions from wastewaters: a review. *J. Environ. Manage.* **2011**, 92 (3), 407-418; [10.1016/j.jenvman.2010.11.011](http://dx.doi.org/10.1016/j.jenvman.2010.11.011).
134. Verplanck, P.L.; Taylor, H.E.; Nordstrom, D.K.; Barber, L.B. Aqueous stability of gadolinium in surface waters receiving sewage treatment plant effluent, Boulder Creek, Colorado. *Environ. Sci. Technol.* **2005**, 39 (18), 6923-6929.
135. Verplanck, P.L.; Furlong, E.T.; Gray, J.L.; Phillips, P.J.; Wolf, R.E.; Esposito, K. Evaluating the behavior of gadolinium and other rare earth elements through large

- metropolitan sewage treatment plants. *Environ. Sci. Technol.* **2010**, *44* (10), 3876-3882.
136. Kiddee, P.; Naidu, R.; Wong, M.H.; Hearn, L.; Muller, J.F. Field investigation of the quality of fresh and aged leachates from selected landfills receiving e-waste in an arid climate. *Waste Manage.* **2014**, *34* (11), 2292-2304.
137. Giesy, J.P.; Alberts, J.J. Conditional stability-constants and binding-capacities for copper(ii) by ultrafilterable material isolated from 6 surface waters of wyoming, USA. *Hydrobiologia* **1989**, *188*, 659-680; 10.1007/BF00027834.
138. Lebron-Paler, A.; Pemberton, J.E.; Becker, B.A.; Otto, W.H.; Larive, C.K.; Maier, R.M. Determination of the acid dissociation constant of the biosurfactant monorhamnolipid in aqueous solution by potentiometric and spectroscopic methods. *Anal. Chem.* **2006**, *78* (22), 7649-7658; 10.1021/ac0608826.
139. Zhang, Y.; Miller, R. Effect of a *Pseudomonas* rhamnolipid biosurfactant on cell hydrophobicity and biodegradation of octadecane. *Appl. Environ. Microbiol.* **1994**, *60* (6), 2101-2106.
140. Lebron-Paler, A. Solution and interfacial characterization of rhamnolipid biosurfactant from *P. aeruginosa* ATCC 9027. , The University of Arizona, 2008.
141. Zhang, L.; Pemberton, J.E.; Maier, R.M. Effect of fatty acid substrate chain length on *Pseudomonas aeruginosa* ATCC 9027 monorhamnolipid yield and congener

- distribution. *Process Biochem.* **2014**, *49* (6), 989-995;
10.1016/j.procbio.2014.03.003.
142. Schnitzer, M.; Hansen, E.H. Organo-metallic interactions in soils: 8. an evaluation of methods for determination of stability constants of metal-fulvic acid complexes. *Soil Sci.* **1970**, *109* (6), 333-&; 10.1097/00010694-197006000-00001.
143. Clark, J.; Turner, R. An examination of the resin exchange method for the determination of stability constants of metal-soil organic matter complexes. *Soil Sci.* **1969**, *107* (1), 8-11.
144. Schubert, J. The use of ion exchangers of the determination of physical-chemical properties of substances, particularly radiotracers, in solution: I. theoretical. *J. Phys. Chem.* **1948**, *52* (2), 340-350.
145. Schubert, J.; Richter, J. The use of ion exchangers for the determination of physical-chemical properties of substances, particularly radiotracers, in solution: II. the dissociation constants of strontium citrate and strontium tartrate. *J. Phys. Chem.* **1948**, *52* (2), 350-357.
146. Lawrance, G.A. Stability, In *Introduction to coordination chemistry*. Wiley: Chichester, U.K, **2010**.
147. Randhawa, N.S.; Broadbent, F. Soil organic matter-metal complexes: 6 stability constants of zinc-humic acid complexes at different pH values. *Soil Sci.* **1965**, *99* (6), 362-366.

148. Schnitzer, M.; Skinner, S. Organo-metallic interactions in soils: 5. stability constants of Cu^{++} -, Fe^{++} -, and Z^{++} -fulvic acid complexes. *Soil Sci.* **1966**, *102* (6), 361-365.
149. Miller, M.; Ohlrogge, A. Water-soluble chelating agents in organic materials: I. characterization of chelating agents and their reactions with trace metals in soils. *Soil Sci. Soc. Am. J.* **1958**, *22* (3), 225-228.
150. Alexandratos, S.D.; Kung, S. Preface to the special issue: uranium in seawater. *Ind Eng Chem Res* **2016**, *55* (15), 4101-4102.
151. Krestou, A.; Panias, D. Uranium (VI) speciation diagrams in the $\text{UO}_2^{2+} / \text{CO}_3^{2-} / \text{H}_2\text{O}$ system at 25° C. *European Journal of Mineral Processing and Environmental Protection* **2004**, *4* (2), 113.
152. Irving, H.; Williams, R.J.P. 637. The stability of transition-metal complexes. *J. Chem. Soc.* **1953**, , 3192; 10.1039/JR9530003192.
153. Richens, D.T. Introduction, In *The chemistry of aqua ions: synthesis, structure, and reactivity : a tour through the periodic table of the elements*. J. Wiley: Chichester; New York, **1997**.
154. Cantrell, K.; Byrne, R. Rare-earth element complexation by carbonate and oxalate ions. *Geochim. Cosmochim. Acta* **1987**, *51* (3), 597-605; 10.1016/0016-7037(87)90072-X.
155. Shannon, R. Revised effective ionic radii and systematic studies of interatomic distances in halides and chalcogenides. *Acta Crystallographica Section A: Crystal*

- Physics, Diffraction, Theoretical and General Crystallography* **1976**, 32 (5), 751-767.
156. Smith, D.W. Ionic hydration enthalpies. *J. Chem. Educ.* **1977**, 54 (9), 540.
157. Parr, R.G.; Pearson, R.G. Absolute hardness: companion parameter to absolute electronegativity. *J. Am. Chem. Soc.* **1983**, 105 (26), 7512-7516.
158. Markich, S.J. Uranium speciation and bioavailability in aquatic systems: an overview. *ScientificWorldJournal* **2002**, 2, 707-729; 10.1100/tsw.2002.130 [doi].
159. Barakat, M.A. New trends in removing heavy metals from industrial wastewater. *Arab. J. Chem.* **2011**, 4 (4), 361-377; 10.1016/j.arabjc.2010.07.019.
160. Shah, A.; Shahzad, S.; Munir, A.; Nadagouda, M.N.; Khan, G.S.; Shams, D.F.; Dionysiou, D.D.; Rana, U.A. Micelles as soil and water decontamination agents. *Chem. Rev.* **2016**, 116 (10), 6042-6074.
161. Rebello, S.; Asok, A.K.; Mundayoor, S.; Jisha, M. Surfactants: toxicity, remediation and green surfactants. *Environmental chemistry letters* **2014**, 12 (2), 275-287.
162. Southward, A.J.; Southward, E.C. Recolonization of rocky shores in Cornwall after use of toxic dispersants to clean up the Torrey Canyon spill. *Journal of the Fisheries Research Board of Canada* **1978**, 35 (5), 682-706.

163. Hamdan, L.J.; Fulmer, P.A. Effects of COREXIT® EC9500A on bacteria from a beach oiled by the Deepwater Horizon spill. *Aquat. Microb. Ecol.* **2011**, *63* (2), 101.
164. Zuijdgheest, A.; Huettel, M. Dispersants as used in response to the MC252-spill lead to higher mobility of polycyclic aromatic hydrocarbons in oil-contaminated Gulf of Mexico sand. *PloS one* **2012**, *7* (11), e50549.
165. Paul, J.H.; Hollander, D.; Coble, P.; Daly, K.L.; Murasko, S.; English, D.; Basso, J.; Delaney, J.; McDaniel, L.; Kovach, C.W. Toxicity and mutagenicity of Gulf of Mexico waters during and after the Deepwater Horizon oil spill. *Environ. Sci. Technol.* **2013**, *47* (17), 9651-9659.
166. Kleindienst, S.; Paul, J.H.; Joye, S.B. Using dispersants after oil spills: impacts on the composition and activity of microbial communities. *Nature Reviews Microbiology* **2015**, *13* (6), 388-396.
167. Pacwa-Płociniczak, M.; Płaza, G.A.; Piotrowska-Seget, Z.; Cameotra, S.S. Environmental applications of biosurfactants: recent advances. *International journal of molecular sciences* **2011**, *12* (1), 633-54.
168. Zhang, Y.; Miller, R. Effect of rhamnolipid (biosurfactant) structure on solubilization and biodegradation of n-alkanes. *Appl. Environ. Microbiol.* **1995**, *61* (6), 2247-2251.

169. Stanghellini, M.E.; Miller, R.M. Biosurfactants: their identity and potential efficacy in the biological control of zoosporic plant pathogens. *Plant disease*. **1997**, *81* (1), 4.
170. Magalhaes, L.; Nitschke, M. Antimicrobial activity of rhamnolipids against *Listeria monocytogenes* and their synergistic interaction with nisin. *Food Control* **2013**, *29* (1), 138-142; 10.1016/j.foodcont.2012.06.009.
171. Abdel-Mawgoud, A.M.; Hausmann, R.; Lépine, F.; Müller, M.M.; Déziel, E. Rhamnolipids: detection, analysis, biosynthesis, genetic regulation, and bioengineering of production, In *Biosurfactants*. Springer: 2011; pp. 13-55.
172. Mulligan, C.N. Environmental applications for biosurfactants. *Environmental pollution*. **2005**, *133* (2), 183-198.
173. Schenk, T.; Breitschwerdt, A.; Kessels, G.; Schuphan, I.; Schimdt, B. A biosynthetic route to [14C]-labelled rhamnolipids. *J. Labelled Compd. Radiopharmaceut*. **1997**, *39* (8), 705-710.
174. Bauer, J.; Brandenburg, K.; Zähringer, U.; Rademann, J. Chemical synthesis of a glycolipid library by a solid-phase strategy allows elucidation of the structural specificity of immunostimulation by rhamnolipids. *Chemistry—A European Journal* **2006**, *12* (27), 7116-7124.
175. Andra, J.; Rademann, J.; Howe, J.; Koch, M.; Heine, H.; Zähringer, U.; Brandenburg, K. Endotoxin-like properties of a rhamnolipid exotoxin from

- Burkholderia (Pseudomonas) plantarii*: immune cell stimulation and biophysical characterization. *Biol. Chem.* **2006**, *387* (3), 301-310; 10.1515/BC.2006.040.
176. Abdel-Mawgoud, A.M.; Lepine, F.; Deziel, E. A stereospecific pathway diverts beta-oxidation intermediates to the biosynthesis of rhamnolipid biosurfactants. *Chem. Biol.* **2014**, *21* (1), 156-164; 10.1016/j.chembiol.2013.11.010.
177. Coss, C.S. Minimally competent lewis acid catalysts. General methods for the synthesis and separation of diastereomeric mixtures of monorhamnolipids of *Pseudomonas aeruginosa* with peracetate glycoside donors. Ph.D. Dissertation, University of Arizona, 2012.
178. Liu, W.; Gan, J.J.; Qin, S. Separation and aquatic toxicity of enantiomers of synthetic pyrethroid insecticides. *Chirality* **2005**, *17* (1), S127.
179. Wong, C.S. Environmental fate processes and biochemical transformations of chiral emerging organic pollutants. *Analytical and Bioanalytical Chemistry* **2006**, *386* (3), 544-558; 10.1007/s00216-006-0424-3.
180. Mueller, T.A.; Kohler, H.-E. Chirality of pollutants - effects on metabolism and fate. *Appl. Microbiol. Biotechnol.* **2004**, *64* (3), 300-316.
181. Smith, S.W. Chiral toxicology: it's the same thing...only different. *Toxicological Sciences* **2009**, *110* (1), 4-30; 10.1093/toxsci/kfp097.

182. Bartha, R.; Pramer, D. Features of a flask and method for measuring the persistence and biological effects of pesticides in soil. *Soil Sci.* **1965**, *100* ((1)), 68-70; 10.1097/00010694-196507000-00011.
183. United States Environmental Protection Agency. *Fate, transport and transformation test guidelines: OPPTS 835.3140 ready biodegradability-- CO₂ in sealed vessels (headspace test)*. October **2008**.
184. Bulich, A. Utility of the microtox luminescent bacterial assay for the rapid assessment of aquatic pollution. *2nd Interagency Workshop on In-Situ Water-Quality Sensing: Biological Sensors April 28-30, 1980, Pensacola Beach, Florida. National Oceanic and Atmospheric Administration Report, 1981.* p 173-184, 4 Fig, 2 Tab, 11 Ref **1981**.
185. Truong, L.; Reif, D.M.; St Mary, L.; Geier, M.C.; Truong, H.D.; Tanguay, R.L. Multidimensional in vivo hazard assessment using zebrafish. *Toxicol. Sci.* **2014**, *137* (1), 212-233; 10.1093/toxsci/kft235 [doi].
186. Palos-Pacheco, R.; Eismín, R.J.; Coss, C.S.; Wang; Kegel, L.M.; Maier, R.M.; Polt, R.; Pemberton, J.E. Synthesis and characterization of four diastereomers of monorhamnolipids. **In Preperation**.
187. OECD *Test no. 301: ready biodegradability*. Organisation for Economic Co-operation and Development: 1992.

188. Place, B.J.; Perkins, M.J.; Sinclair, E.; Barsamian, A.L.; Blakemore, P.R.; Field, J.A.
Trace analysis of surfactants in Corexit oil dispersant formulations and seawater.
Deep Sea Research Part II: Topical Studies in Oceanography **2016**, *129*, 273-
281.
189. Uña, G.V.; García, M.J.N. Biodegradation of non-ionic dispersants in sea-water.
Eur. J. Appl. Microb. Biotechnol. **1983**, *18* (5), 315-319.
190. Campo, P.; Venosa, A.D.; Suidan, M.T. Biodegradability of corexit 9500 and
dispersed south Louisiana crude oil at 5 and 25 C. *Environ. Sci. Technol.* **2013**, *47*
(4), 1960-1967.
191. White, H.K.; Lyons, S.L.; Harrison, S.J.; Findley, D.M.; Liu, Y.; Kujawinski, E.B.
Long-term persistence of dispersants following the Deepwater Horizon oil spill.
Environmental Science & Technology Letters **2014**, *1* (7), 295-299.
192. Unites States Environmental Protection Agency. Technical overview of ecological
risk assessment - analysis phase: ecological effects characterization.
[https://www.epa.gov/pesticide-science-and-assessing-pesticide-risks/technical-
overview-ecological-risk-assessment-0](https://www.epa.gov/pesticide-science-and-assessing-pesticide-risks/technical-overview-ecological-risk-assessment-0)
193. Fuller, C.; Bonner, J.; Page, C.; Ernest, A.; McDonald, T.; McDonald, S.
Comparative toxicity of oil, dispersant, and oil plus dispersant to several marine
species. *Environmental Toxicology and Chemistry* **2004**, *23* (12), 2941-2949.

194. Franzetti, A.; Di Gennaro, P.; Bevilacqua, A.; Papacchini, M.; Bestetti, G.
Environmental features of two commercial surfactants widely used in soil
remediation. *Chemosphere* **2006**, *62* (9), 1474-1480.
195. Tarkpea, M.; Hansson, M.; Samuelsson, B. Comparison of the microtox test with the
96-hr LC50 test for the harpacticoid *Nitocra spinipes*. *Ecotoxicol. Environ. Saf.*
1986, *11* (2), 127-143.
196. Nałecz-Jawecki, G.; Rudź, B.; Sawicki, J. Evaluation of toxicity of medical devices
using spirotax and microtox tests: I. toxicity of selected toxicants in various
diluent. *J. Biomed. Mater. Res.* **1997**, *35* (1), 101-105.
197. Leal, J.S.; Gonzalez, J.; Comelles, F.; Campos, E.; Ciganda, T. Biodegradability and
toxicity of anionic surfactants. *Acta Hydrochim. Hydrobiol.* **1991**, *19* (6), 703-
709.
198. Lechuga, M.; Fernández-Serrano, M.; Jurado, E.; Núñez-Olea, J.; Ríos, F. Acute
toxicity of anionic and non-ionic surfactants to aquatic organisms. *Ecotoxicol.*
Environ. Saf. **2016**, *125*, 1-8.
199. Johann, S.; Seiler, T.; Tiso, T.; Bluhm, K.; Blank, L.M.; Hollert, H. Mechanism-
specific and whole-organism ecotoxicity of mono-rhamnolipids. *Sci. Total*
Environ. **2016**, *548*, 155-163.
200. George-Ares, A.; Clark, J. Aquatic toxicity of two Corexit® dispersants.
Chemosphere **2000**, *40* (8), 897-906.

201. Braunbeck, T.; Böttcher, M.; Hollert, H.; Kosmehl, T.; Lammer, E.; Leist, E.; Rudolf, M.; Seitz, N. Towards an alternative for the acute fish LC (50) test in chemical assessment: the fish embryo toxicity test goes multi-species—an update. *ALTEX* **2005**, *22* (2), 87-102.
202. Hogan, D.E.; Pemberton, J.E.; Maier, R.M. Rhamnolipid biosurfactants preferentially complex rare earth elements. **In Preparation.**
203. Hogan, D.E.; Veres-Schalnat, T.A.; Pemberton, J.E.; Maier, R.M. Biosurfactant Complexation of Metals and Applications for Remediation, In *Biosurfactants : Research Trends and Applications*, Mulligan, C.N.; Mudhoo, A.; Sharma, S.K., Eds.; CRC Press: London, GBR, 2014; pp. 277.
204. *Coping with water scarcity: a strategic issue and priority for system-wide action*; UN-Water Scarcity Initiative: New York, NY;
http://www.un.org/waterforlifedecade/pdf/2006_unwater_coping_with_water_scarcity_eng.pdf.
205. Hoekstra, A.Y.; Mekonnen, M.M.; Chapagain, A.K.; Mathews, R.E.; Richter, B.D. Global monthly water scarcity: blue water footprints versus blue water availability. *PLoS One* **2012**, *7* (2), e32688.
206. Mekonnen, M.; Hoekstra, A. Global water scarcity: monthly blue water footprint compared to blue water availability for the world's major river basins. *Value of Water Research Report Series. UNESCO-IHE* **2011**.

207. Fuller, A.C.; Harhay, M.O. Population growth, climate change and water scarcity in the southwestern United States. *Am. J. Environ. Sci.* **2010**, *6* (3), 249-252; 10.3844/ajessp.2010.249.252 [doi].
208. Gerten, D.; Lucht, W.; Ostberg, S.; Heinke, J.; Kowarsch, M.; Kreft, H.; Kundzewicz, Z.W.; Rastgooy, J.; Warren, R.; Schellnhuber, H.J. Asynchronous exposure to global warming: freshwater resources and terrestrial ecosystems. *Environmental Research Letters* **2013**, *8* (3), 034032.
209. 2030 Water Resource Group. Charting our water future: economic framework to inform decision-making. **2009**.
210. *Water recycling FAQs*; The University of Arizona Cooperative Extension: cals.arizona.edu/pubs/water/az1568.pdf.
211. Sebba, F. Concentration by ion flotation. *Nature* **1959**, *184*, 1062-1063. 10.1038/1841062a0.
212. Pinfeld, T.A. Ion flotation, In *Adsorptive bubble separation techniques*, Lemlich, R., Ed.; Academic Press: New York, 1972; pp. 53.
213. Matis, K.; Mavros, P. Recovery of metals by ion flotation from dilute aqueous solutions. *Sep. Purif. Methods* **1991**, *20* (1), 1-48.
214. Lemlich, R.; Arod, J. *Adsorptive bubble separation techniques*. Academic Press: New York, 1972.

215. Thalody, B.; Warr, G.G. Ion flotation: a laboratory experiment linking fundamental and applied chemistry. *J. Chem. Educ.* **1999**, *76* (7), 956-958.
216. Klassen, V.I.; Mokrousov, V.A. 16 Frothers and flotation froths, In *An introduction to the theory of flotation*. Butterworths: London, 1963; pp. 143.
217. Myers, D. Chapter nine: foams, In *Surfactant science and technology*, 2nd ed. VCH: New York, 1992; pp. 249.
218. Jacobelli-Turi, C.; Maracci, F.; Margani, A.; Palmera, M. Separation of metallic ions by foaming: studies in Italy, In *Adsorptive bubble separation techniques*, Lemlich, R., Ed.; Academic Press: New York, 1972; pp. 265.
219. Abbasi, H.; Noghabi, K.A.; Hamed, M.M.; Zahiri, H.S.; Moosavi-Movahedi, A.A.; Amanlou, M.; Teruel, J.A.; Ortiz, A. Physicochemical characterization of a monorhamnolipid secreted by *Pseudomonas aeruginosa* MA01 in aqueous media. An experimental and molecular dynamics study. *Colloids and Surfaces B: Biointerfaces* **2013**, *101*, 256-265.
220. Salmani, M.H.; Davoodi, M.; Ehrampoush, M.H.; Ghaneian, M.T.; Fallahzadah, M.H. Removal of cadmium (II) from simulated wastewater by ion flotation technique. *Iranian Journal of Environmental Health Science and Engineering* **2013**, *10* (1), 1.
221. Matis, K.; Stalidis, G.; Zoumboulis, A. Flotation of germanium from dilute solutions. *Sep. Sci. Technol.* **1988**, *23* (4-5), 347-362.

222. Klassen, V.I.; Mokrousov, V.A. *An introduction to the theory of flotation*. Butterworths: London, 1963.
223. Fuerstenau, D.W.; Healy, T.W. Principles of mineral flotation, In *Adsorptive bubble separation techniques*, Lemlich, R., Ed.; Academic Press: New York, 1972; pp. 53.
224. Klassen, V.I.; Mokrousov, V.A. 17 Size and flotability of particles, In *An introduction to the theory of flotation*. Butterworths: London, 1963; pp. 143.
225. Klassen, V.I.; Mokrousov, V.A. 21 Formation of air bubbles, In *An introduction to the theory of flotation*. Butterworths: London, 1963; pp. 143.
226. Morgan, J.D.; Napper, D.H.; Warr, G.G.; Nicol, S.K. Kinetics of recovery of hexadecyltrimethylammonium bromide by flotation. *Langmuir* **1992**, 8 (9), 2124-2129.
227. Liu, Z.; Doyle, F.M. A thermodynamic approach to ion flotation. I. kinetics of cupric ion flotation with alkylsulfates. *Colloids Surf. Physicochem. Eng. Aspects* **2001**, 178 (1), 79-92.
228. Doyle, F.M. Ion flotation—its potential for hydrometallurgical operations. *Int. J. Miner. Process.* **2003**, 72 (1), 387-399.
229. Martell, A.E.; Hancock, R.D. Chapter 7: stability constants and their measurement, In *Metal complexes in aqueous solutions*. Plenum Press: New York, 1996; pp. 217.

230. Rossotti, F.J.C.; Rossotti, H. *The determination of stability constants: and other equilibrium constants in solution*. McGraw-Hill: New York, 1961.
231. Schubert, J. Applications of ion exchange to the separation of inorganic cations, In *Ion exchange: theory and application*, Nachod, F.C., Ed.; Academic Press Inc.: New York, 1949; pp. 167.
232. Marcus, Y.; Kertes, A.S. *Ion exchange and solvent extraction of metal complexes*. Wiley-Interscience: New York [etc.]; London, 1969.
233. MacCarthy, P.; Mark, H.B. A further examination of the Schubert ion-exchange method as applied to soil organic matter-metal ion interactions. In *Biological implications of metals in the environment: proceedings of the Fifteenth Annual Hanford Life Sciences Symposium at Richland, Washington, September 29-October 1, 1975*, Drucker, H.; Wildung, R.E.; United States Energy Research and Development Administration Technical Information Center; United States Energy Research and Development Administration Division of Biomedical and Environmental Research; Pacific Northwest Laboratory, Eds.; Technical Information Center, Energy Research and Development Administration: Oak Ridge, Tenn., 1977; .
234. Schubert, J.; Russel, E.R.; Myers, L.S., Jr Dissociation constants of radium-organic acid complexes measured by ion exchange. *J. Biol. Chem.* **1950**, *185* (1), 387-398.

235. Zunino, H.; Galindo, G.; Peirano, P.; Aguilera, M. Use of the resin exchange method for the determination of stability constants of metal-soil organic matter complexes. *Soil Sci.* **1972**, *114* (3), 229-233.
236. Galindo, G.; Zunino, H. Some limiting factors of the ion-exchange equilibrium method for determining apparent formation constants of mononuclear complexes. *Talanta* **1978**, *25* (8), 447-450.
237. MacCarthy, P.; Mark, H.B. A discussion of Schubert's ion-exchange equations. *Talanta* **1979**, *26* (12), 1177-1178.
238. Cheng, M.H.; Patterson, J.W.; Minear, R.A. Heavy metals uptake by activated sludge. *Journal (Water Pollution Control Federation)* **1975**, , 362-376.
239. Li, N.C.; Westfall, W.M.; Lindenbaum, A.; White, J.M.; Schubert, J. Manganese-54, uranium-233 and cobalt-60 complexes of some organic acids. *J. Am. Chem. Soc.* **1957**, *79* (22), 5864-5870.
240. Li, N.C.; Doody, B.E.; White, J.M. Some metal complexes of glycine peptides, histidine and related substances. *J. Am. Chem. Soc.* **1957**, *79* (22), 5859-5863.
241. Schubert, J.; Lind, E.L.; Westfall, W.M.; Pflieger, R.; Li, N.C. Ion-exchange and solvent-extraction studies on Co (II) and Zn (II) complexes of some organic acids. *J. Am. Chem. Soc.* **1958**, *80* (18), 4799-4802.
242. Fronaeus, S. The use of cation exchangers for the quantitative investigation of complex systems. *Acta Chem. Scand.* **1951**, *5*, 859-871.

243. MacCarthy, P. Some comments on the derivation of Schubert's ion-exchange equations. *Soil Sci.* **1977**, *123* (3), 207.
244. Schubert, J. Ion exchange studies of complex ions as a function of temperature, ionic strength, and presence of formaldehyde. *J. Phys. Chem.* **1952**, *56* (1), 113-118.
245. Ringbom, A. The analyst and the inconstant constants. *J. Chem. Educ.* **1958**, *35* (6), 282.
246. Burgot, J. Chapter 26: conditional stability constants, In *Ionic equilibria in analytical chemistry*. Springer Science & Business Media: 2012; pp. 485.
247. Schubert, J.; Richter, J.W. Cation exchange studies on the barium citrate complex and related equilibria. *J. Am. Chem. Soc.* **1948**, *70* (12), 4259-4260.